Reflex: A Closed-Loop Tactile Feedback System for Use in Upper Limb Prosthesis Grip Control

by

Luke E. Osborn

A thesis submitted to The Johns Hopkins University in conformity with the requirements for the degree of Master of Science in Engineering.

Baltimore, Maryland

June, 2014

Abstract

Tactile sensing provides valuable insight to the environment in which we interact with. Upper limb amputees lack the sensations that generates the necessary information to stably grasp the wide variety of objects we interact with on a daily basis. Utilizing tactile sensing to provide feedback to a prosthetic hand provides a mechanism for replacing the grip control functionality of the mechanoreceptors found in human skin. Novel customizable, low cost tactile sensors for monitoring the dynamics of an object grasped by a prosthetic hand are developed and presented as part of this thesis. The response of sensors placed on a prosthetic hand provides information regarding the state of a grasped object, particularly contact and slip.

The sensors are made up of various textile materials, including stretchable interfacing layers and conductive traces. Essentially a force sensitive resistor, each sensor is shaped into stretchable cuff that can be placed around the finger of a prosthetic hand. An outer rubber layer on the sensor provides compliance, which is found to enhance grasping performance with a prosthesis.

Two control algorithms were developed as part of the closed-loop tactile feedback

system, called Reflex, to enhance grasping functionality with a prosthesis. A *Contact Detection* strategy uses force information to effectively reduce the user's electromyography (EMG) signals, which are used to control the prosthesis. Essentially, the goal of this strategy is to help a user grab fragile objects without breaking them. A second strategy, *Slip Prevention*, uses the derivative of a force signal to detect slip of a grasped object. Instances of slip trigger electrical pulses sent from the prosthesis control unit to close the hand in an effort to prevent additional slip.

The Reflex system, comprised of two control strategies along with flexible textile based force sensors on the fingers of a prosthesis, was shown to improve the grasping functionality of a prosthesis under normal use conditions. Able body participants were used to test the system. Results show the sensors' ability to greatly enhance grasping fragile objects while also helping prevent object slip. The compliant nature of the sensors enables users to more confidently pick up and move small,fragile objects, such as foam peanuts and crackers. Without sensors and tactile feedback, users had a higher likelihood of breaking objects while grabbing them. The addition of sensors reduced this failure rate, and the failure rate was reduced even further with the implementation of control algorithms running in real-time. The Slip Prevention strategy was also shown to help reduce the amount of object movement after a grasp is initiated, although the most benefit comes from the compliant nature of the sensors.

Reflex is the first closed-loop tactile feedback system with multiple control strategies that can be used on a prosthetic hand to enhance grasping functionality. The

ABSTRACT

system allows one to switch between Contact Detection or Slip Prevention control strategies, giving the user the ability to use each control as needed. Feedback from the textile sensors directly to the prosthesis control unit provides valuable information regarding grasping forces. This research aims to help improve prosthetic technology so that one day amputees will feel as if their device is a natural extension of their body.

Primary Reader: Nitish Thakor, PhD

Secondary Reader: Youseph Yazdi, PhD

Secondary Reader: Albert Chi, MD

Acknowledgments

Thanks to Dr. Nitish Thakor for his time, support, and guidance over the past year and a half. His valuable input has helped bring this project to where it is today. A special thanks to Drs. Albert Chi, Youseph Yazdi, and Marin Kobilarov for taking the time to read and review this monstrous document. A very special thanks to Megan Hodgson and James Su for their help with all things software and hardware related, to Martin Vilarino for his optimism and willingness to help at every turn, to Dr. Rahul Kaliki for his insight regarding sensor designs and the experimental protocol, to Michelle Zwernemann for her help with the IRB process, and the rest of Infinite Biomedical Technologies for their support and good cheer during the course of my masters program. Thanks to Wang Wei Lee for his help with designing and constructing the early prototypes of the tactile sensors. Thanks to Ayushi Sinha for her help with all things LaTeX related. This work would not have been possible without the help of those listed as well as the countless others who have helped along the way.

Dedication

This thesis is dedicated to my parents (Cindy and Steve) who managed to teach this hard headed boy the value of dedication, patience, and hard work, to my siblings who somehow manage to be even more goofy than myself, and to all of those close to me who always manage to put a smile on my face and remind me that there is indeed a world outside of these laboratory walls.

Contents

List of Tables

List of Figures

Chapter 1

Introduction

This chapter provides an introduction to the aims of this document and the motivation behind the contained research.

1.1 Overview

The human hand is an exquisite, sensitive part of our bodies that has the ability to comfortably hold a vast number of objects. Whether the object is large and robust or small and fragile, our dexterous hands play an important role in interacting with objects on a daily basis. Unfortunately for upper limb amputees, this sophisticated level of functionality is not currently available in commercial prostheses. Although large efforts have been made to solve issues pertaining to objects slipping and deforming while grasped by a prosthetic hand, there is still a major barrier between current

prostheses and the quick, reliable functionality of a natural hand. Even though it is not an immediate possibility to simply reconstruct a fully functioning human hand out of a prosthesis, steps can be taken to enhance an amputee's daily life by making the use of their prosthesis a more natural experience.

The multi-fingered dexterous hand, capable of performing a vast number of highly complicated movements, has enabled humans to communicate and interact with their surroundings since the existence of mankind. The motor and sensory cortices of our brain are devoted to analyzing the sophisticated sensory inputs - such as touch, pain, temperature, and proprioception - we experience from our surrounding environment. These multifarious inputs are then taken to turn the human arm and hand, made up of over 40 individual muscles, into a well-oiled machine of precision and functionality [1].

1.1.1 Prosthesis Attributes and Drawbacks

While advances in prosthesis control can be expected to greatly enhance functionality and reliability for amputees across the globe, there are still major issues pertaining to grasping and holding objects with a bionic hand. Prostheses that are myoelectric controlled typically use a proportional EMG control scheme to open and close the hand [22, 23]. In other words, an amputee can control the amount he or she opens and closes the device based on the magnitude of muscle flexion or extension contractions. EMG signals can be rather noisy and require complex filtering techniques which often induce a noticeable time delay between when an amputee wants to control

his or her prosthesis and when the device actually responds. Because of this delay, there is an inherent risk of accidentally dropping or breaking grasped objects [24] . Another contribution to this problem stems from the lack of proprioceptive feedback. It is often hard for the amputee to know, with certainty, how well an object is grasped by his or her prosthesis. Extensive research has sought to rectify this issue through solutions such as tactile feedback and even direct neural feedback [25, 26]. As cutting edge as these ideas may seem, there is still a downfall. Even by directly stimulating the peripheral nervous system with information related to the amount of applied prosthesis grip force, there will still be a time delay that is longer than the response of an actual human hand. The reason is that these types of feedback are still forced to depend on the time delays linked to filtering sensors and EMG signals [24]. Humans tend to be very good at detecting if an object is about to slip out of their hands. We have an incredible number of mechanoreceptors on our fingertips that quickly send dynamic information regarding loads applied during a grasping task [27]. We are also able to estimate the friction at the object interface, which in turn allows us to control the amount of force we apply to the object itself [28] . The challenge remains to translate the high functionality of the human hand, in terms of grasping functions, into a useful prosthesis for amputees. Surveys of upper limb amputees have shown that the enhanced ability to prevent grasped objects from slipping as well as becoming deformed or breaking is an area that could use improvement [29, 30]. Detecting and preventing slip is an extremely challenging problem that has been researched for

many decades [24, 31–36]. While there are a great number of issues that create a barrier between modern upper limb prostheses and natural human arms and hands, solving the problem of object slip and deformation in prosthetic hands would be a significant leap forward for both prosthetic and robotic technologies across the world.

The i-limb^{TM}(Fig. 1.1a) by Touch Bionics (Livingston, UK), one of the more advanced commercially available hands for upper limb amputees, has helped bridge the gap between prosthetic devices and real human hands [2]. Current bionic hands can perform a range of functional grips and tasks, such as a key grip, precision grip, a power grip, and even an index point [37]. For a myoelectric prosthesis, these different modes can be achieved through a series of individual muscle contractions or co-contractions of two muscles. For a trans-radial upper limb amputee, the two muscles available to act as inputs to a myoelectric device are typically the flexor and extensor muscles of the forearm. One of the major challenges of upper limb prostheses is quickly and reliable changing between different grip modes. The entire system is under actuated in the sense that the user has, typically, only two inputs to control a wide range of commands. This has led to novel solutions such as the **morph**^{TM}device by Infinite Biomedical Technologies (IBT) (Baltimore, USA) (Fig. 1.1b) that can easily change grip modes via RFID technology [3].

Ground breaking research, particularly from Paolo Dario and others at Scuola Superiore Sant Anna (Pisa, Italy) as well as Shadow Robot Company (London, UK), has led to the design and development of the anthropomorphic dexterous ShadowHand^{TM}(Fig.

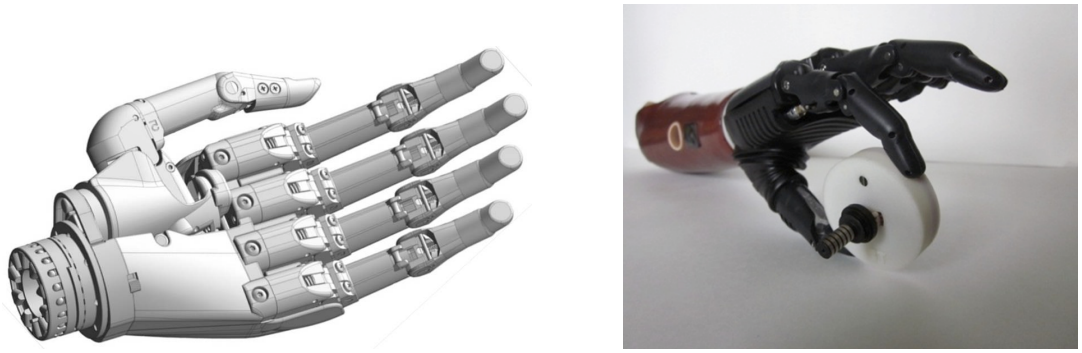

(a) (b)

Figure 1.1: State of the art upper limb prosthetic devices: (a) the i-limb hand by Touch Bionics [1, 2] and (b) IBT's **morph** [3]

1.2) [4,5]. While this hand is commercially available and is being used by the National Aeronautics and Space Administration (NASA) as well as Carnegie Mellon University for research purposes, the hand is not meant for use in everyday myoelectric upper limb prostheses because of its extremely steep costs [5]. However, the development of the ShadowHand is an exciting leap for prosthetic technology because of its high dexterity. It was designed by Shadow Robot Company to move as a typical human would with four fingers that contain two one-axis joints connecting to the distal, middle, and proximal phalanges as well as one universal joint that links the finger to the metacarpal. Although the thumb contains only a one-axis joint between the distal and proximal phalanges, there is a joint at the bottom of the metacarpal as well as one between the metacarpal and the thumb, which allows the hand to mimic palm-curling movements. An extra one-axis joint on the smallest finger's metacarpal further en-

Figure 1.2: ShadowHand [4]

hances this curling movement [4,5,38]. The addition of wrist joints allowing for flexion and extension gives the ShadowHand a total of 20 degrees of freedom stemming from the 24 joints. The hand itself is controlled by a complex array of 40 actuators that utilize airflow to command the joints [4, 5, 38]. Although the translation of human hand movements into an anthropomorphic robotic hand, via the ingenuity and hard work of countless researchers, has become a reality, there is not much commercial practicality for the ShadowHand itself as upper limb prosthesis despite its extremely functional capabilities because of its high costs. The consumer needs a prosthesis that is durable, affordable, and functional.

Historically, weight has been a major drawback for bionic hands but current advances in biomaterials has helped to significantly reduce this barrier [1]. Although

many prosthetic hands now have similar weights to a natural hand, the residual limb of an amputee undergoes additional stress and torque in order to support the terminal device that is only connected to his or her body through a hard-shelled socket. In addition, improvements in battery life have given way to increased efficiency as well as time between re-charging a prosthesis, which has been especially beneficial for amputees who wear a prosthesis for at least 8 hours a day [39]. Table 1.1 compares current prosthetic hands available today.

1.1.2 Current Solutions

In an effort to solve the issues with prosthetic hand grasping, researchers have resorted to a variety of sensors and complex algorithms to help prevent unnecessary failures in grasping functions. The aforementioned ShadowHand utilizes sensitive tactile force sensors on the tips of each finger (Fig. 1.3). This array of 36 sensors can very accurately determine the amount of force applied by each finger on the hand. However, because of the high costs of this hand and precision sensors, it is not a viable option for amputees. The use of force sensitive resistors is one of the most common approaches to diminishing the problem of object slip and deformation. The constant feedback from the force sensors allows researchers to measure the amount of force applied during a grasping task. With this knowledge, one could reduce the hands motor speed to more delicately grasp an object.

The Ottobock (Berlin, Germany) SensorHand Speed^{TM}is a commercially available

Table 1.1: Comparison of commercial prosthetic hands

Device Name	**Manufacturer**	**Weight**	**Grips**	**Cost**	**Max Grip**	**Features**
bebionic	RSL Steeper	557g	14	$30,000	140 N	Proportional speed control [40]
i-limb Ultra	Touch Bionics	515g	24	$50,000	100 N	Automatic thumb rotation [2]
MC Hand	Motion Control	609g	1	$15,000	98 N	Safety release fingers [41]
SensorHand Speed	Ottobock	460g	1	$18,000	100 N	Double speed [42]
Dexterous Hand	Shadow Robot	41200g	32*	$120,000	80 N	Human kinetics [5]
Luke Hand	DEKA	3600g	6	$100,000	80 N	Multiple control inputs [43]

*20 degrees of freedom and 24 joints, mimics human movement

Figure 1.3: ShadowHand tactile fingertip sensor [5]

prosthesis that uses a three-axial force sensor on the end of the thumb to allow for autonomous force control [44,45]. This sensor determines when the ratio of normal to tangential force (see Fig. 2.3) is unfavorable, outside of a predetermined threshold, between the hand and object interface and automatically increases the applied grip force. This algorithm is useful in that it tries to predict when an object might slip accidentally and compensates by tightening the hand. Essentially, if the tangential force becomes too large then the system assumes that this indicates an increase in shear force, which is related to a slipping object. The downside to this method is that it can inadvertently increase the force too much, which could potentially break the object. Another issue is that the coefficient of friction between the hand and object dictates the tangential forces, thus some object textures and surfaces can cause the SensorHand Speed's grip control algorithm to misidentify instances of slip.

Engeberg et al have taken the principles of preventing slip through applied force

analysis and engineered a novel proportional derivative force controlling system to further enhance the grasping capabilities of a bionic hand [18, 24, 36, 46–51]. The first approach taken was to implement a biomimetic prosthetic hand controller that changes grip force based on the angular acceleration of the wrist, the grip force derivative, as well as the actual applied grip force. The grip force derivative is the rate of change of the tangential force component. Large changes in the grip force derivative are associated with quick changes in the tangential force, indicating object movement. Previous work has shown the benefit of using grip force and grip force derivative feedbacks as a way of controlling the prosthesis grasping functions [46, 48]. In [36], a FlexiForce$^{\text{TM}}$by Tekscan (South Boston, USA) force sensitive resistor was placed on the thumb of an Ottobock myoelectric hand and a potentiometer that measured rotational position of the terminal device relative to the arm was attached to the wrist rotating unit. In addition, a gyroscope was added to the wrist to determine the wrist's angular velocity. The voltage input, E_H, into the hand itself can be expressed by the following equation:

$$E_H = K_P(F_d + K_W \left|\frac{d\dot{\theta}}{dt}\right| - K_N D \left|\frac{dF}{dt}\right| - K_N F) \tag{1.1.1}$$

where F_d is the desired grip force, $\dot{\theta}$ is the angular velocity of the wrist, F is the measured grip force, and the K values are all proportional constants of each component. To test the experimental set-up, upper limb amputees were asked to grasp an aluminum object and then rotate their wrist unit. The voltage input to the hand was continuously monitored to adjust for any object slippage that may occur [36].

The results show that by measuring wrist movement, grip force derivative, and applied grip force, the hand itself can be programmed to automatically compensate for changes due to the users movements. This allows the user to move his or her prosthesis without having to consciously monitor the amount of applied grip force on the object being held. Overall, this is useful in that it allows the hand to compensate for potential incidents of object slip without additional input from the user.

One major issue discovered with the previous solution was the relatively long delay time between when the hand detected a slip situation and when the motors were actually able to compensate for the applied grip force. This being an obvious issue, a new slip prevention control scheme was evaluated [24]. Instead of band-pass filtering the force derivative in order to amplify high frequency vibrations that occur when a grasped object slides relative to the fingers, an integral sliding mode slip prevention algorithm was used to not only smoothly and quickly compensate for changes in grip force but to also reduce the amount of object deformation. Although this approach did not solve the time delay between slip detection and hand reaction, it did show that the deformation of a held object can be reduced by using an integrated approach. The integration approach assumes that there are two possible instances: when slip occurs and when it does not occur. Unlike the standard sliding mode slip prevention (SMSP) control system that often increases the amount of applied force in predetermined amounts when slip is detected, the integral sliding mode slip prevention (ISMSP) controller integrates the variation of the slip signal when slip is detected to create a

smooth increase in the applied grip force once slip actually occurs [24]. This steady and not excessive increase in grip force reduces the amount of object deformation that occurs. The results of this experiment show that the standard proportional derivative (PD) control scheme, like that used in the Ottobocks SensorHand Speed, as well as the SMSP control system deform objects more than the ISMSP [24]. The ISMSP provides a way to successfully reduce the occurrence of object slip while also reducing the amount of deformation, through smooth increases in applied grip force that the held object receives. This is especially useful for amputees who might have problems with breaking delicate and fragile objects, such as wine glasses. This is a huge step forward in upper limb prosthetic technology because it shows that systems can be made to more accurately model a natural human hand that doesn't exert anexcessive amount of force to hold an object in place.

1.2 Tactile Feedback

Humans use their hands on a daily basis for a wide variety of actions, such as gestures, extremely fine manipulations, and grasping objects. This versatile system relies on a complicated biomechanical structure that contains not only numerous degrees of freedom but a large number of sensitive receptors embedded in the skin, joints, and muscles. Extensive research has shown how our hands behavior changes in such a quick and seamless fashion to accommodate for our daily interactions [10,

52–57]. The functionality of our hands and fingers allow us to take full advantage of the surrounding environment, whether it be by performing fine movements to manipulate objects or determining the shape, weight, and material of an object. The mechanoreceptors in the human hand provide a closed tactile feedback loop, providing us with valuable information regarding our surroundings.

Upper limb amputees lose their ability to decode their surroundings via the approximately 17,000 cutaneous mechanoreceptors in the glabrous skin of the human hand [58]. Commercial upper limb prostheses do not provide a stable replacement for the tactile sensors lost due to amputation. Because such a large portion of humans daily living relies on the explorative role and motor skills of the hand, there is a pitfall when it comes to the psychophysical detection of objects through tactile sensing for upper limb amputees.

1.3 Force Sensor Technology

Highly precise contact force sensors that can be used with prosthetic hands in both compliant, low-force interactions, such as shaking hands, as well as determining when the state of a held object have been developed over recent years [6, 59]. This novel work has led to a bio-inspired anthropomorphic artificial hand that mimics the biomechanical features as well as the sensory system of a natural hand. The focus of the hand sensors specifically deal with the signals that pertain to grasping tasks

and control stability during a task, such as lifting or replacing an object. Overall, to mimic a natural hand, the bionic hand must be able to determine the contact and release between the fingers and an object, the release and replacement of an object to any given environment, and the slip that occurs between the fingers and object interface. The sensors used on the fingers of the bionic hand were made up of copper electrodes that wrapped around the phalanx (Fig. 1.4). These sensors were used to determine contact between the fingers and an object. In addition, three-axial force sensors were mounted on the fingers to monitor the amount of force applied at an object interface. The results showed that by implementing the force and contact sensors, the bionic hand was able to successfully perform grasping tasks and discriminate between different sections of the task while accurately compensating for changes that occurred at the finger and object interface. These developments are extremely pertinent to upper limb prosthetic technology, particularly as it applies to grasping functions, because it indicates the types of sensors capable of turning a dexterous bionic hand into a more fluid and natural functioning machine.

Work has led to more advanced phalanx sensors in an attempt to make prosthetic hands even more lifelike [59]. A particular study showed the effects of sensor placement and response due to low force social touching interactions, particularly shaking hands. The idea is that with lifelike compliant sensors, an amputee would no longer feel like his or her prosthesis was a rudimentary replacement for a lost body part, but rather a dynamic extension of his or her own body. The results suggest that a highly

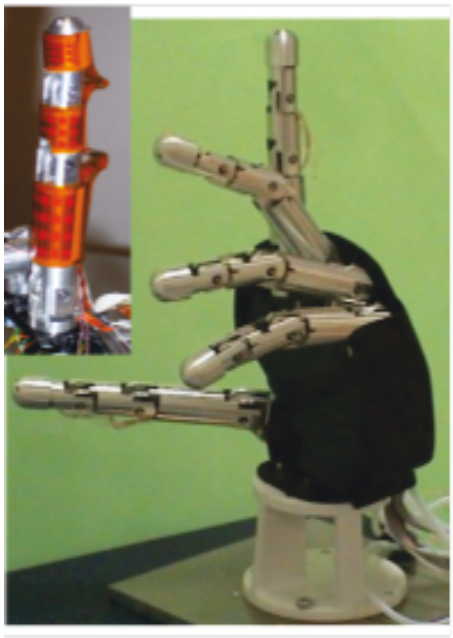

Figure 1.4: Bionic hand and contact sensors [6]

precise array of sensors on a prosthetic hand is the gateway to the next generation of upper limb prostheses. This has spurred an even more in depth development of novel tactile feedback sensors that can have applications in prosthetic technology [59].

Loeb et al from the University of Southern California have also put forth tremen-

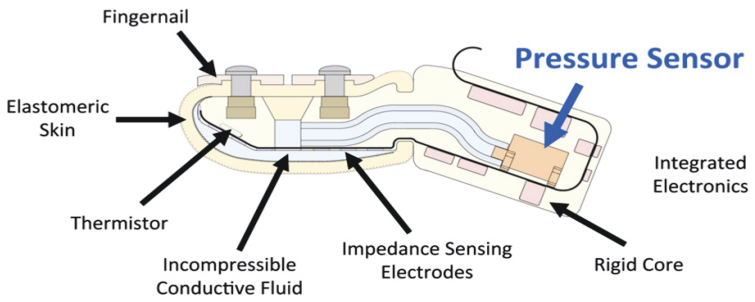

Figure 1.5: BioTact fingertip sensor [7]

dous efforts in solving the problems with object slip and deformation [7, 34, 60, 61]. In particular, they use simple control algorithms combined with state of the art fingertip sensors, as seen in Fig. 1.5, known as the BioTac^{TM} [7, 34, 35, 60–62]. The BioTac is the most advanced and functional fingertip sensor commercially available for prosthetic hands. It has the capability of accurately identifying over 200 hundred different materials based solely on the micro-vibrations between the fingertip and a surface. When the fingers move over a surface, micro-vibrations are generated; each type of material produces possesses different texture qualities, which can be detected by the BioTac through the vibrations. This gives way to an ultra-smart fingertip that can classify more materials than the typically human being [7, 62]. In addition to detecting micro-vibrations, the BioTac uses a thermistor to detect temperature as well as impedance sensing electrodes, a conductive fluid, and a pressure sensor to determine applied forces. It is made up of a rigid bone-like core that is covered with a silicone skin. The space between the skin and the bone is filled with a liquid that gives the entire sensor a biomimetic compliance that is similar to natural fingertips [35, 63]. The skin itself can be replaced and contains no electronics, making the sensor robust enough to be used in an upper limb prosthesis. Contact and forces can be measured form both the pressure sensor as well as the impedance electrodes. This multi-faceted sensor has proven to take upcoming prosthetic technology a step further. The most recent study with the BioTac involves a novel contact detection algorithm to allow amputees to handle delicate objects while reducing the risk of breaking them [35].

A prosthetic hand is equipped with the BioTac sensors and an algorithm is used to reduce the motor gain, essentially making the hand less sensitive to the user's EMG signals, once contact has been detected between an object and the hand itself. By taking this approach, the user now has more control over small increments of force adjustments, which reduces the risk of inadvertently crushing an object by applying too much grip force. The results showed that using the contact detection algorithm, amputees were not only better at picking up and not breaking fragile objects such as egg shells and packing peanuts but they were also more comfortable performing these tasks than without contact detection [35]. In addition, it was discovered that over 75% of the improvement over the subject's prosthesis was due to the physical compliance of the BioTac itself [35]. Although the contact detection further enhanced the amputee's ability to handle delicate objects, the biomimetic and compliant fingertips were the major reason behind the high levels of improvement and functionality.

1.4 Thesis Objectives

This work focuses on utilizing tactile input to more efficiently handle objects by upper limb amputees who use dexterous prosthetic limbs. Sensor development builds upon the idea of recreating a multi-fingered dexterous hand that mimics the human sensory system. Not enough emphasis has been placed on creating a low cost system that can interface with any upper limb prosthesis. Specialized anthropomorphic

prosthetic hands are too expensive for everyday use by an upper limb amputee. The costly solutions that are on the market today prevent users from readily accessing a prosthetic system that utilizes tactile information to enhance its functionality. There is a need to provide a functional solution that is appealing to users of all economic statuses.

Currently there is no solution that can interface with a variety of prosthetic hands to make use of tactile information. A simple cosmesis, such as one made from a silicone rubber covering for a prosthetic hand, with the ability to detect forces at different parts of the hand via basic sensors can relay information regarding the interface between a prosthetic hand and any objects that it interacts with. Modern prosthetic technology has made enormous leaps in the past decade, but there is still a gap between connecting an amputee and his or her prosthetic device with the surrounding area. By providing a cheap covering that can be donned and doffed for practically any prosthetic hand, amputees will morph their terminal device from a sophisticated yet 'tactilely' senseless extension of their body to a more fluid and natural component of their daily lives.

The low cost design of this device will allow amputees to utilize tactile feedback to more securely grasp and handle objects while not being burdened by any major fiscal implications that are typical of prosthesis enhancement. Complex and highly accurate fingertip sensors, although functional, are not the best option for solving this issue. Instead, a simple covering that can measure grasping forces is more practical

for creating a closed tactile feedback loop.

The current methods and solutions described previously have all shown ways to improve the problems upper limb amputees are having while grasping, holding, and handling objects with their prosthetic hand; however, there are only a few options for commercially available hands and sensors that can be used to help resolve these issues. The hardware that is currently available can often be too expensive or not practical enough for everyday use. There is still a need to design and develop sensors that are functional like the BioTac but are also cheap and robust enough for everyday use.

In addition to cost, there is inevitably a relatively large delay between when a sensor detects slip or excessive object deformation and when the hand can adjust. It has been reported that the natural human hand takes a mere 70 ms to react to changes of a held object, whereas current methods can take at least 10 times longer with a reaction time closer to 750 ms - a noticeable delay [60, 64]. This lag is due to the band-pass filtering that is required for processing signals from the sensors as well as the calculations and adjustments that must be made within the control algorithms. To resolve this issue, one could bypass the often-complex algorithms of hand control and use the sensor feedback as an input directly to the hand motors. However, a large portion of the delay time can be attributed to the hand motors themselves. While the internal design of prosthetic hands is beyond the scope of this research, it would benefit amputees if quicker, more precise motors were implemented in bionic hands.

Given the current findings, it would benefit upper limb amputees, particularly for grasping and handling tasks, if the tips of their terminal devices implemented a more lifelike compliance, such as that demonstrated by the BioTac. Compliant fingertips, even without any type of tactile feedback, could make it easier for users to grasp and hold objects such as a coffee mug or even a toothbrush. This in itself would be a great leap forward for commercial upper limb prostheses because it would allow amputees more freedom and confidence in the daily activities.

Combining grip force feedback with robust yet compliant fingertip sensors would create a system that is highly capable of detecting and preventing object slip or accidental breaking. However, there are still issues regarding the accuracy and reliability of current sensors.

Chapter 2

Sensing and Control

This chapter provides a detailed look at current tactile sensing technologies as well as the algorithms implemented in robotic control methods. In particular, how these technologies are used for upper limb prosthetic devices is investigated.

2.1 Current Sensors

There are countless uses for commercial pressure and force sensors. Applications can include gait analysis, brake pad design, evaluating hip replacements, posture studies, spring design, orthodontic evaluations, footwear research, bed monitoring, muscle activity, robotics and prosthetics technologies, and even seat belt design, just to name a few. Because force and pressure readings can provide crucial information regarding a system and its function, there are a multitude of sensors capable of

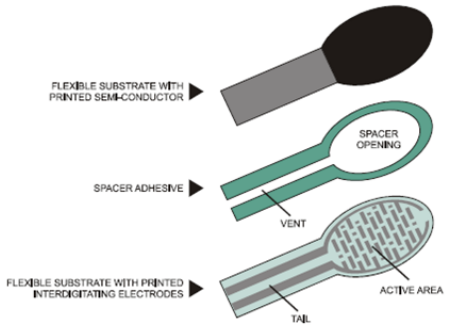

Figure 2.1: Force sensitive resistor construction [8]

detecting this information.

2.1.1 Commercial Sensors

2.1.1.1 Force Sensitive Resistor

Commercial sensors are common and readily available. A basic force sensitive resistor (FSR), a simple device with crossing conductive layers that changes resistance based on the amount of applied force, can act as a functional force sensor. Companies such as Interlink Electronics (Camarillo, USA) and Tekscan (South Boston, USA) make a variety of force and pressure measuring sensors. Figure 2.1 shows the construction of a basic FSR and Fig. 2.2 shows a FlexiForce [8, 9].

Engeberg et al used a simple FlexiForce FSR to monitor the applied grip force during prosthetic wrist rotations. The feedback controller implemented makes adjustment to the angular wrist velocities of the prosthetic hand [36]. Another recent development in upper limb prosthesis feedback came from the Functional Neural In-

Figure 2.2: Commercially available force sensitive resistor, FlexiForce by Tekscan [9].

terface Lab at Case Western Reserve University in Cleveland, OH. A single FSR placed on the pointer phalanx of a prosthetic hand allows force measurements while pulling stems off cherries. When activated, the force sensor triggers a vibrotactile motor which allows the user to know if he or she is grasping an object [65].

For robotic or prosthetic grasping applications, it is desirable to maintain a high level of sensitivity while also utilizing a relatively large sensor operating range. It is hard to generalize human grasping forces, but it has been reported that typical grasping forces for a precision grip are between 1 - 50 N for small sized objects (Fig. 2.3) [10]. Obviously, grip force required to stably hold an object is dependent on object weight, size, material, and shape; however, for grasping in upper limb prosthetic devices the force range of interest is 0.5 - 20 N [18]. Many upper limb prosthetic hands are delicate machines that are limited in the grasping force. For this reason, it is favorable to use a sensor that can easily detect small changes in grip force.

2.1.1.2 Polyvinylidene Fluoride

Polyvinylidene fluoride (PVDF), a stable thermoplastic fluoropolymer, has piezoelectric properties and can be manufactured into tactile sensor arrays, strain gauges,

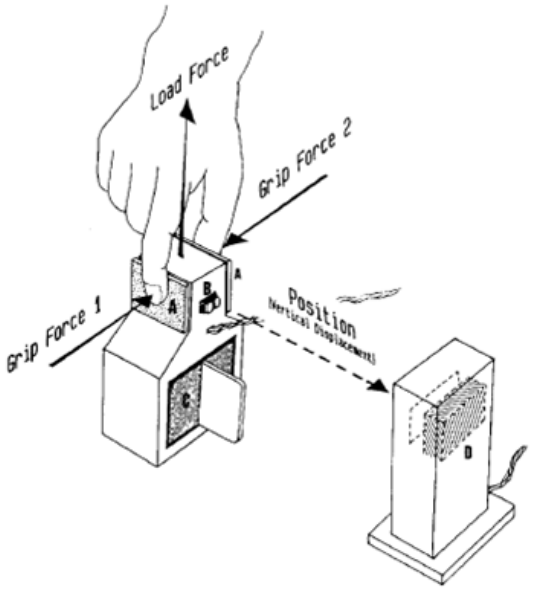

Figure 2.3: Diagram showing grip force (normal to object surface) and load force (parallel to movement of object) [10].

or even audio transducers. These piezoelectric sensors are designed by sandwiching a compression film between two PVDF films. The softness of the center film determines the sensitivity and the operating range of the sensor. The bottom layer is activated by an electrical pulse and creates mechanical contractions in the PVDF film acting as a receiver. This layer reacts to the mechanical changes with a time varying voltage. Typically, this signal is then amplified and fed into a demodulator that compares the output voltages of the two plates. This is shown in Fig. 2.4.

A PVDF tactile sensor was placed inside a silicon rubber skin in [66] to act as a slip sensor. Movement across the outer surface of the rubber skin created vibrations, which were picked up by the internal PVDF sensor. However, the use of an accelerometer

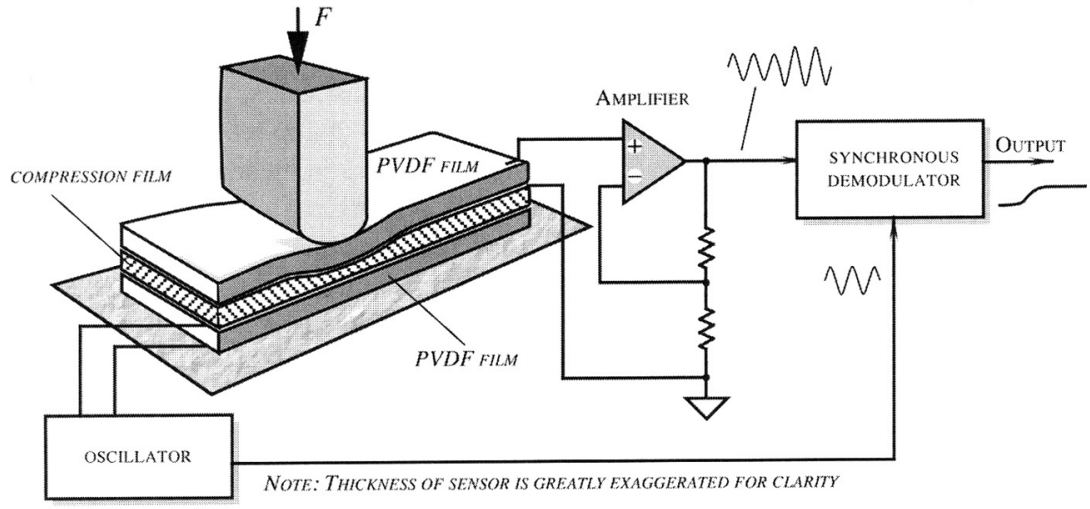

Figure 2.4: An active PVDF tactile sensor [11].

as well as tangential and normal force sensors was necessary to limit the slip of an object while controlling a multi-linked robotic finger [66].

2.1.1.3 Capacitive Pressure

Capacitive sensors consist of a plate capacitor, in which, the distance between plates or the effective area is changed by the applied force, which consequently shifts their relative position. Capacitive sensors can be made very small, which is ideal for dense sensor array that require dynamic measurements. This sensing technology is popular among tactile sensors based on microelectromechanical systems (MEMS) and microfabrication [67–69]. Capacitive tactile sensors are found commercially in products from Pressure Profile Systems and, more commonly, Apple's line of personal electronics [70, 71]. A study utilizing capacitive tactile sensors investigated the com-

pliance of lifelike prosthetic finger phalanges during low-force interactions, such as shaking hands [59].

2.1.2 State of the Art Sensing

While many tactile sensors are available on the market, there are often times when it is more desirable to create customized sensors depending on the intended use. A general FSR may not be appropriate for an application that requires multiple sensing areas over a small area while also minimizing costs.

2.1.2.1 Piezoresistive

Customized fingertips were prototyped by Cotton et al for a prosthetic hand [12, 31]. Fig. 2.5 shows the sensing layers of the fingertip. The piezoresistive layers act as strain sensor, which behave similarly to the slow adapting mechanoreceptive afferent units in the fingers. When a force is applied to the end of the structure (Fig. 2.5), the fingertip bends and the resistance of the piezoresistive layers change proportionally to the applied force [12, 31].

2.1.2.2 BioTac

As mentioned in Section 1.3, the BioTac (Fig. 2.6) from the University of Southern California and Syntouch (Los Angeles, USA) leads the way in terms of sensor technology and functionality in an integrated fingertip for robotic hands. The BioTac

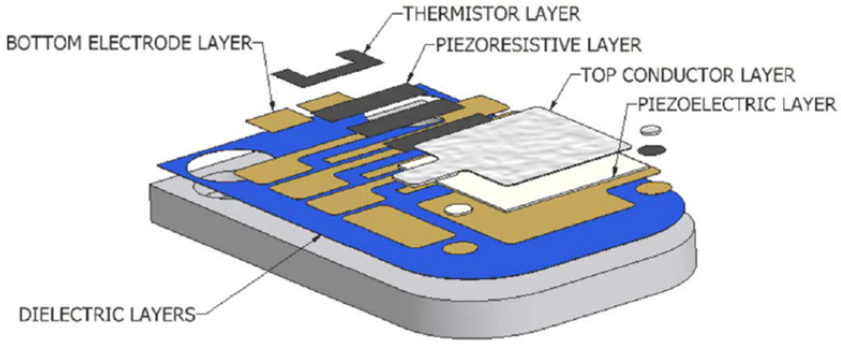

Figure 2.5: The printed layers used to create a fingertip with piezoresistive sensing [12].

is made up of a compliant outer rubber layer that houses internal conductive fluid. A rigid core gives the fingertip its shape. The impedance changes of the internal fluid, detected by electrodes, correspond to the amount of force on the BioTac [7]. The pressure sensor inside the BioTac is capable of detecting vibrations from surface textures, thus giving the device an added element of functionality. The cost of an individual BioTac sensor is $5,000, not including the materials required to integrate the sensors to an existing prosthesis [62]. The device itself is at the leading edge of sensor technology, but its high costs make it a very expensive solution to an already expensive prosthesis.

2.1.2.3 TakkStrip

Designed in the Harvard Biorobotics Lab (Cambridge, USA), the TakkStrip (Fig. 2.7) consists of barometric sensor chips coated in polyurethane elastomer, which act

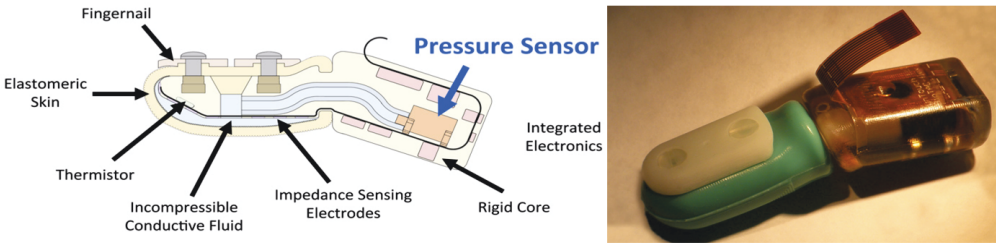

Figure 2.6: The BioTac from Syntouch [7].

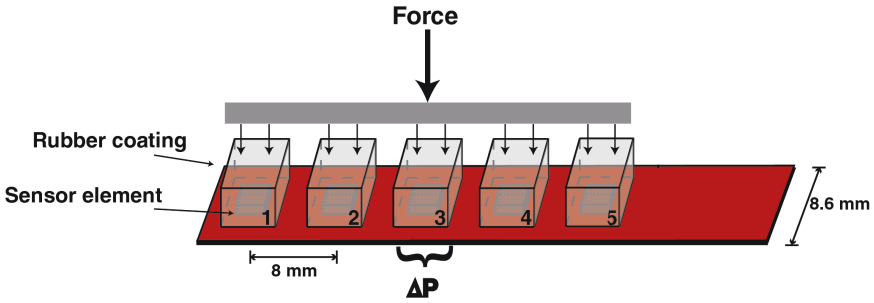

Figure 2.7: Sensor layout of the TakkStrip.

as highly sensitive (0.01 N) pressure sensors [72, 73]. Targeted for use with robotic grasping tasks, the sensors are robust in nature thus allowing for operation in a wide variety of environments while maintaining sensitive and accurate measurements. The TakkStrip is used in conjunction with OpenHand project at Yale as well as in a recent study in which it was shown that the sensor is capable of detecting grasped object movement within a prosthetic hand [74, 75]. Although it can accurately detect pressure changes that are characteristic of an object slipping from the grasp of a prosthesis, the TakkStrip is greatly limited in its operating range as it saturates after an applied pressure of approximately 1 N. Thus, the TakkStrip is more useful for detecting small changes in applied grip force in low-force manipulations.

2.1.2.4 Modular Prosthetic Limb

The most advanced dexterous prosthetic arm is the Modular Prosthetic Limb (MPL), developed by the Applied Physics Lab (Laurel, USA) at Johns Hopkins University. The MPL is capable of human-like strength and dexterity with a neural interface for intuitive and natural closed-loop control. The arm uses more than 100 customized sensors that rely information regarding position, contact, torque, temperature, acceleration, drive voltages and currents, and force [13, 76]. The sensors in the hand are shown in Fig. 2.8. The extreme functionality of this device comes at a great financial cost, resulting in the MPL being used primarily for research and demonstrative purposes. While the progress made in prosthetics technology is realized through the MPL, it does not offer an everyday solution for enhancing upper limb prostheses.

2.1.2.5 Synthetic Skin Sensing

The past few years has seen a rapid development of exciting flexible, skin-like electronics. John Rogers from the University of Illinois at Urbana-Champagne showed the feasibility of integrating circuits on flexible sheets of plastic [77]. This, along with work from Takao Someya from the University of Tokyo, has led to electronic skin, illustrated in Fig. 2.9, that can be used for temperature or pressure sensing [14, 77]. This new technology shows promise in providing new ways of integrating sensors on robotic hands; however, there havent been any studies to show the functionality of this new electronic skin for tactile sensing in prosthetic hands.

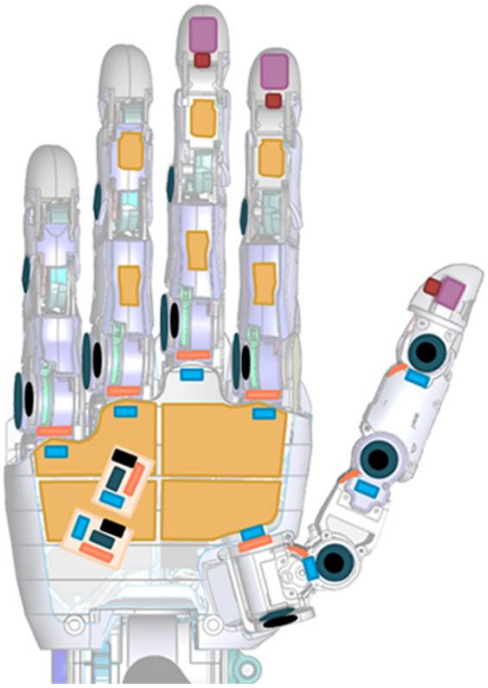

Key	Sensor	Number
	Absolute Position Sensor	21
	Contact Sensor	10
	Torque Sensor	14
	Joint Temperature Sensor	17
	3-Axis Accelerometer	3
	3-Axis Force Sensor	3
	Additional Sensors	41

Figure 2.8: Sensor placement on the MPL hand [13].

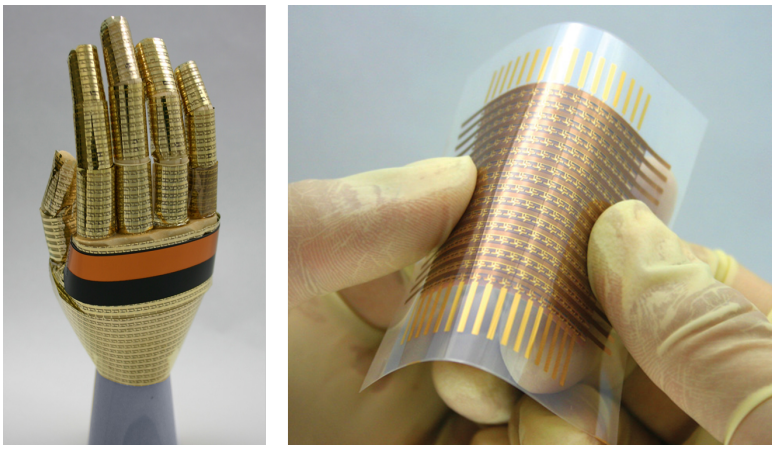

Figure 2.9: Flexible electronic skin [14].

Figure 2.10: Tactile array sensor with embedded PVDF strips [15].

2.1.2.6 Biomimetic Sensing

While biomimetic, an academic buzzword that is sure to capture attention, is just a fancy way of saying that something is modeled after a biological system, the Biomimetics and Dexterous Manipulation Laboratory at Stanford University (Stanford, USA) has developed a tactile sensing system that attempts to differentiate between object-hand and object-world interactions during a grasping or manipulation task with a robotic hand [15, 78]. With multiple sensing elements in a customized fingertip (Fig. 2.10), slip signals are analyzed to determine differences between object movement that is a result of outside perturbations, such as when inserting a key into a lock, or slip between the hand and the object, if the key slips out of the grasp [78].

2.1.2.7 Textile 'Neuromorphic' Sensing

The Singapore Institute for Neurotechnology (SINAPSE) at the National University of Singapore has recently developed flexible, textile sensors that are capable of measuring applied forces [16, 79]. Operating as a basic force sensitive resistor, criss-crossing conductive traces are separated by a piesoresistive fabric layer. These sensing elements, illustrated in Fig. 2.11, are in between two stretchy, fusible interfacing layers, a non-conductive elastic fabric to provide structure and shape to the sensors. A close collaboration between Johns Hopkins and SINAPSE has led to the design and development of customized textile sensors for prosthetic hands. The benefit from these sensors arises in their extremely low costs and customization. Multiple sensing elements can be placed to measure forces at the most pertinent places of a prosthetic hand. With a workable sensing area as small as 1 cm^2, a single sensor can hold numerous taxels, (taxel stems from a contraction formed from the words 'tactile' and 'pixel') depending on its overall size. Its 'neuromorphic' behavior can be attributed to the sensor's ability to respond to repeated stimuli, creating a spiking output. This output can be treated as the firing or afferent nerve fibers, which can be used for signal interpretation and analysis.

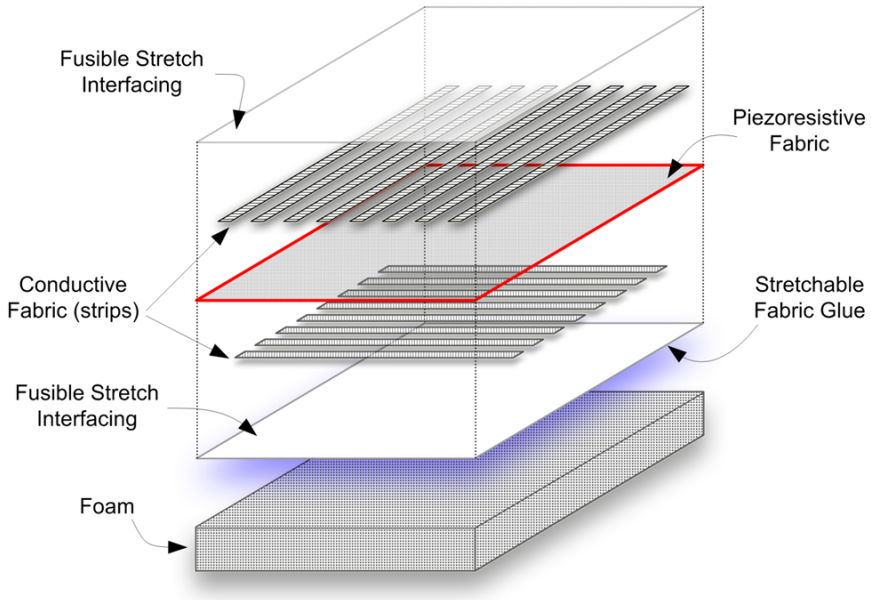

Figure 2.11: Components of the textile force sensitive resistor developed by SINAPSE [16].

2.1.3 Sensor Comparison

There are a multitude of sensors that are capable of detecting tactile forces during grasping or manipulation tasks. The high financial costs of the BioTac and other highly functional research sensors act as a deterrent when choosing an appropriate sensor for use on prosthetic hands. A comparison of sensors if shown in Table 2.1. These SINAPSE sensors served as early prototypes to the ones developed for this project.

Table 2.1: Sensor comparison

Sensor	Cost	Specifications					Limitations	Benefits	Manufacturer
		Operating Range	Sensitivity	Sampling Rate	Sensing Size	Type			
TakkStrip	$149	0 - 1.5 N	0.01 N	70 Hz	36 mm^2	Barometric pressure	Slow sampling, low range	Sensitive	TakkTile [73]
FlexiForce	$20	0 - 111 N	0.1 N	ADC dependent	71 mm^2	FSR	Not robust, can rip/break	Cheap, easy to get	Tekscan [6]
Interlink FSR	$6	0 - 10 N	0.1 N	ADC dependent	13 mm^2	FSR	Low range	Cheap, easy to get	Interlink [5]
BioTac	$5,000	0 - 50 N	36.5 Pa	ADC dependent	320 mm^2	Impedance and pressure	Expensive	Multi-modal sensing	SynTouch [62]
Textile Neuromorphic	$2	0 - 30 N	0.1 N	ADC dependent	9 mm^2	FSR	Low repeatability, poor spatial resolution	Customizable, flexible	SINAPSE [79]
Tekscan Grip	$19,000	0 - 50 N	0.1 N	850 Hz	6 $mm^2/_{sensor}$	FSR array	Not conformable	High resolution	Tekscan [6]
TactoLogic Pad	>$10,000	0 - 3 mN	40 mN/V	100 Hz	0.09 mm^2	Piezoresistive MEMS	Fragile, limited range	3-axis force sensing	TactoLogic [80]
FingerTPS	$6,000	0 - 20 N	0.2 N	40 Hz	100 mm^2	Capacitive	Low spatial resolution	Robust	Pressure Profile System [70]

2.2 Grasping Control Algorithms

Traditional methods for controlling a prosthetic hand are either through a body-powered cabling system, or through electromyography (EMG). A two-site control method is used to trigger opening and closing of the prosthesis. Advanced devices offer multiple grip patterns, such as a tripod (3-fingered) grasp, a power grasp, or even a finger pinch grasp [1]. However, an amputee is still largely restricted to using his or her EMG signals to open/close the hand or switch grips. The user must rely on visual information to properly grasp objects.

The task of grasping is a complicated issue that has been researched for many years; however the reach and grasp model can be broken into three sub-tasks: (1) the transport phase, which involves reaching for an object, (2) the contact phase where an object is grasped, and (3) the transformation phase in which the object is manipulated. A large portion of grasping control theory is focused on the first two phases, which has found applications mainly in industrial robotics. The third phase is particularly pertinent in controlling a prosthetic hand. Upper limb amputees use their prosthesis as an extension of their body, a tool for daily tasks; thus, a more biomimetic approach for control is essential. Two classes of problems predominate in the manipulation of grasped objects: (1) detecting object slippage by a sensor and (2) real-time force control of a gripping apparatus to grasp the object. The design procedures for creating a grasping controller can be classified into three major approaches: (1) model-based controllers [80–83], adaptive controllers [84, 85], and

controllers based on intelligent methods [17, 86–88]. Model-based controllers allow accurate finger positioning; however, this is only useful for repetitive industrial robotic grasping of the same object [89]. This is because the gripping apparatus is designed to grasp a target object in a specific way. Any change to the target object causes the model to breakdown.

2.2.1 Feedback Control in Industrial Applications

Work presented by Touvet et al utilizes multimodal sensory and motor information for positioning a mechanical hand and grasping an object with a control scheme that provides object-dependent and intelligent reach and grasp capabilities. The model, which is based on a multi-network architecture, incorporates multiple Matching Units (MU) that are trained by a statistical learning algorithm (LWPR). The MUs integrate the multimodal signal to provide estimations for object-dependent grasp configurations [90]. The use of the MUs provides a way to enhance reaching and grasping in mechanical hands by eliminating explicit calculations of inverse kinematic solutions and thus avoiding the need for an optimization process; however, it does not address the third phase of grasping tasks. Another strategy for grasping control involves finger motion planning while monitoring force signals to detect contact and grasping stability; however, it fails to address the issue of dynamic changes to an object after it is grasped [91]. One approach to detecting slip was presented by Goeger et al which classifies slip as a representation of peaks over a large range in the frequency

domain [92].

More recently, SynTouch used the BioTac sensor to help determine the firmness of fruit [7]. The idea is that agricultural applications can benefit from automating the process to determine if a fruit is ready for picking.

2.2.2 Prosthesis Feedback Control

Controllers that are designed to contact a variety of objects and shapes as well as focusing on how these objects are manipulated are better suited for the dynamic task of prosthesis grasping. Some controllers were developed to focus on grasping objects that are fragile and delicate, such as glass and fruits. Coupled with a PID controller, a particularly functional control algorithm adjusts the fingers of a mechanical hand based on fuzzy logic, as illustrated by Figs. 2.12 and 2.13 [17]. The fuzzy logic controller is based on results from research on human behavior during grasping tasks. The rules for the controller were derived from the center of distribution of the frequency response of a piezoelectric sensor signal in the fingers. It has been found that incipient slip occurs when the center of distribution lies around 5 Hz, whereas when greater than 8 Hz then the object is slipping. Similarly, stable grasp generates 2-3 Hz [93].

Compared to a standard proportional-integral-derivative (PID) controller, the fuzzy logic controller response time was much quicker while also reducing the maximum amount of grasping force. A PID controller requires adjustment of gains with

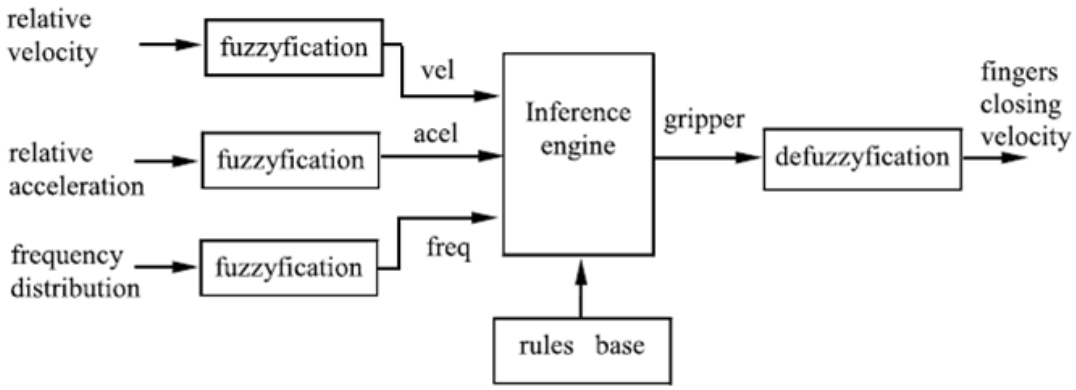

Figure 2.12: Structure of the fuzzy logic controller [17].

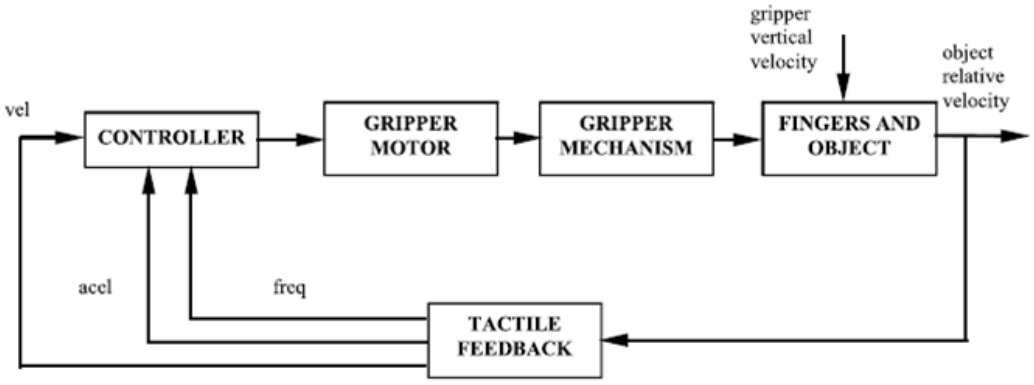

Figure 2.13: Block diagram of gripper control from Glossas et al [17].

every grasping task whereas the fuzzy logic controller does not require any changes for any given grasping task, thus making it ideal for grasping delicate and sensitive objects without requiring knowledge of the objects weight, size, or shape.

Other controllers use learning algorithms based on artificial feed forward neural networks that adjusted the grasping control scheme after detecting instances of slip [94]. After learning when slip occurs, the model is able to adjust how to grasp a cylindrical object to prevent future slip. This work validates the use of neural networks in controlling grasping tasks in anthropomorphic hands, but it is limited to grasping only one object of a particular shape and size while capable of learning only after slip has already occurred [94].

Another proposed prosthesis controller uses a derived force vector to determine object movement across a hand. The controller runs an optimization process to minimize the force applied across the entire hand [95].

Control strategies to intelligently close fingers on a robotic hand have been investigated [96]. This controller uses a family of Lagrange's equations of motion to express the dynamics of robotic fingers to restrict contact to certain parts of the fingers in order to improving grasping. Essentially, sensory feedback provides information regarding what parts of the robotic hand are making contact with an object, the controller compensates by shifting the hand in a way that distributes the grip forces appropriately so that the object is supported in a stable manner. However, this type of control is impractical for use on commercial prosthetic hands because it

would require changes in the mechanical design of the prosthesis.

The most closely related work in terms of hand grasping control for an upper limb prosthesis has been developed by Engeberg et al. In [18], a sliding mode slip prevention (SMSP) controller, as outlined in Fig. 2.14, offers a robust design for grasped object slip prevention without requiring any knowledge of the coefficient of friction μ, a parameter that is utilized in commercially available prosthetic hands that implement slip prevention algorithms [18, 24, 36, 42]. In the control design, the derivative of shear force between a grasped object and a hand is taken to amplify vibrations that occur during slip. A standard proportional-derivative (PD) controller for slip prevention that feeds back the force signal will increase the applied grip force when an object is lifted because there is an increase in force from the object, even though slip does not occur. This causes unnecessary grasping forces that could potentially destroy the object. On the other hand, the SMSP controller increases applied grip force in discrete, predetermined amounts only after slip occurs. The problem with this approach is that the grasped objects may be deformed more than necessary [18]. There is also the potential that the grip force increments are inadequate or too small; especially for situations where the hand and grasped object interface has low friction.

The sliding mode slip prevention controllers presented by Engeberg et al introduced a slip-dependent state, e_s, into the error equation

$$e = x_1 D - x_1 - e_s \tag{2.2.1}$$

The slip-dependent state depends on whether or not the grasped object has slipped;

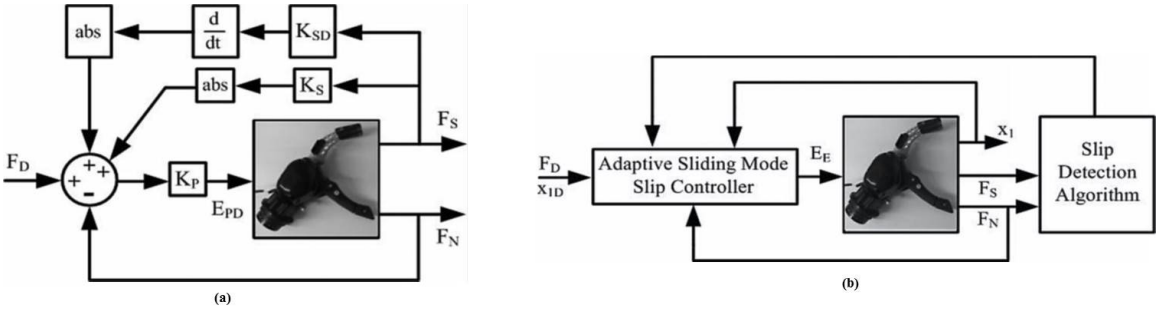

Figure 2.14: Diagram of (a) PD and (b) sliding mode shear force feedback slip prevention control algorithms [18].

this creates an error state that is a function of whether or not the grasped object has slipped. When slip is detected by the SMSP controller the grip force may increase very rapidly, thus making the controller too aggressive with the possibility of excessively crushing an object [18]. To help remove the issue of unintentionally crushing grasped objects that slip, one can redefine the slip-dependent state as

$$e_s = C \int \gamma dt \tag{2.2.2}$$

where γ has a value of 0 if slip does not occur and a value of 1 if slip does occur. The definition integrates the slip signal when detected so that the applied grip force increases smoothly, thus theoretically reducing the amount of deformation that occurs while preventing object slip. Because slow, gradual adjustments are made to correct for prosthesis grip, delicate objects can be manipulated with a lower risk of breaking.

Each of these control algorithms provide ways of improving prosthesis grasping. While each of these methods show some benefit for an amputee, none have been implemented as part of a real-time, closed-loop tactile feedback system for human

use. In some cases, complex algorithms can slow down the prosthesis control unit, thus reducing response time of the prosthesis. The goal of this work is to implement a control method that does not require excessive computational effort while also utilizing tactile feedback in a closed-loop fashion.

Chapter 3

Sensor Design and Characterization

This chapter details the design, modeling, and characterization of the sensors used for this closed-loop tactile feedback system. The most important aspect of utilizing tactile information on a prosthetic hand is ensuring that the sensors used to capture this valuable information are suitable for the application. The goal is to develop low cost sensors that have the ability to measure applied forces during grasping tasks with a prosthetic hand. The sensors must be functional and easily customizable so as to be placed on any prosthetic hand.

3.1 Design Considerations

Before tackling the challenge of creating a system that is functionally similar to the reach and grasp strategy found in healthy humans as mentioned in Section 2.2, it is necessary to understand the underlying principles that make up these controls. In particular, it is useful to investigate the internal planning and sensing mechanisms during grasping; however, it should be noted that the same structure and strategies found in human grasping do not necessarily offer the best solution for improving grasping through tactile feedback in prosthetic or robotic systems.

3.1.1 Human Grasping

The motor and sensory cortices of our brain are devoted to analyzing the complex sensory inputs, such as touch, pain, temperature, and proprioception, we experience from our surroundings. These multifarious inputs are then used to turn the arm and hand, made up of over 40 individual muscles, into a well-oiled machine of precision and functionality [1]. This versatile system relies on a complicated biomechanical structure that contains not only numerous degrees of freedom but a large number of sensitive receptors embedded in the skin, joints, and muscle that make up the pathways for tactile sensing [10, 52, 57].

Reaching for an object requires a breakdown of a complex spatial problem. Information regarding limb and eye position as well as the target location need to be

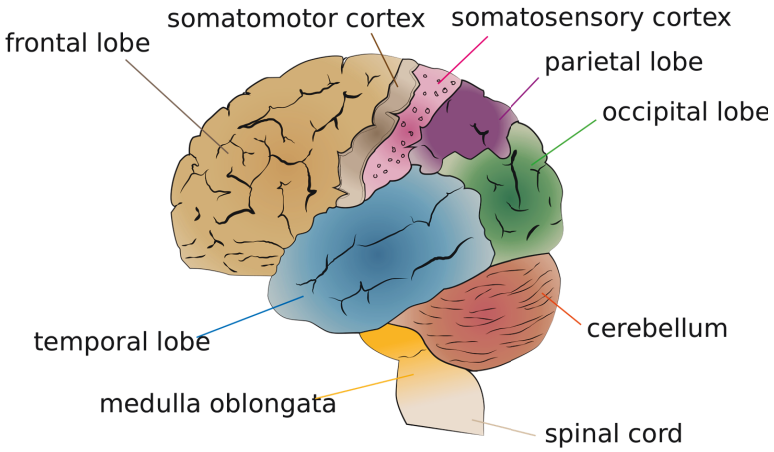

Figure 3.1: Sections of the human brain [19]

integrated into a common spatial representations [97]. Say that a person sees an object he or she wishes to reach out and pick up off a table, such as a glass of water. From a high level neurophysiological perspective, the posterior parietal cortex receives information from the visual cortex in the occipital lobe regarding the target object (*i.e.* the glass of water). This information is dissected by the premotor cortex, found in the somatomotor cortex as seen in Fig. 3.1, to plan the reaching and grasping movement before being passed along to the motor cortex, which ultimately triggers muscle movements [20]. There is evidence that the information sent to the spinal cord from the primary motor cortex is also relayed to the intermediate zone of the cerebellum [97, 98].

Grasping is viewed in neurophysiology as changes in grip aperture, the posture assumed by all digits along the reaching action. For cases where a precision grip is used, this aperture can be described as the distance between the thumb and index

finger. Evidence for specialized neural circuits in grasping has been shown through studies involving lesions in the human primary motor cortex or corticospinal fibers. These lesions greatly disrupt grasping. The cortical areas activated in humans during grasping are the inferior frontal gyrus (IFG), the anterior intraparietal sulcus (AIP), as well as the premotor cortex [97]. After an object has been grasped, information from the mechanoreceptors of the hand regarding the status of the grasped object are sent to the central nervous system, which is then processed by the posterior parietal cortex. An amazing feature of this biological system is the reflex pathway in which afferent axons are used to carry nerve impulses to the spinal cord and back to the muscles through efferent axons, creating a high speed, closed-loop system as seen in Fig. 3.2. This pathway is especially important during grasping tasks as it allows us to manipulate objects in a stable manner without relying on cognitively expensive processing, such as using visual feedback, to make minute hand adjustments. The reflex pathway allows quick hand adjustments to prevent grasped objects from slipping, crushing, or becoming unbalanced. Quick reaction times in healthy humans, approximately 70 ms, allows us to manipulate countless objects in practically an endless number of ways as we can efficiently adjust for dynamic changes in the grasped object [60, 64].

A combination of visual and somatosensory inputs are applied with sensorimotor memories for fingertip force adjustments during grasping. Vision identifies common objects, which automatically calls relevant stored information in order to make para-

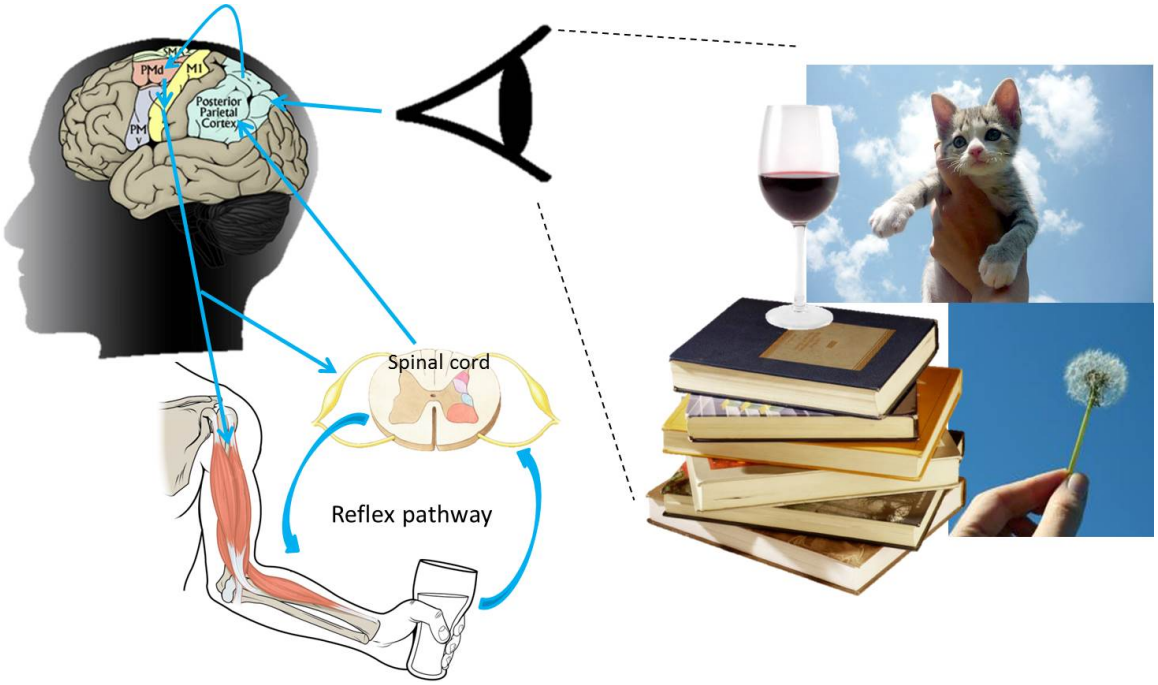

Figure 3.2: Neurophysiology of grasping

metric adaptions for motor commands before being executed, essentially anticipating upcoming force requirements to grasp the target object [54, 55]. For object shape and size, humans often use visual geometric cues for anticipatory control, relying on feedforward models that represent relationships between visual cues and force requirements. However, during manipulation, the formation of object properties and its constant change primarily depends on signals from tactile sensors in the hand in what has been called *discrete event, sensory-driven control* [54, 55]. The basis of this control lies in the comparison of somatosensory inflow with an internal sensory signal that represents a predicted afferent input. A disturbance in the execution of a task due to an error in a parameter of the internal sensorimotor signal is reflected with

a mismatch between the actual and predicted afferent input. When a mismatch between the signals is detected a corrective pattern is triggered, using a forward model. This also updates any of the pertinent internal models, thus changing specifications in the model parameters [55]. Is has been discovered that this type of updating occurs primarily during the initial contact with an object or, if there is an error in the expected value for an object's weight, during object lift-off [55]. While a large portion of the reaching and grasping task can be attributed to the coordination and movement of skeletal muscles, maintaining a grasp and manipulating the target object relies primarily on the cutaneous mechanoreceptors in the glabrous skin of the hand.

3.1.2 Perceived Tactile Sensing

The perceived tactile sensations in the human hand include texture, form, and motion (*i.e.* surface features and whether it is moving across the skin) as well as global features such as shape and size. The skin can be broken up into two major components based on the receptors (1) glabrous skin and (2) hairy skin. The cutaneous receptors in glabrous skin are made up of four different afferent types: slowly adapting type 1 (SA1), rapidly adapting (RA), Pacinian (PC), and slowly adapting type 2 (SA2). RA and PC are classified as rapidly adapting because they respond to the transient period when probes are entered or released in the receptive fields. They do not respond to sustained stimuli. SA1 and SA2 afferents are slow adapting because they respond to sustained skin deformation and stimuli [58, 99–101].

Table 3.1: Cutaneous mechanoreceptors found in the glabrous skin of a human hand and their corresponding functions.

Receptor		Responds To	Perception Function
SA1	Merkel	Curvature	Form, texture
RA	Meissner	Motion	Slip, grip
SA2	Ruffini	Stretch	Hand shape, lateral force
PC	Pacinian	Vibration	Slip, probes

Two principal mechanoreceptors in the superficial skin layers are the Meissner's corpuscle, an RA receptor that is mechanically connected to the papillary dermis ridge (the upper most dermis layer), and the Merkel disk, a SA1 receptor that responds to compressing strain from the skin. Deeper in the subcutaneous tissues are the Pacinian corpuscle, similar to the Meissner's corpuscle as it responds to rapid indentations of the skin but not steady pressure, and the Ruffini ending, SA2 receptors that link subcutaneous tissue to stretch in the skin on the palm and around joints. The Ruffini ending receptors help make up our perception of the shapes of the objects we grasp. Fig. 3.3 shows the location and morphology of the different mechanoreceptors in human skin. Although all four mechanorecptors are excited by indentation and movement of the skin, they each signal different information [20, 58, 101, 102]. Table 3.1 shows a schematic of the mechanoreceptor types and their related features, as described in [99].

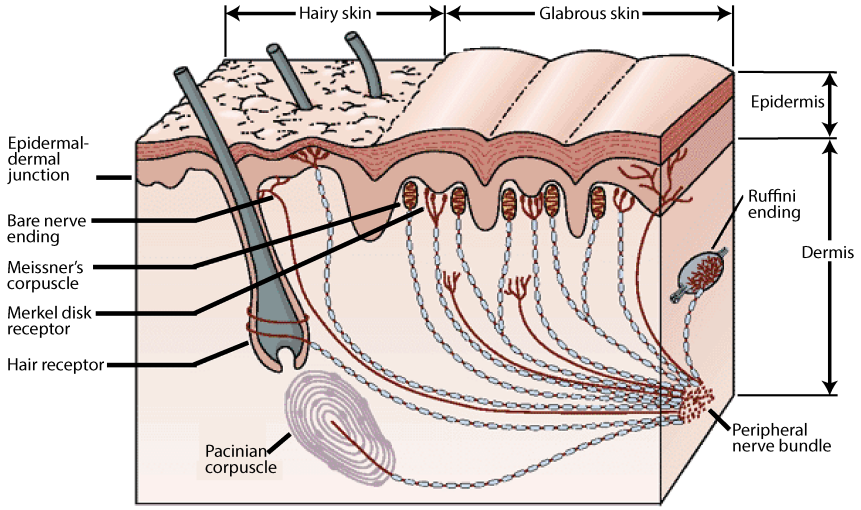

Figure 3.3: The mechanoreceptors in human skin. Receptors are found in superficial skin between the dermis-epidermis interface [20].

3.1.3 Sense of Slip

The ability to perceive incipient slip during grasping is very importatnt for maintainined stability during manipulation tasks [101]. The onset of slip is initiated at the edges of object contact, as the load over the contact area is highest in the center of contact and much lower at the boundaries. This phenomenon generates detectable skin vibrations, which are picked up by the Pacinian corpuscles as they are most sensitive to vibrations. The information regarding the direction of object slip is provided from the Meissner (RA) corpuscles [21, 99, 101]. Visual cues about the shape of an object as well as sensorimoter memory of previous grasping experiences provides information necessary to predict grasping and manipulation expectancies for a given object. Our impressively quick reflex is triggered when we experience a mis-

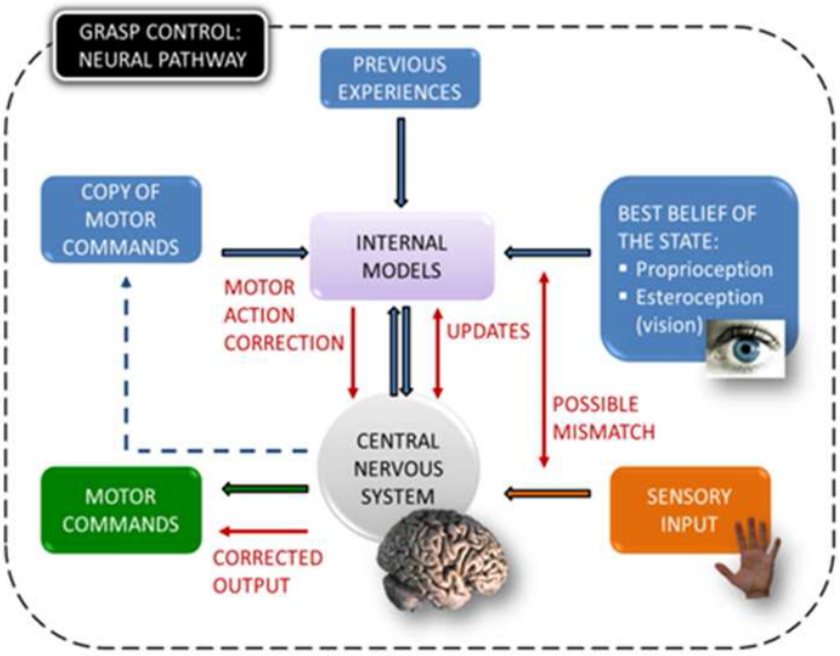

Figure 3.4: The neural pathway for grasping control in humans [21].

match between what we predicted and the actual sensory information we receive [52]. A neural pathway diagram showing grasp control is seen in Fig. 3.4. It has been demonstrated that humans can control grasping force very efficiently with forces approximately 10% above the minimum required value to prevent slip [103]; thus, our ability to predict, perceive, and react during grasping and manipulation tasks is one of the many intrinsic and complex physiological systems we utilize on a daily basis.

3.1.4 Prosthesis Grasping

Perhaps the most basic strategy to prevent slip comes from regulating the normal component of grip force to its least effective value; however, additional information

regarding the tangential force components are necessary to determine the dynamic state of a grasped object. Kyberd et al claim that force sensor information to detect object slip is more robust than using specialist single-site sensors as a force vector can be developed to determine object movement within a grasp [95].

Recent groundbreaking work by Hsiao et al discusses the direction of sensory feedback for upper limb prostheses using models based on human mechanoreceptors and neural pathways [104]. The current downside to this approach is the sheer complexity of providing extensive feedback to the amputees themselves; however, this is the direction prosthesis control must go as it advances in the future. Other work in this direction has shown a model to provide tactile feedback through electrical stimulation in the residual peripheral nerves to convey velocity, acceleration, and jerk from a prosthetic hand to an amputee [105]. Of course another issue is the timing delay ($\sim$750 ms) between when an amputee receives information regarding object slip and when he or she is able to cause the prosthesis to react, unlike humans who are capable of contracting muscles for corrective behavior within 70 ms of receiving information of object slip [60,64]. As a result, it is currently more applicable to create closed-loop tactile feedback directly to the prosthesis from force sensors. In addition, an amputee may become desensitized to the effect of electrical stimulation over time.

Currently, amputees rely on visual cues to grasp objects with their prosthetic device. Two-site proportional control is used by placing electrodes on the flexor and extensor muscles of the residual limb to measure electromyography (EMG) signals

from the amputee. These signals are used to open and close the prosthesis as well as change the grip mode of the prosthesis by performing pre-determined muscle contractions, such as a co-contraction of both the flexor and extensor muscles. The joint angles and hand position of the prosthesis during opening and closing by an amputee is programmed into the hand by the manufacturer. As a result, an amputee can only choose to increase or decrease hand aperture, as opposed to individual fingers, during grasping. Some commercial hands use the amount of current supplied to the prosthesis motors to determine the physical resistance at the fingertips of the device. This principle is employed in top-of-the-line prosthetic hands, such as the i-limb or bebionic, in an effort to prevent burning out the prosthesis driving motors as well as breaking the fingers if it experiences large amounts of physical resistance. While this strategy is very useful in the general sense, there are objects that may break before providing enough resistance to stop the prosthesis from closing too far, such as an egg or a cracker.

3.1.5 Slip Sensing for Prostheses

Systems that detect object slip for robotics is not a new area of research [106], but has made large improvements recently [12, 18, 31, 35, 48]. The use of pressure and force sensing during grasping tasks has shown the ability to detect force changes at the prosthesis and object interface [18, 60, 75, 107]. The next step becomes what to do with these sensor values and how these signals effect the prosthesis. While novel

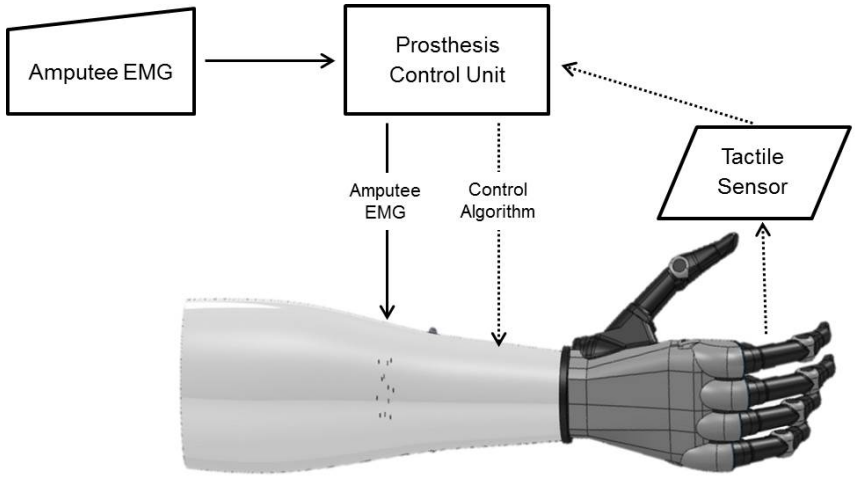

Figure 3.5: Basic diagram of the Reflex tactile feedback system. The users EMG signals control the prosthesis while additional information from tactile sensors is fed into the control unit to monitor the applied grip forces of the hand.

control strategies have been recently developed [18], there is yet to be a closed-loop tactile feedback system with slip prevention that is implemented on amputees. Fig. 3.5 shows a diagram of the Reflex system implemented in this work. The user's EMG signal is sent through the prosthesis control unit to the terminal device. In addition, information from the tactile sensors is received and processed by the control unit. Based on the incoming signal and control algorithm, hand adjustments are made. For example, if an object is moving during a grasping task, the control unit will make a decision to close the hand a certain amount to correct for the object instability.

The SensorHand by Ottobock (Berlin, Germany) is a commercial device that offers a primitive form of force sensing to help improve grasping. Essentially, a series of strain gauges are used to determine the distribution of the applied grip force across the

terminal device. A mismatch between the strain gauges indicates that the prosthesis is experiencing an unequal distribution of grasping force, which triggers an increase in grip force. The increase in grip force stems from a measured increase in shear force [44]. There are assumptions made in the SensorHand, such as a constant coefficient of friction value, that present certain challenges. One challenge stems from the fact that slip is not actually detected but rather grip force is increased in a proportional manner that corresponds to measured shear forces. This causes some objects to be crushed upon lifting even if slip is not present because of the increase shear force measured by the prosthesis.

Most commercial prosthetic hands lack the ability to perform tactile sensing as it pertains to grasping or interacting with the environment. Adding an element of sensing to a prosthesis can often require extensive manipulation of the prosthesis' phalanges or even designing new phalanges and fingertips that must be built into the device [12,60]; in addition, this introduces a financial burden on an already expensive piece of equipment to the end user. There is a need to develop a tactile sensing system that is low cost, easily customizable, compatible with a variety of commercial upper limb prosthetic devices, and does not require extensive manipulation or redesigning of the prosthesis.

3.2 Sensor Design

A specialized textile force sensitive resistor (FSR) was designed and built to measure applied forces during grasping tasks with a prosthetic hand. Based on previous work and a close collaboration with the Singapore Institute for Neurotechnology (SINAPSE), the textile force sensors are designed using several crossing traces of conductive fabric, which are separated by a piezoresistive textile layer [16]. Fig. 3.6 shows the textile sensor cuff design in which flexible materials are used to allow the sensor to be placed on a prosthesis phalanx. A textile bi-directional stretch fusible interfacing serves as the foundation of the sensors. The conductive traces are used to sandwich a piezoresistive fabric layer, as mentioned, while an outer stretchy covering acts as a protective barrier between the conductive traces and the environment. A small rubber patch is cured directly over the conductive trace crossing areas. The rubber layer acts as a compliant gripper to help increase the tackiness of the sensor cuff. The nature of the textile FSRs allows them to easily be fit on different regions of a prosthetic hand. The stretchable material that makes up each sensor cuff allows it to fit snugly against the surface of the prosthesis. The added benefit to this design is that it enables the sensors to be placed on different makes and models of upper limb prosthetic devices.

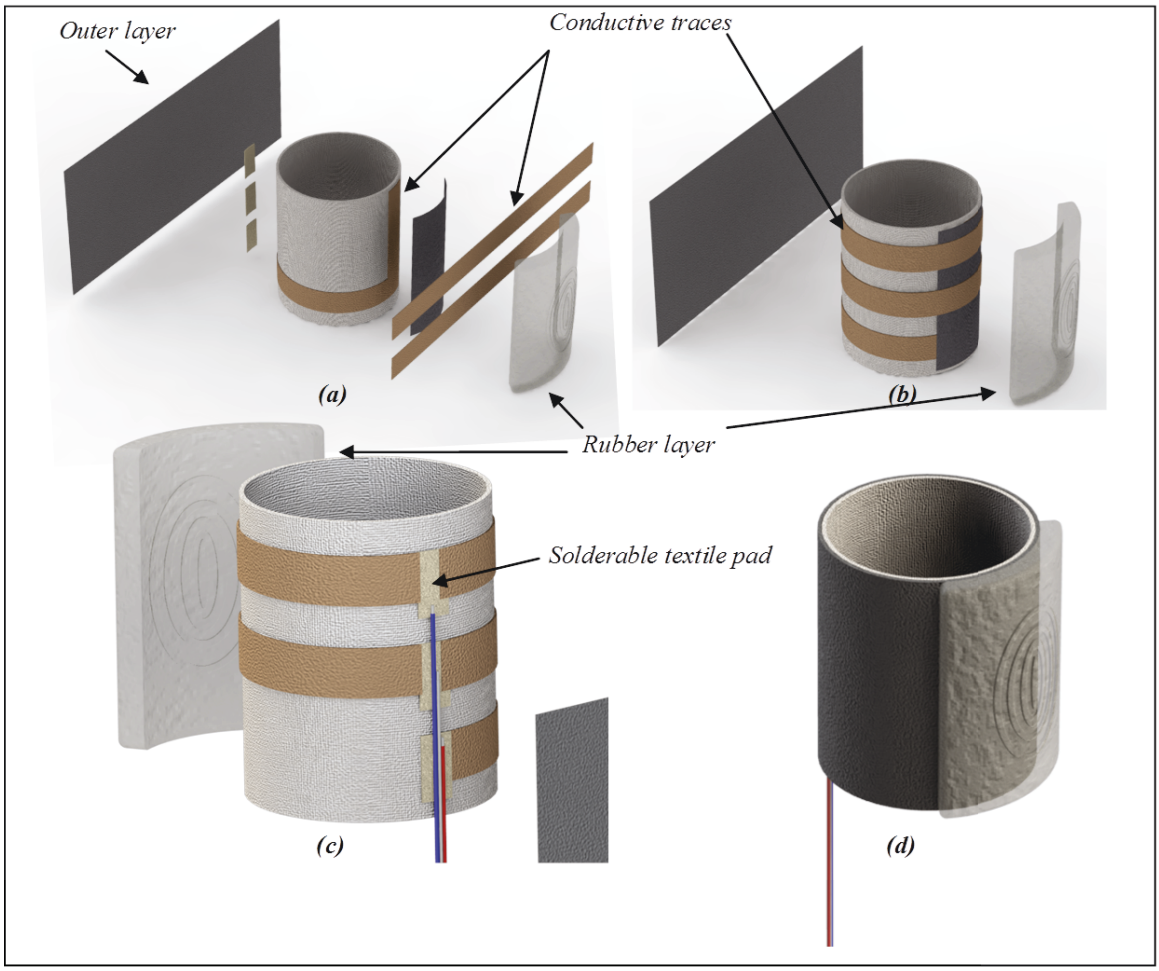

Figure 3.6: Textile sensor cuff design. Flexible and stretchy materials allow the sensor to be placed on a prosthesis phalanx. (a) shows an exploded view of all the components and (b) shows how the conductive traces are wrapped around the inner cuff. (c) shows the textile solderable pads used to create the hard-to-soft connection between the textile cuff and wires, and (d) shows a completed sensor with the outermost rubber fingertip-like layer.

3.2.1 Sensor Materials

A variety of materials are used to make each textile sensor cuff. FusiKnit Tricot (fusible interfacing) (NR-3102, Fabric.com, USA) is a lightweight tricot, a special type of knitting where yarn zigzags vertically following a single column of knitting as opposed to a single row, and acts as the backing and foundation of the textile sensor. Ironically, tricot is traditionally used in lingerie. The conductive traces are cut from LessEMF's (Latham, USA) Stretch Conductive Fabric (#A321), which offers 100% stretch in the length direction and approximately 65% along the width. It has a surface resistivity of $< 0.5\ ^{\Omega}/_{sq}$. The piezoresistive layer is made up of Velostat from Eeonyx (Pinole, USA). Solderable pads (Fig. 3.6(c)) are cut from LessEMF's ShieldIt Super (#1220), which is a rugged rip-stop polyester substrate with nickel and copper plating with a hot melt adhesive backing so that it can be ironed onto other fabrics. Its resistivity is approximately $1\ ^{\Omega}/_{sq}$, making it ideal for creating a hard-to-soft connection between the textile cuff and wires. The cuff is then coated with a layer of a 95% cotton - 5% lycra fabric, which is manufactured by Kaufman (Los Angeles, USA) and purchased on Fabric.com.

The rubber covering is Dragon Skin 10 from Smooth-On (Easton, USA), a high performance silicone rubber that once cured becomes very strong and stretchy. An in-depth analysis of rubber type and performance is performed in Section 3.3.1. Table 3.2 shows the materials and their roles used to create the sensor cuffs.

Table 3.2: Materials used in making the sensor cuffs

Material	**Manufacturer**	**Purpose**	**Notes**
Fusible interfacing	FusiKnit	Cuff backing	Adhesive back
Conductive fabric	LessEMF	Conductive traces	100% stretch, conductive
Velostat	Eoynx	Layer between traces	Piezoresistive, stretchable
ShieldIt	LessEMF	Solder pads	Adhesive backing, Ni/Cu plating, solderable
Stretch fabric	Kaufman	Outer fabric layer	Stretchable
Dragon Skin 10	Smooth-On	Outer rubber layer	Compliant

3.2.2 Sensor Fabrication

The sensors are fabricated using the materials mentioned in the previous section as well as a standard cutting mat, a rotary cutter, and a clothes iron, which serves as the heat source for the heat activated adhesives on the back of the fusible interfacing and the solderable pads. Fig. 3.7 shows all the components of the textile based sensor. The fabrication steps are shown in Fig. 3.8 and are as follows: (a) the conductive traces are fixed to the fusible interfacing by applying heat; (b) the same method is used for the piezoresistive layer, which is placed over the first conductive trace; (c) the remaining two conductive traces are laid in place and secured to the backing layer; (d) the two portions of the fusible interfacing are then heated and secured to each other; (e) the solderable pads are then placed on the ends of the conductive traces;

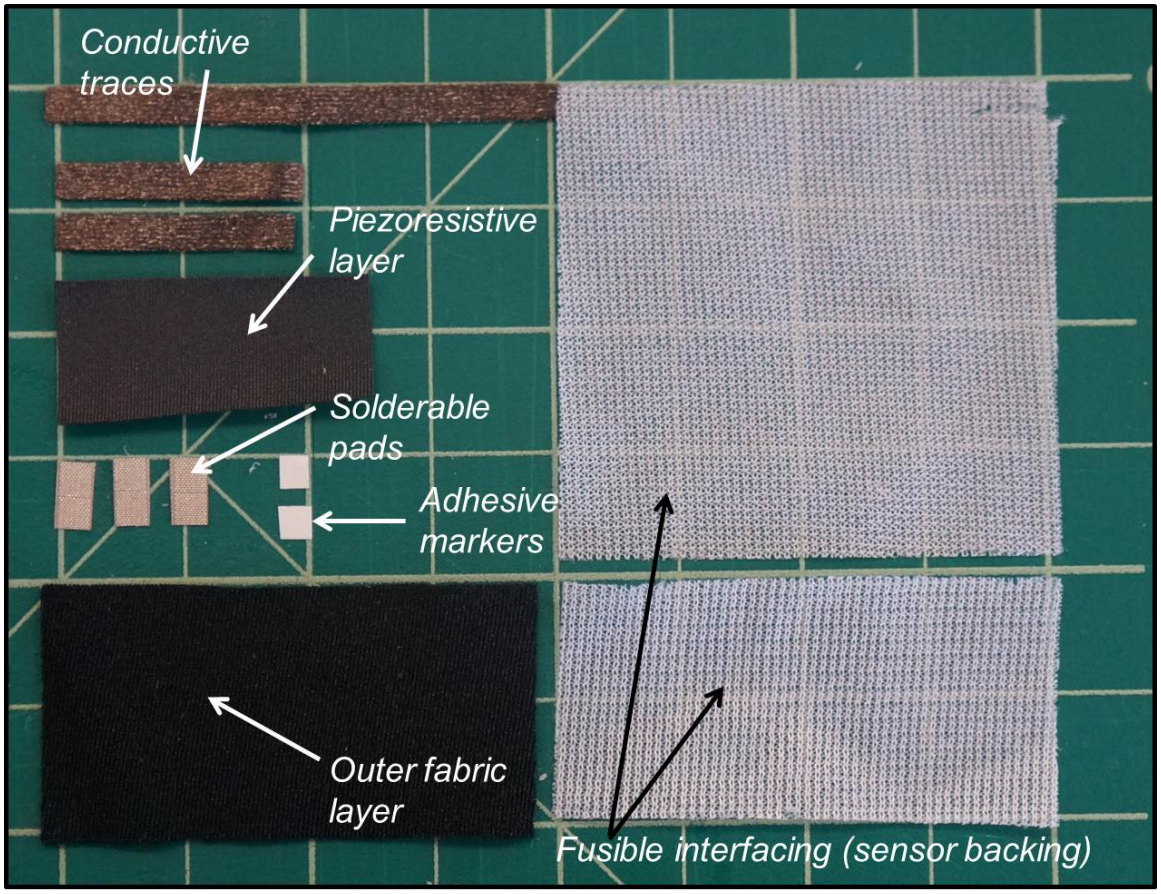

Figure 3.7: Components of the textile based force sensor.

(f) the fusible interfacing is cut to allow folding; and (d) adhesive strips are placed on the back of the outer fabric layer. Fig. 3.9 shows a completed sensor. The remaining steps for fabrication are to (a) solder wires to the sensor and fold it into a cuff, using a heating element to activate the adhesive; (b) place the adhesive markers to indicate the sensing elements; and (c) coat with the rubber layer using a custom mold.

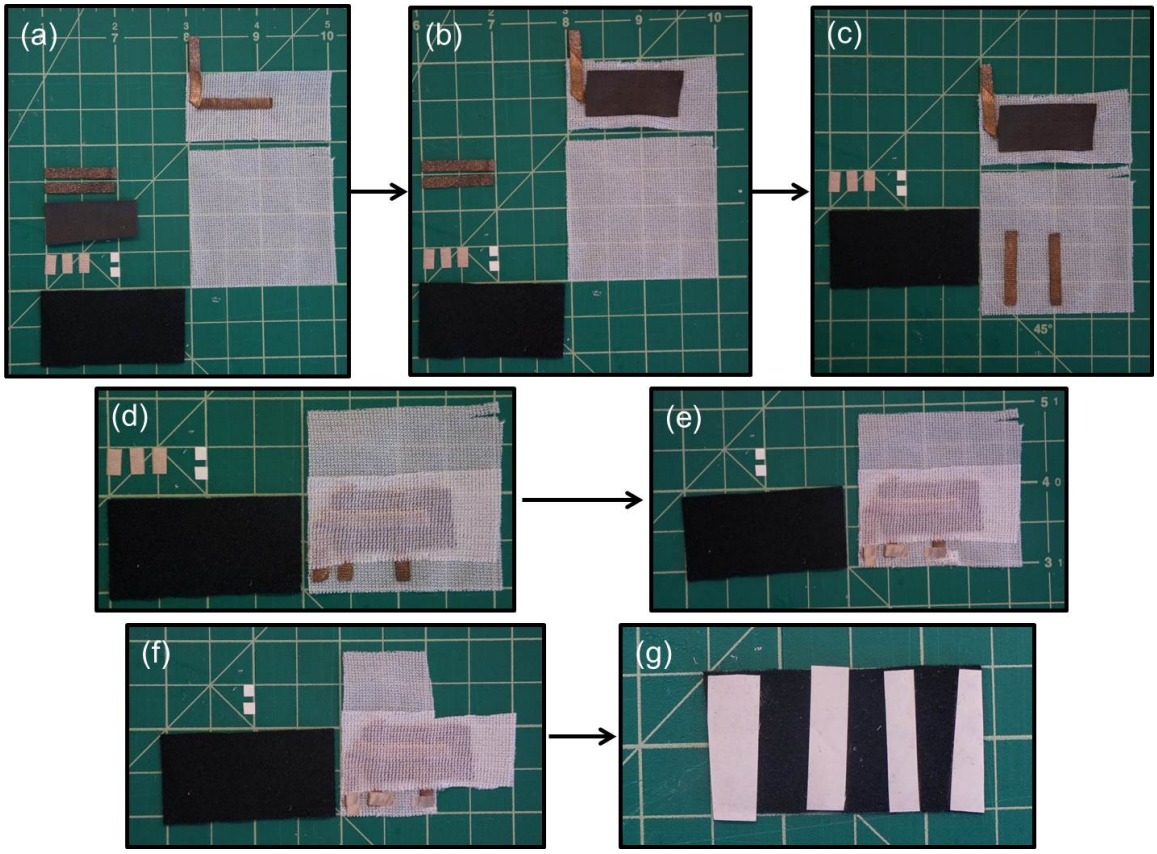

Figure 3.8: Fabrication steps to make the sensor cuff. (a) place the common conductive trace on the fusible interface; (b) apply piezoresistive layer; (c) apply remaining traces; (d) fix fusible layers together; (e) apply solderable pads; (f) cut fusible layer; (g) apply adhesive backing to outer fabric layer.

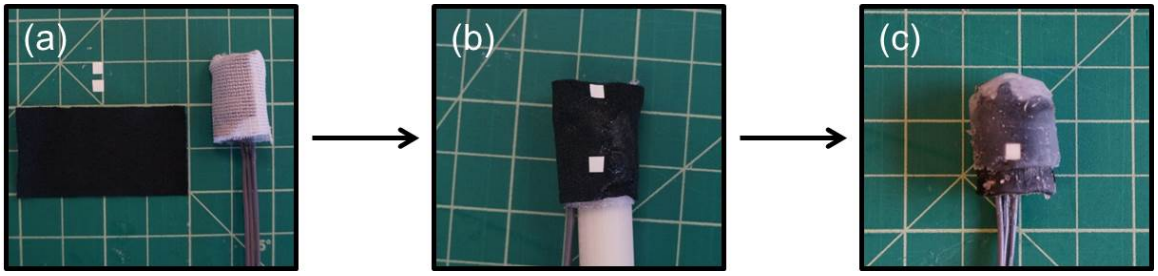

Figure 3.9: Steps to cover and coat sensor: (a) solder wires and folding the sensor into a cuff; (b) apply adhesive markers showing sensing regions; (c) coat with rubber layer using a mold.

3.2.3 Sensor Placement

The sensors are placed on different parts of the prosthesis. Fig. 3.10 shows the textile FSR placement on different regions of a bebionic^{TM}from RSLSteeper (Leeds, UK) prosthetic hand. The stretchable material within each cuff allows for sensor placement on a range of different prosthetic hand makes and models. This image is used to illustrate the areas that the sensors can be easily added to a prosthetic hand. Each sensor cuff has multiple sensing elements.

One could employ an algorithm to decide sensor design, including placement on the prosthesis, based on the prosthesis. A statistical analysis of the main areas of contact during grasping could be performed to find optimal sensor placement on a prosthetic hand. The bebionic prosthetic hand used in this work closes in a way that makes the thumb and index finger the primary areas of contact during grasping. As a result, the final sensor placement is on the tips and distal regions of the thumb, index,

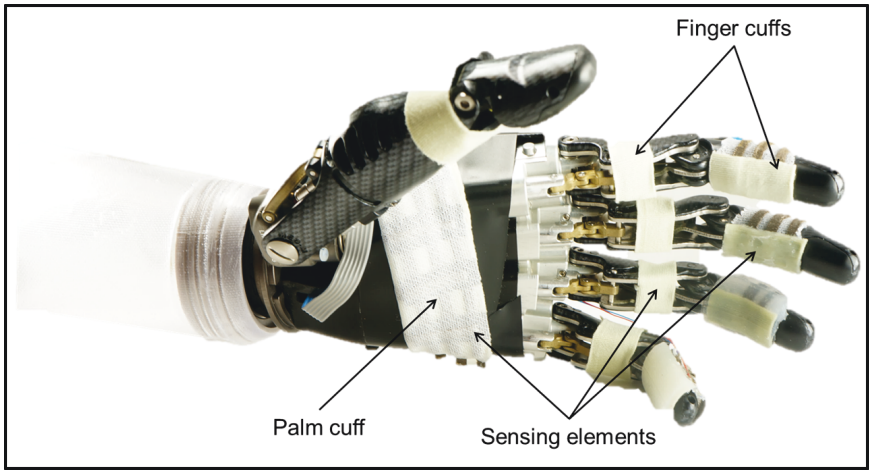

Figure 3.10: Prototype textile FSR placement on different regions of a bebionic prosthetic hand. The stretchable material within each cuff allows for sensor placement on a range of different prosthetic hand makes and models. A palm sensor cuff is constructed as well using similar methods as the finger cuff sensors.

and middle fingers (see Section 5.1.1). Fig. 3.10 shows the customizable nature of the sensor cuffs in that different regions of the prosthesis could be covered by sensing elements.

3.3 Sensor Characterization

Characterization for the textile FSRs was carried out using an analog to digital converter (LabJack U12) while a series of normal forces were applied to the sensing areas of the cuff. A total of 8 sensors were used to establish an expected sensor response curve. Each sensor's response is slightly different in terms of resistance

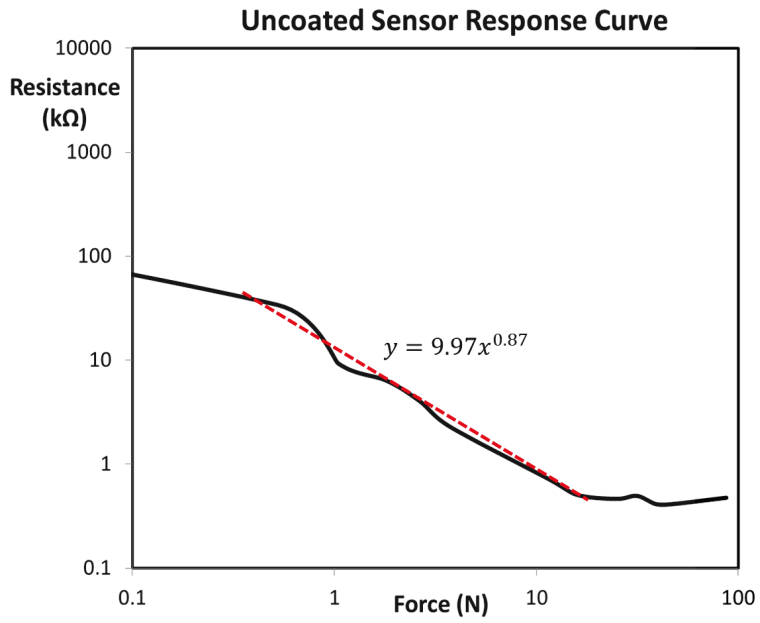

Figure 3.11: Sensor transfer function for a range of applied normal loads. Changes in sensor resistance are measured and plotted against the corresponding force value. The operating range of the sensor is quantified by a power trendline and is given by $y = 9.969x^{0.87}$.

change for an applied force due to the slightly different sizes of the conductive traces across all sensors. Although each trace is cut to be 1 cm in width, even slight variations can cause a change in the sensor response. As a result, the general trend for the sensors is seen in Fig. 3.11 with a log-linear regression. The operating range for the sensors is defined as the linear section of the sensor response curve on a log-log scale, which was found to be 0.6 ± 0.2 N — 20 ± 5 N. The transfer function for the sensor's operating range in Fig. 3.11 can be quantified by a power trendline given by $y = 9.97x^{0.87}$ with a coefficient of determination equal to 0.92.

To validate the functionality of the textile FSR, it is necessary to compare it to other sensors already in use. A direct comparison to commercially available force and pressure sensors was performed to characterize the relative performance and functionality of the textile FSR. Fig. 3.12 shows the output of the textile FSR sensor along with the FlexiForce FSR by Tekscan (Boston, USA) and the TakkStrip pressure sensor by TakkTile (Cambridge, USA) [9, 73]. The textile FSR and the FlexiForce were characterized using a data acquisition board (LabJack U12), while the TakkStrip was analyzed using an Arduino Uno through an I^2C interface [72]. Each sensor was subject to a normal force directly on its sensing area, the average sensor response was used in creating Fig. 3.12. It should be noted that the FlexiForce response in Fig. 3.12 uses a separate scale from the TakkStrip and textile cuff sensor. The TakkStrip output is converted to an equivalent resistance for easier comparison to the other sensors. The TakkStrip, while extremely sensitive, saturates after an applied load of approximately 1 N or higher, thus limiting its operating range. On the other hand, the FlexiForce is better suited for higher force applications as it offers a larger operating range. The textile FSR, as seen more clearly in the inset of Fig. 3.12, is comparable to the TakkStrip in that it offers a similar response except for the fact that the textile FSR is responsive for a larger range of applied normal forces. The textile FSR appears better suited for applications with prosthetic hands as grasping forces tend to range from 0.5 — 20 N for these devices, although this range can have some variation as it is largely dependent on object size, shape, and weight [18].

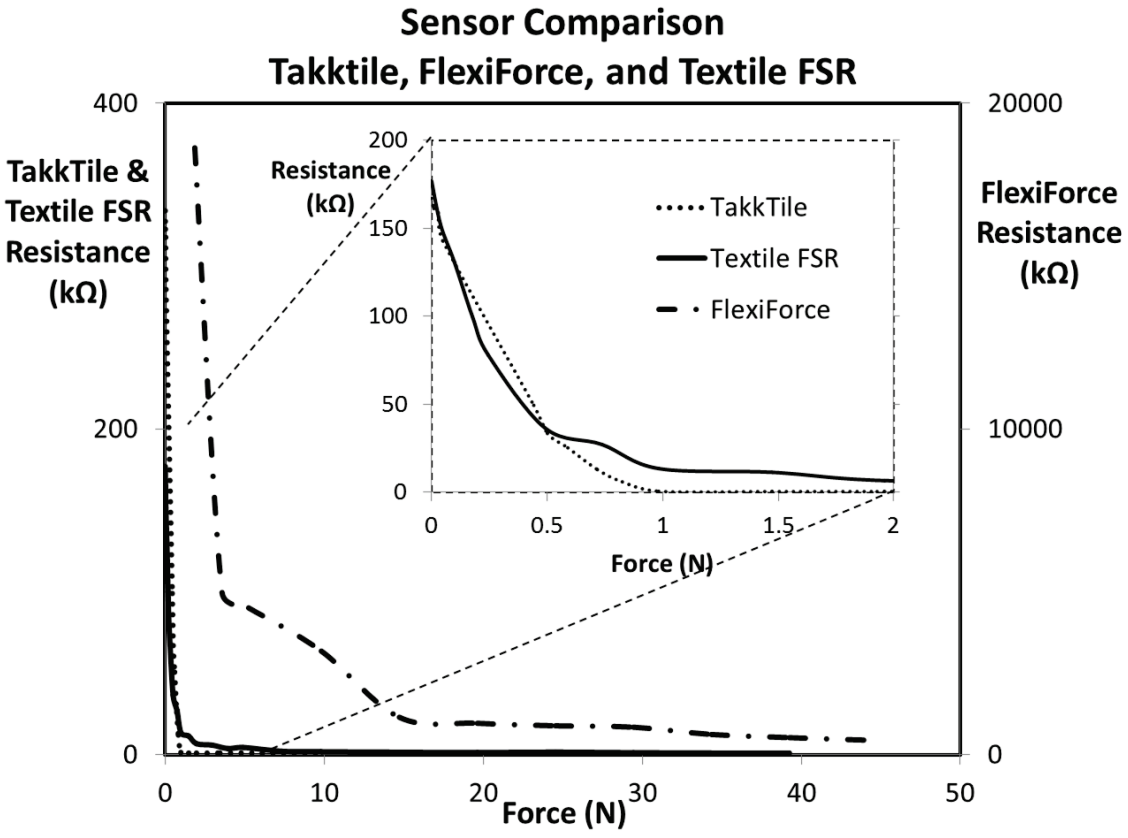

Figure 3.12: Comparison of sensor behavior for the textile FSR, the FlexiForce, and the TakkStrip. The inset shows a zoomed in version of the region showing the difference between the textile FSR and the TakkStrip.

3.3.1 Rubber Coating Characterization

Additional testing was performed to evaluate the effect of different rubber coatings on the sensing element. Fig. 3.13 shows the response of the textile FSR when subject to a 3 mm layer of different silicone based rubbers. The outer rubber layer is a multi-functional component of the system as it provides extra protection between the sensing elements and the environment while also offering additional compliance to the textile cuff surface. Table 3.3 shows the different silicone rubbers used and their respective properties. The results in Fig. 3.13 show that increasing the durometer of the rubber layer decreases the sensor sensitivity but extends the operating range. Dragon Skin 10 was chosen as the most suitable rubber coating for the sensors as it maintained sensor sensitivity while offering appropriate compliance when subject to applied loads. Although Ecoflex's lower durometer gives way to a more compliant rubber layer, its low viscosity allows the rubber to seep through the textile fibers and soak the internal conductive traces of the cuff. This results in either completely removing any connection between the traces or else reducing the conductance between traces. This phenomenon is seen in Fig. 3.13 where the sensor with Ecoflex requires a larger activation force. Similarly, Sil 945 is a high durometer rubber which ultimately causes the sensor to be unresponsive due to the hardness and low compliance of the rubber layer. In order to successfully coat the textile sensor cuffs, the viscosity of the rubber must be above 20,000 cPs before curing. This ensures that the rubber will not soak through the fabric weaves and remove the conductivity of the traces.

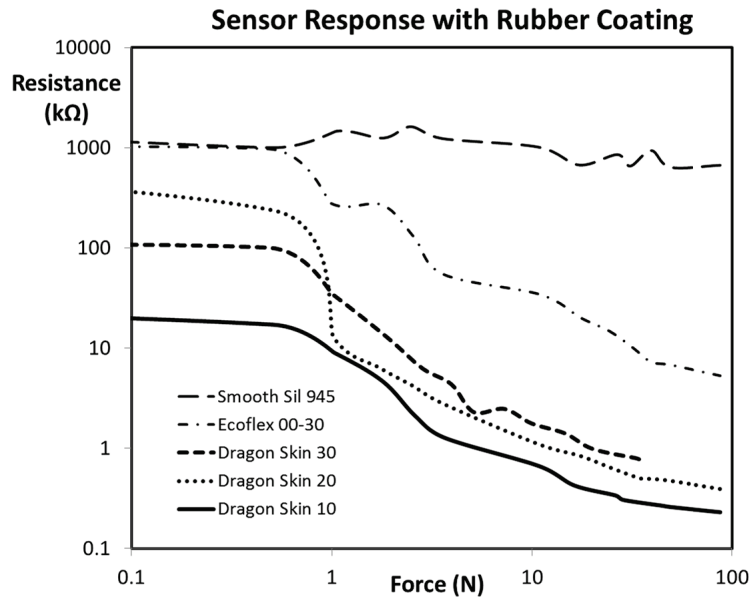

Figure 3.13: Sensor response for different rubber materials.

The nonlinear response of the coated sensors is due to the nonlinear mechanics of the rubber layer during compression.

3.3.2 Sensor Drift and Loading

Extended testing was performed on the sensors to estimate the amount of drift experienced over time. Fig. 3.14 shows the response of an unloaded sensor over a period of 20 min. Drift is estimated using a linear regression model on the steady state output of a sensor. The results show that the drift of an unloaded sensor is insignificant as the variation between individual sensors is greater than the variation of a sensor's unloaded output over time. This could also be an artifact of temperature change, although the resources to perform such an evaluation are unavailable at this

Table 3.3: Comparison of silicone rubbers used on textile sensors

Material	**Mixed Viscosity (cPs)**	**Elongation at Break**	**Shore Hardness**
Ecoflex	3,000	900%	00-30
Dragon Skin 10	23,000	1000%	10A
Dragon Skin 20	20,000	620%	20A
Dragon Skin 30	30,000	364%	30A
Sil 945	40,000	320%	45A

time. To help reduce the effect of temperature on the operation of the sensors, all tests and experiments were performed in a laboratory setting at 21 °C and 45% relative humidity.

A load of 1 N was applied to a sensor and the response was measured for approximately 20 min to understand how the sensor output changes under an applied force. The response follows a power trendline given by $R_{Drift} = 6.8t^{-0.1}k\Omega$ where t is in min, as seen in Fig. 3.15. After loading, the relative changes in sensor resistance are more significant than when unloaded. A variation of $2k\Omega$ when the sensor resistance is $< 20k\Omega$ is a significant change. A high-pass filter with a low cut-off frequency can be applied to remove the sensor drift; however, only in rare occasions will an amputee hold an object with his or her prosthesis for an extended period of time. Thus, it is

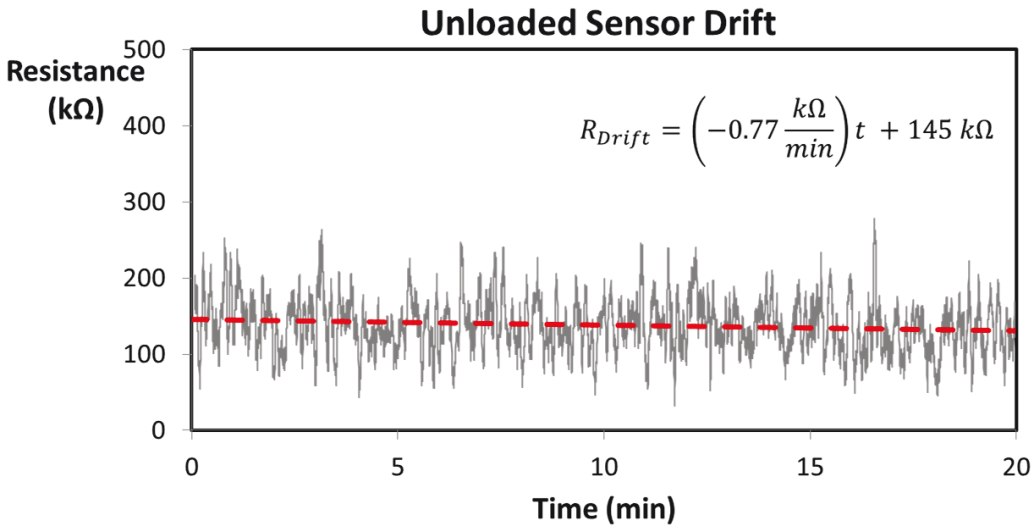

Figure 3.14: Unloaded sensor response over an extended time. The red line indicates a very slight negative trend line of the unloaded sensor response. The slope of the drift is estimated to be $-0.77\ ^{k\Omega}/_{min}$.

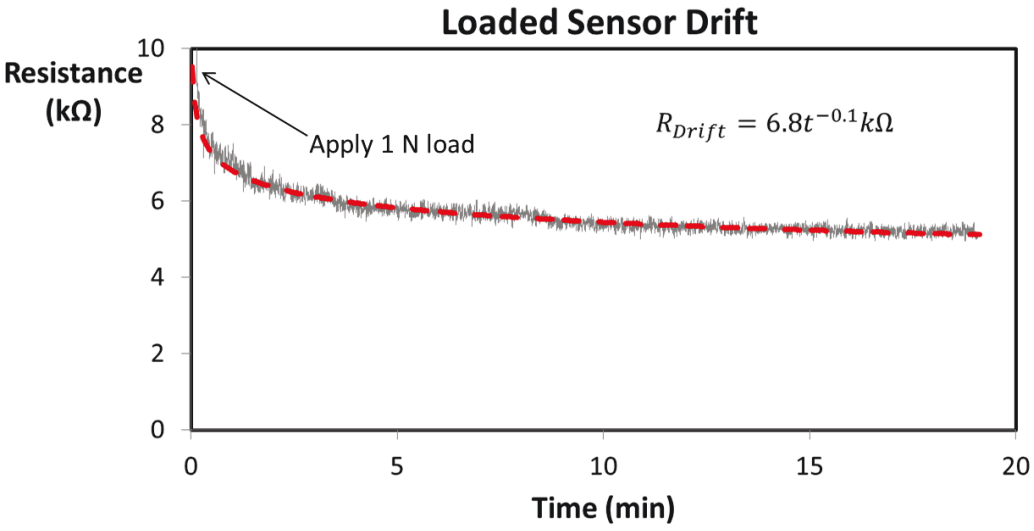

Figure 3.15: Sensor response over an extended time with a 1 N load. The response follows a power trendline given by $R_{Drift} = 6.8t^{-0.1} k\Omega$ where t is in min.

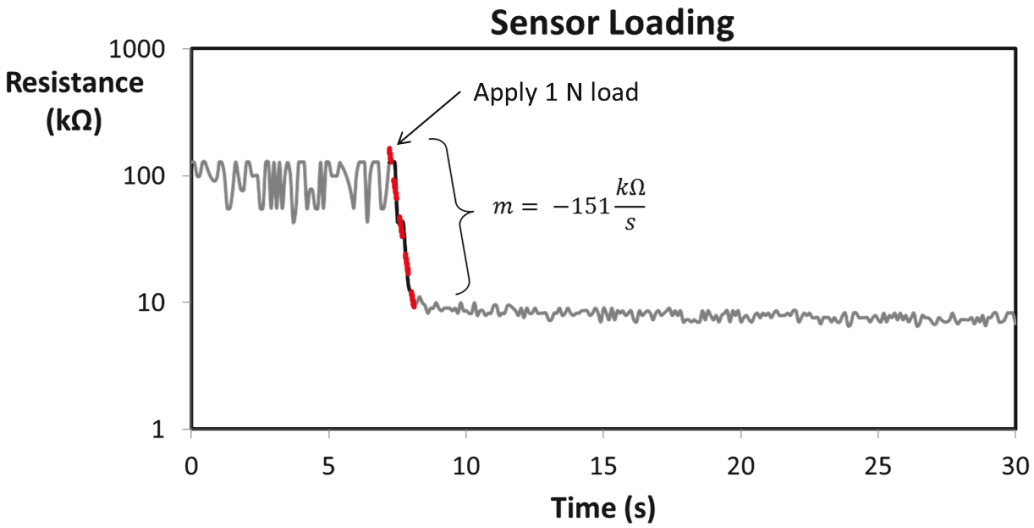

Figure 3.16: A 1 N force is applied to the sensor, which produces a transient period in which the textiles of the sensor begin to settle under the load. This settling period is quantified as the time it takes the sensor to reach a relatively steady value once loaded. A linear regression with a slope of $-151\ {}^{k\Omega}/_{s}$ can be used to describe the initial response of the sensor when going from unloaded to loaded.

not expected that the sensors will experience loading for more than a few minutes.

A zoomed in plot of the sensor loading with 1 N is seen in Fig. 3.16. The short period ($\sim$ 6.5 — 7 s) before the sensor output reaches a relatively stable value can be attributed to the settling time of the textiles after they experience a force. The compliant nature of the textiles causes this small delay in the sensor response during loading. The slope of this loading section is estimated using a linear regression line with a slope of $-151\ {}^{k\Omega}/_{s}$.

3.4 Force Sensing Model

The textile FSRs are designed to be easily placed on the finger of an existing prosthesis, thus eliminating any need for special disassembly or mechanical manipulation of the device. The textile FSR cuff (Fig. 3.6) can be slipped on the mid and distal regions of a prosthetic phalanx. A simple model top down view of the sensor cuff on a finger is seen in Fig. 3.17 and shows the sensor as it undergoes an applied normal and tangential load, the forces experienced during grasping. The rubber coating on the sensor cuff is designed to move as it undergoes these forces. This movement enables the sensor to detect changes in both normal and tangential directions as the rubber causes corresponding stresses in the sensing areas.

Solidworks from Dassault Systémes SolidWorks Corp. (Vélizy-Villacoublay, France) was used to model the textile sensor. A finite element method and analysis were performed on the rubber layer of the textile FSR to predict stresses, displacements, and strains during loading, which are discretized using tetrahedral elements. Normal and tangential forces are applied in the simulations using values that are typical during grasping. The resulting displacements of the rubber component from the simulations can be seen in Fig. 3.18. The distortion energy theory can be used to understand the behavior of the interface between the rubber layer and the textile cuff itself. This theory predicts that yielding will occur when the distortion energy per unit volume exceeds the distortion strain energy per unit volume for simple tension or compression of a material [108, 109].

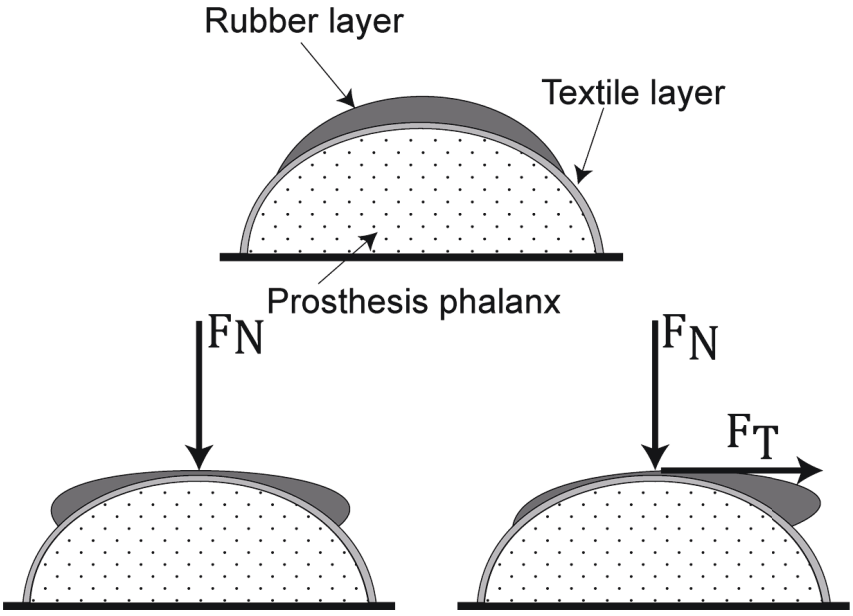

Figure 3.17: Top down view of the sensor cuff as it is fixed to a prosthesis phalanx. The rubber coating is designed to move when under applied normal and tangential loads. This enables the sensor to detect changes in both normal and tangential directions as the movement of the rubber layer causes corresponding stresses in the sensing areas.

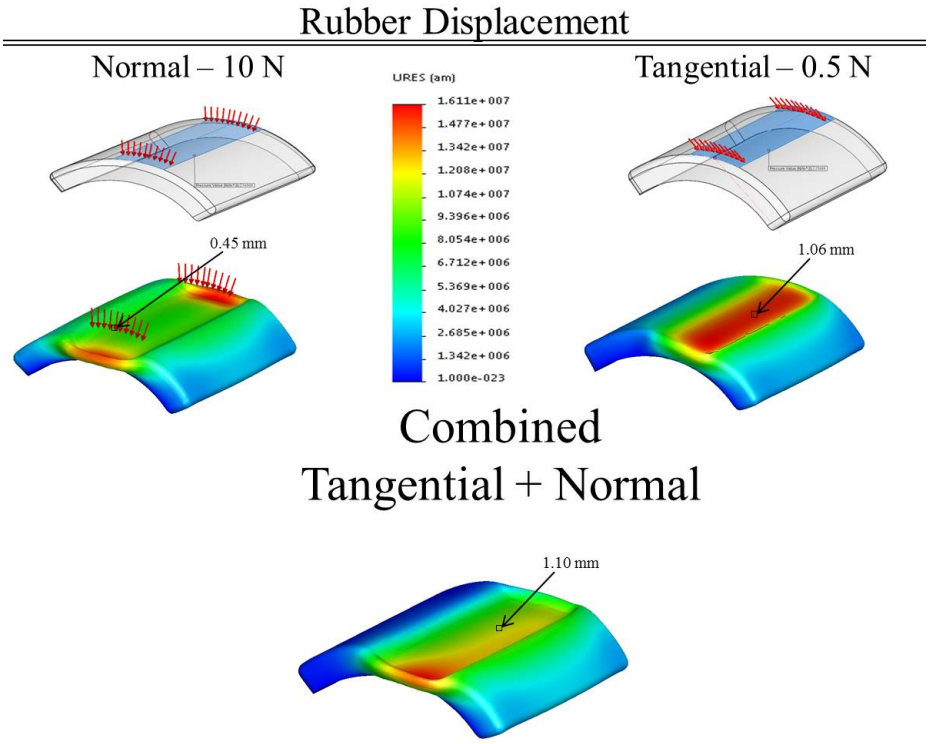

Figure 3.18: Simulated displacement of the textile FSR outer rubber component under normal and tangential loads.

The total strain per unit volume, u, can be expressed as:

$$u = \frac{1}{2}\left[\epsilon_1\sigma_1 + \epsilon_2\sigma_2 + \epsilon_3\sigma_3\right] \tag{3.4.1}$$

where σ_1, σ_2, and σ_3 are the prinicpal stresses of the volume ($\sigma_1 > \sigma_2 > \sigma_3$) and strain, ϵ. Originating from Hooke's Law, axial strain along an axis can be expressed as a relation between the stress (σ) along the axes of 3 dimensional space [109]:

$$\epsilon_x = \frac{1}{E}\left[\sigma_x - \nu(\sigma_y + \sigma_z)\right] \tag{3.4.2}$$

where ν is Poisson's ratio which is the negative ratio of transverse to axial strain. Using the known relationship for ϵ (strain), a substitution can be made using 3.4.2 to produce:

$$u = \frac{1}{2E}\left[\sigma_1^2 + \sigma_2^2 + \sigma_3^2 - 2\nu(\sigma_1\sigma_2 + \sigma_2\sigma_3 + \sigma_3\sigma_1\right] \tag{3.4.3}$$

The strain energy can be broken into two parts: distortion energy (u_d), which is responsible for changing shape, and the strain energy per unit volume (u_v), which is due to dilation (change in volume). u_v can be expressed as [109]:

$$u_v = \frac{1-2\nu}{6E}\left[\sigma_1^2 + \sigma_2^2 + \sigma_3^2 + 2\nu(\sigma_1\sigma_2 + \sigma_2\sigma_3 + \sigma_3\sigma_1\right] \tag{3.4.4}$$

Subtracting u_v (3.4.4) from u (3.4.3) provides the distortion energy (u_d):

$$u_d = u - u_v = \frac{1+\nu}{3E}\left[\frac{(\sigma_1-\sigma_2)^2 + (\sigma_2-\sigma_3)^2 + (\sigma_3-\sigma_1)^2}{2}\right] \tag{3.4.5}$$

Simplifying the distortion energy using an equivalent stress, called the *von Mises stress*, σ' [108]:

$$u_d = \frac{1+\nu}{3E}\sigma'^2 \tag{3.4.6}$$

The von Mises stress can be though of as a single, equivalent, or effective stress for the entire general state of the stress given by σ_1, σ_2, and σ_3:

$$\sigma' = \sqrt{\frac{(\sigma_1 - \sigma_2)^2 + (\sigma_2 - \sigma_3)^2 + (\sigma_3 - \sigma_1)^2}{2}} \tag{3.4.7}$$

The principal stresses can be expressed in terms of the normal (σ) and shear (τ) stresses [109] given by:

$$\sigma' = \sqrt{\frac{1}{2}\left[\sigma_x - \sigma_y)^2 + (\sigma_y - \sigma_z)^2 + (\sigma_z - \sigma_x)^2\right]} + \sqrt{3(\tau_{xy}^2 + \tau_{yz}^2 + \tau_{zx}^2)} \tag{3.4.8}$$

The resulting von Mises stress experienced by the rubber component of the textile FSR cuff during normal and tangential loading is modeled and shown in Fig. 3.19. The highlighted areas indicate the a region where a textile sensing element is present. It should be noted that an increased stress is present during an applied tangential load. This increased stress is translated to the sensing element of the sensor and detected as an increase in applied force. The onset of object slip during a grasp is accompanied by an increase in tangential force, which is translated through the rubber layer to the textile cuff and rubber interface.

The simulations help explain the expected behavior of the sensor during grasping tasks with a prosthesis. Each sensor is designed to fit over the finger of a prosthetic hand in order to monitor grasping forces. The low cost design using stretchable textiles allows multiple sensing elements to be securely mounted on the fingers of a prosthesis without requiring any hardware changes to the prosthesis itself.

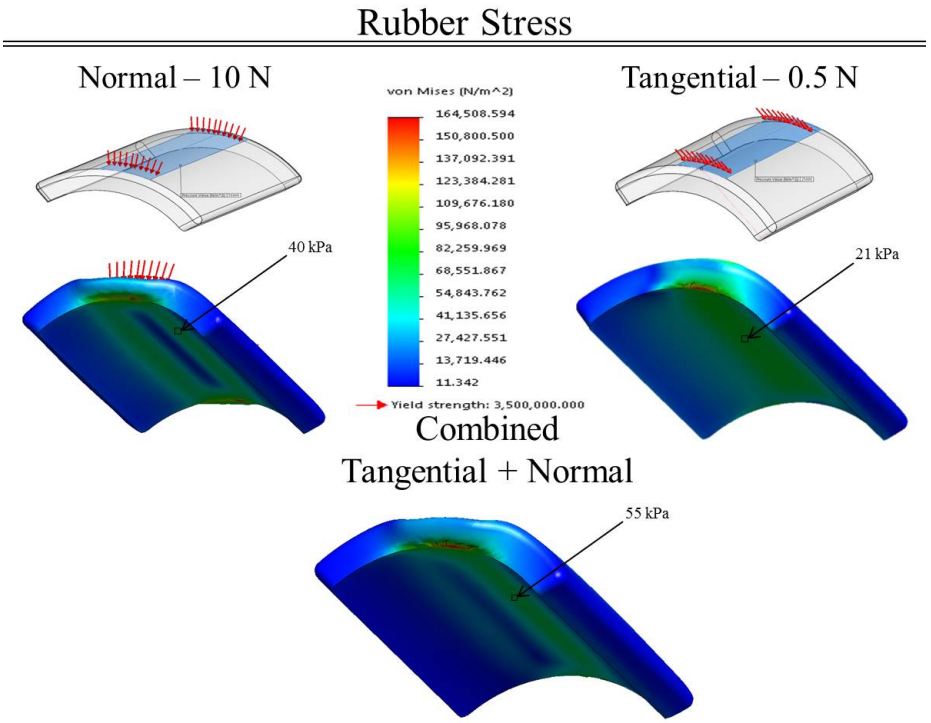

Figure 3.19: Simulated resultant *von Mises* stresses on the rubber layer of the textile FSR. The highlighted areas indicate a region where a sensing element is present. It should be noted that an increased stress is presented during an applied tangential load. This increased stress is realized at the textile cuff and rubber layer interface, thus allowing the onset of object slip to be detected due to the deformation of the rubber layer.

Chapter 4

System Design and Validation

This chapter examines user needs for upper limb prosthetic devices, the integration of the tactile feedback system, and the methods for validating and verifying the system and it's functionality. The combination of the textile force sensor cuffs, prosthesis control hardware, and the control algorithms makes up the tactile feedback system. Operating similarly to the human pathway of the same name, this system is referred to as *Reflex* because it aims to provide a closed-loop tactile feedback mechanism for improving grasping.

4.1 User Needs

Although clinical surveys fail to identify any one single factor that requires focus for the improvement of prostheses or prosthetic provision [30], some surveys suggest

that ability to utilize grip force as a feedback input would be an area of improvement for many users [39]. In particular, some amputees desire the capability to feel the amount of grasping force, which could potentially lower the degree of visual attention required to control grasping with a prosthesis [39]. Sensory feedback is an area identified by some users as being a feature that would enhance a prosthesis [110]. For the Reflex system, feedback is not directed to the user but instead to the terminal device itself. This is because the time delay between notifying a user of changing grip forces from the prosthesis and when the user can react is too large. In order to reduce complexity while also providing a solution for object slip prevention, the sensory feedback is directed to the prosthesis.

Interviews with both prosthetists and amputees gave insight into the user needs for a system that utilizes tactile feedback during grasping tasks. According to one amputee and prosthetist, the addition of rubber tips on the fingers of a prosthesis could greatly enhance the ability to grasp and hold objects. In addition, an internal survey of upper limb prosthesis users shows that nearly 85% of myoelectrically operated prosthesis users see the ability to grasp objects, particularly fragile or delicate objects, as an important feature of a prosthesis [111]. This helps provide the motivation and justification for developing a contact detection algorithm, as described in Section 4.3. Over 90% of amputees with a multi-articulated prosthesis see the ability to prevent grasped objects from slipping as an important feature for prosthetic devices, thus giving way to the development of a slip prevention control strategy for grasping

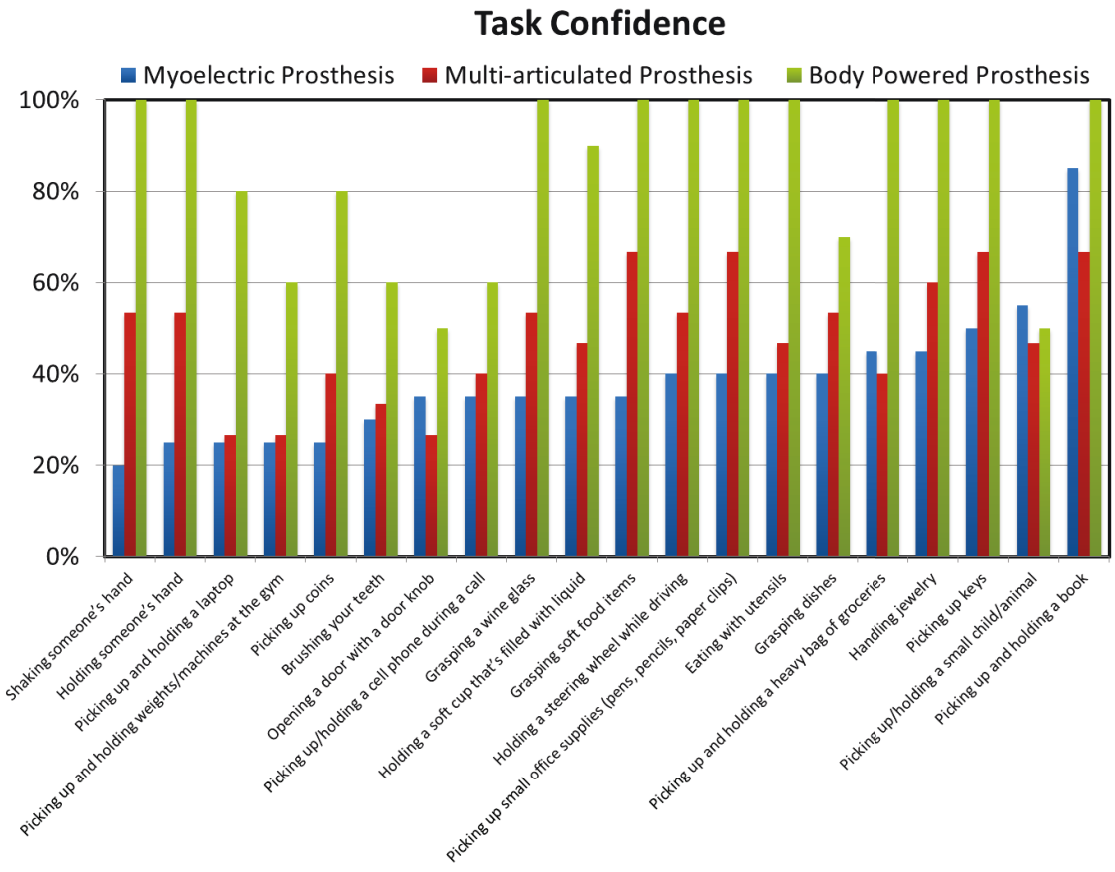

Figure 4.1: Survey results from upper limb amputees regarding their confidence levels performing particular tasks (100% = completely confident). Responses were grouped based on prosthesis type. Users with body powered devices show more confidence in performing tasks when compared to users with myoelectrically operated devices.

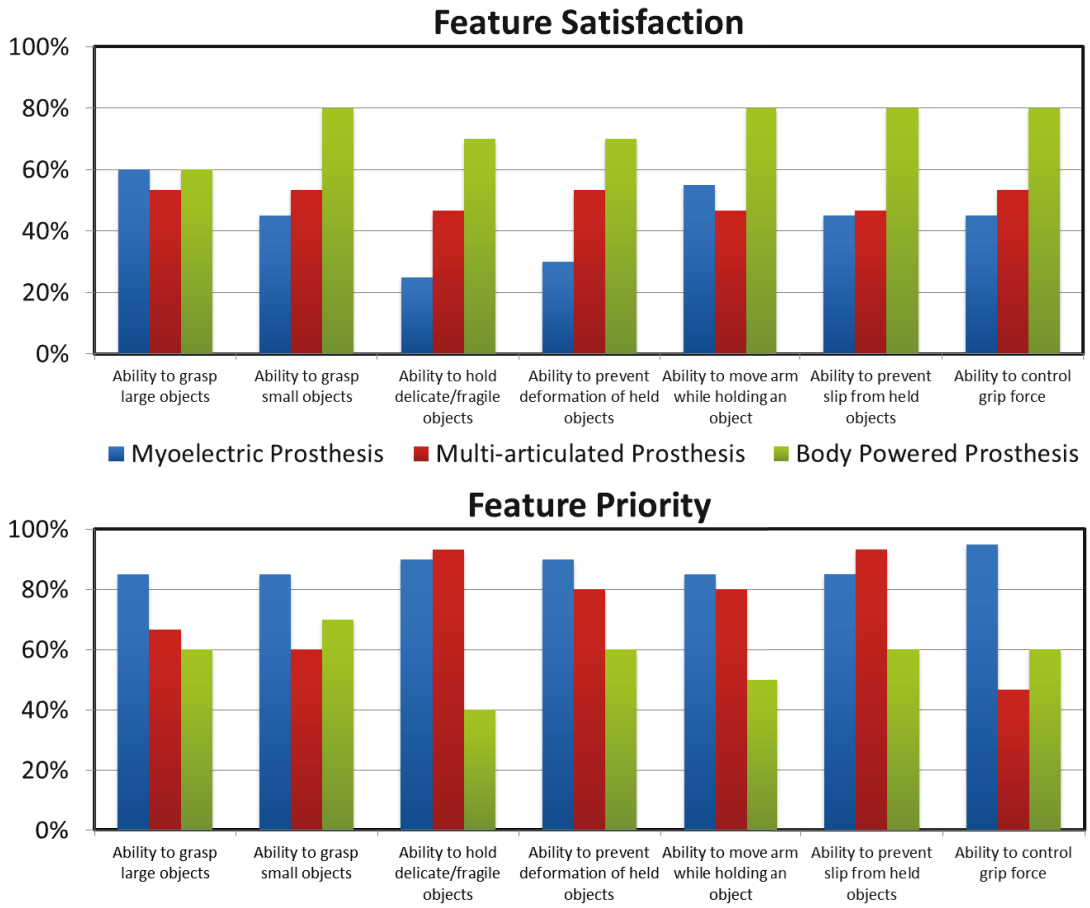

Figure 4.2: Survey results from upper limb amputees regarding the features of their prosthetic devices where 100% indicates complete satisfaction (top) or highest priority (bottom). In general, users with myoelectric or multi-articulated devices were not satisfied with their device's ability to grasp or hold objects, particularly delicate and fragile objects. These same users saw these features, although lacking in their current device, as a priority.

tasks, also described in Section 4.3.2 [111]. Results from the survey are shown in Figs. 4.1 and 4.2. Fig. 4.1 shows the response of upper limb amputees regarding their confidence to complete particular tasks with their prosthesis. Fig. 4.2 assesses particular features of a prosthesis, how satisfied the users are with these features, and if those features are a priority in the daily use of their device. Responses from amputees were categorized based on the type of terminal device used (myoelectric, multi-articulated myoelectric, or body powered). While multi-articulated devices are also myoelectrically controlled, a distinction was made between myoelectric devices that are multi-articulated, such as the i-limb Pulse, and those that operate as a 3-fingered gripper, such as the Ottobock MyoHand. It should be noted that amputees who used a body powered prosthesis were generally more confident in their ability to perform tasks, which can be attributed to the physical feedback users of these devices get through the cable tensions in their systems.

4.2 Reflex System Hardware

4.2.1 Sensor Integration

The textile force sensitive resistors described in Chapter 3 are placed on the distal regions of the thumb, index, and middle fingers of the prosthesis. It was found that these are the major contact points for a prosthesis during grasping using standard grip modes. Each sensor has two sensing areas, thus providing a total of six discrete

points of sensorization on the prosthesis.

4.2.2 Circuit Configuration

The textile force sensors are connected as analog inputs to the prosthesis control unit after being amplified using an instrumentation amplification circuit. Fig. 4.3 shows the force sensor circuit configuration as well as all values used in the circuit. A 7.4 V supply from the prosthesis battery pack is regulated to 5 V. An ICL 7660 voltage converter is used to supply both positive and negative voltages for powering an INA 128 instrumentation amplifier for each sensor. The force sensitive resistors are connected in a voltage divider configuration so that slight changes in the sensor values are more easily picked up by the amplifier. A signal gain of 7.5 was realized by using a R_g value of 8 kΩ (Fig. 4.3). Additional amplifiers can be used to increase the number of sensing elements. A green LED was used to provide visual feedback when the circuit was properly powered. The output of the INA 128 amplifiers was connected to the analog inputs of the prosthesis control unit. A PIC 32MX795F512L microcontroller serves as the processing unit for the controller. Sensor values are monitored in real-time by the control unit. For this work, the Reflex control unit is synonymous with the prosthesis control unit.

The output of the force sensors can be measured using the output voltages from the amplifiers in the circuit diagram. Fig. 4.4 shows the relationship of the sensor resistance (kΩ) to the voltage output (V) of the circuit.

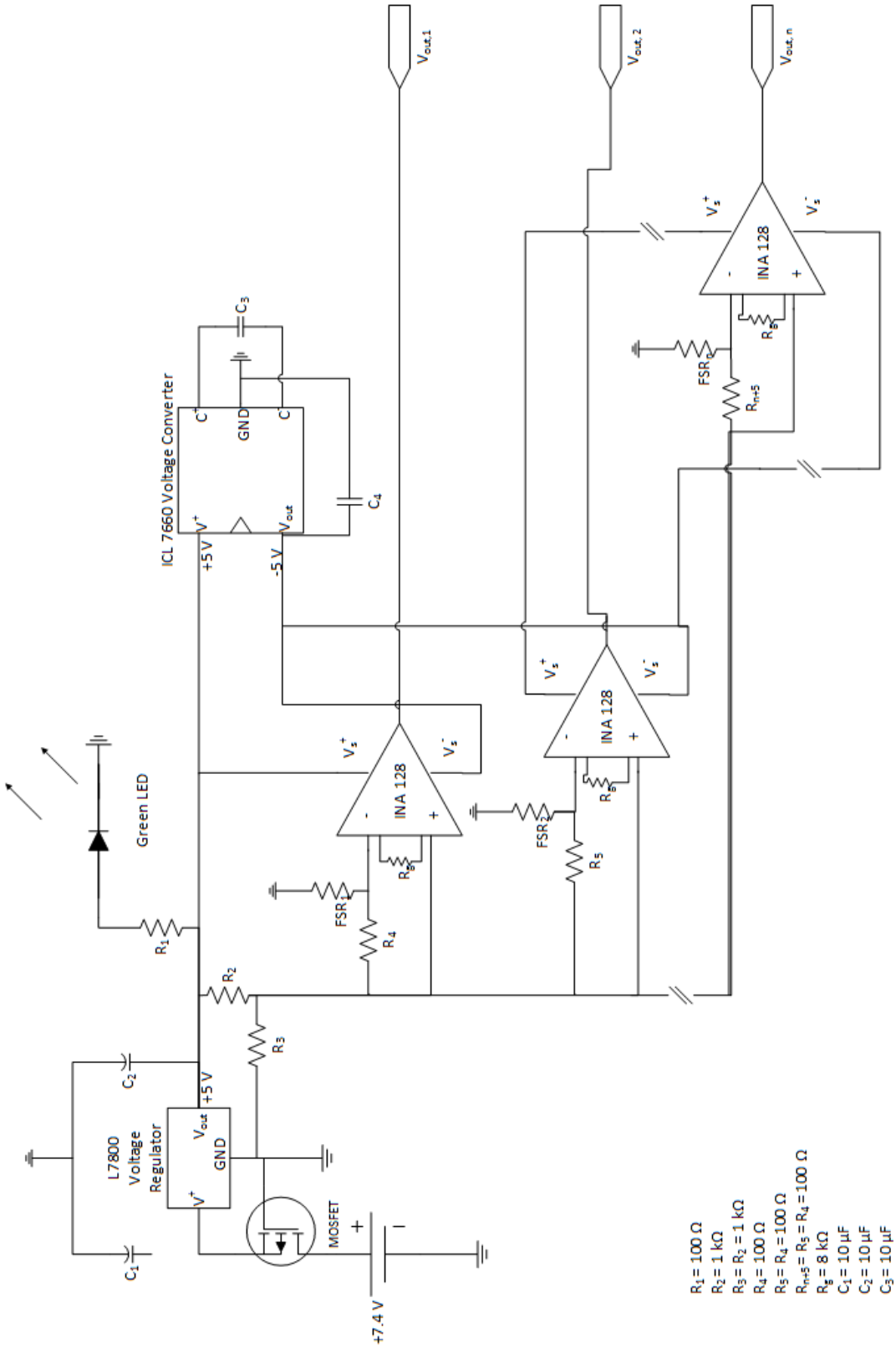

Figure 4.3: Circuit diagram for interfacing force sensors with prosthesis control unit. INA 128's were used to amplify the sensor signals.

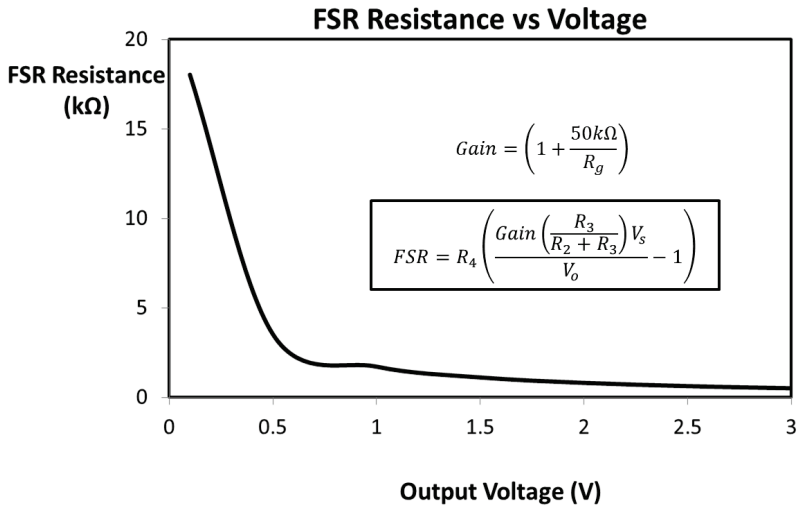

Figure 4.4: Relationship of the FSR resistance (kΩ) and the output votlage of the sensor circuit. The equation shows the effect of the amplifier gain as well as the supply voltage and resistor values of the circuit.

4.3 Reflex Control Algorithms

The force information from the tactile sensors on the prosthesis phalanges is relayed into the control unit of the prosthesis. Two control strategies that utilize the sensor values are implemented. A contact detection scheme is used to adjust the gain of the user's input EMG signal, and a slip prevention strategy uses a numerical derivative to determine when objects are slipping from within the grasp of the prosthesis.

4.3.1 Contact Detection

The Contact Detection control algorithm uses applied grip force to determine a gain reduction on the user's EMG signal used to control the prosthesis. This scheme allows the user to have a finer amount of control of grip force by reducing the strength of the EMG signal. This is useful for handling delicate or fragile objects as it prevents from accidentally crushing or breaking the object. An example of when this control strategy would be useful is while holding a fragile object such as an egg, Styrofoam cup, or during human interaction, such as a handshake or holding hands. Fig. 4.5 shows how EMG gain adjustments effect the amputee's signals sent to the prosthesis. In a proportional control scheme, a prosthesis will respond differently to changing EMG amplitudes. By reducing the effective EMG signal seen by the prosthesis, it prevents an amputee from having to reduce their muscle contractions to make small adjustments to their device. Instead, they can maintain the same level of contraction strength after grasping an object.

Fig. 4.6 shows different EMG gain levels based on grip force. A negative exponential relationship between grip force and gain is implemented as it provides a quick, yet smoothly decreasing function as force increases. A sigmoidal relationship is not practical as a significant reduction in gain would not occur until a grasping force of greater than approximately 4 N was achieved. On the other hand, an inverse relationship results in a rapid decrease of gain over a very small range of force. A gain reduction threshold of 20% (red horizontal line in Fig. 4.6) is used to set the lower

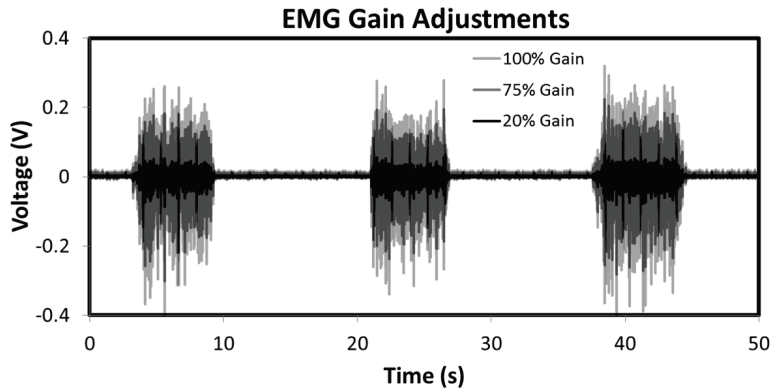

Figure 4.5: EMG signal after gain adjustment. Signals with greater amplitudes result in more movement of the terminal device. By reducing the EMG signal, the user doesn't have to worry about changing the levels of muscle contraction to make small hand adjustments after grasping an object.

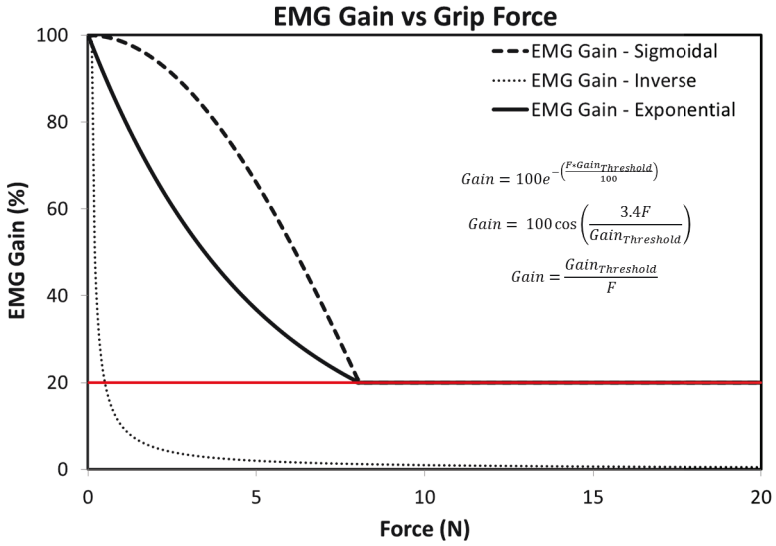

Figure 4.6: EMG Gain curves over a range of applied grip force. The exponential relationship is implemented in the Reflex system as it provides a quicker reduction in EMG gain reduction over a larger range of grip forces.

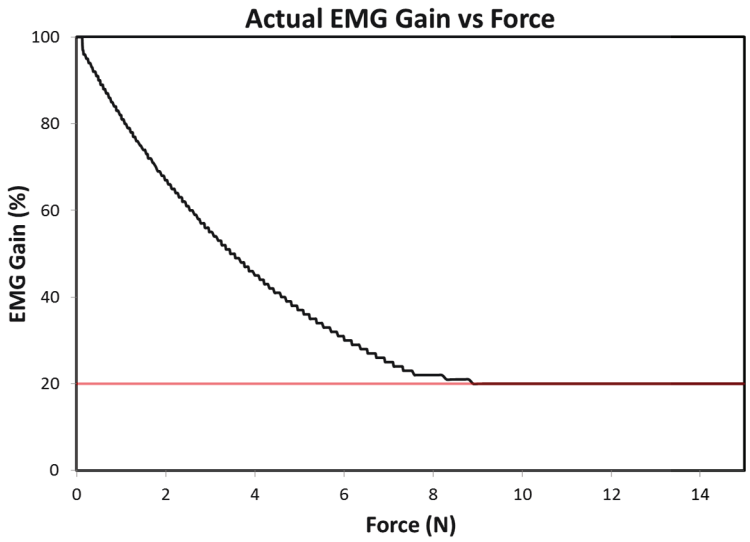

Figure 4.7: Actual EMG Gain curve over a range of applied grip force as measured from the prosthesis control unit. The EMG gain adjustment follows a negative exponential relationship with increasing force. If the sensors measure above 8 N while running this control algorithm then the EMG gain is limited to 20%.

limit of the gain changes. It should be noted that the sigmoidal and exponential EMG gain curves are written shown piecewise functions with a lower EMG limit of 20%, the inverse function is not shown as a piecewise function in this figure to highlight its impracticality for this application.

The Contact Detection algorithm is tested by providing a known force to a sensor and measuring the percent gain adjustment output of the prosthesis control unit. Fig. 4.7 shows the system response when running the Contact Detection control strategy.

4.3.2 Slip Prevention

In many instances, an amputee wishes to hold and maintain a stable grasp on an object, such as a mug of coffee. In this case, it is more desirable to implement the Slip Prevention strategy. A finite difference approximation using Newton's difference quotient takes the numerical derivative of the force sensor signal. The force signal is essentially run through a high-pass filter (differentiator) in the software of the prosthesis control unit in order to highlight areas of rapid changes in the grip force. A large negative change in the grip force indicates a slip at the prosthesis and grasped object interface.

A threshold is set in the software of the control unit to trigger a hand closure for 45 ms if the derivative of the force signal is less than (*i.e.* more negative) -0.02 N/ms. For the Reflex system, a drop in force of 0.02 N over 1 ms is used to quantify an instance of slip. This value was chosen as it is small enough to detect slight movement of a grasped object while also reducing the number of false positives. The time between samples of the force signal is approximately 1 ms, thus resulting in choosing a force derivative threshold of -0.02 N/ms. Fig. 4.8 shows the force derivative signal with the corresponding output signal from the control unit to make hand adjustments. Once a large enough negative spike is realized, a close signal is sent to the prosthesis. For the particular test shown in Fig. 4.8, a slip threshold of 0.08 N/ms is used.

An external hardware switch is used to change between the two control algorithms. Fig. 4.9 shows the circuit diagram of the hardware switch. The prosthesis control

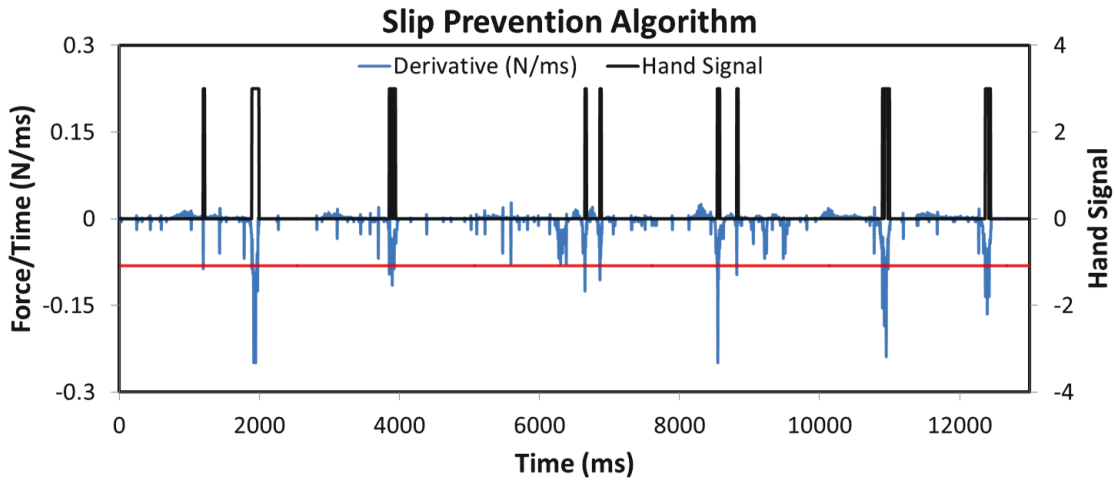

Figure 4.8: Slip Prevention algorithm showing the output of the prosthesis control unit based on the derivative of the force signal. A threshold of -0.08 N/ms is set to determine an instance of slip for this particular test.

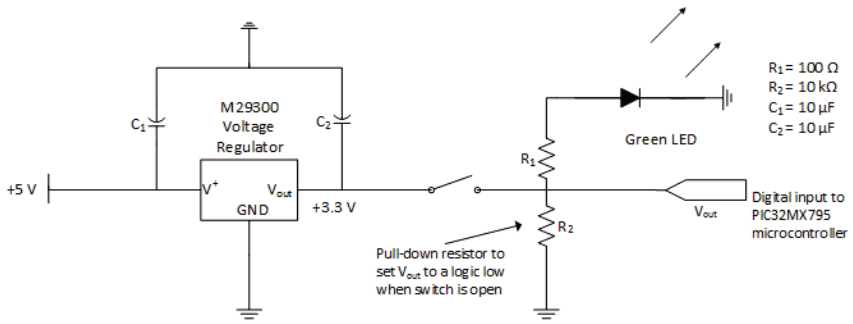

Figure 4.9: Circuit diagram for the switch to determine the control algorithm to be run on the prosthesis.

unit determines the appropriate control algorithm (*i.e.* Contact Detection or Slip Prevention) based on the output of the switch circuit. A logic high indicates that the Slip Prevention algorithm is to be used, whereas a logic low is used to running the Contact Detection strategy. A green LED is illuminated when the switch is closed, indicating that the Slip Prevention algorithm is running.

Measurements were made to determine the prosthetic hand latency after receiving a signal from the control unit. An infrared distance sensor (QRB1114) was used to measure hand movements, and an oscilloscope was used to directly measure the output of the prosthesis controller as well as the distance sensor. The time between when the signal was sent and when the prosthesis actually responded was measured 25 times; the average hand latency is 33.9 ms $\pm$ 1.9 ms.

4.4 Benchtop Experimentation

A series of simple experiments were performed to evaluate the ability of the Reflex system to detect forces while a prosthesis grasps an object. The sensor cuffs were fixed to the distal region of the index and middle fingers of a bebionic prosthetic hand. The movement of the prosthesis was controlled using fixed signal durations to reduce variability across experiments and trials. A tripod grasp was used by the prosthesis to grab a coffee mug and a hockey puck, Fig. 4.10. After a stable grasp is initiated, the object is held by the prosthesis for a few seconds before the hand

Figure 4.10: Prosthesis with attached sensor cuffs grasping an ice hockey puck and ceramic coffee mug.

is slowly opened to simulate object slip. The rate of increasing hand aperture is controlled by modulating the input of the prosthesis motors with a 5% duty cycle for a signal period of 42 ms. Opening at this controlled rate causes a slow decrease in the applied grip force, which eventually will cause the grasped object to slip from the prosthetic hand. This task is repeated at least 3 times with the same object.

The goal of the grasping task is to analyze the ability of the textile sensors to detect object contact as well as the movement of an object within the grasp of a prosthesis. In order to create a closed-loop tactile feedback system that is capable of detecting and preventing grasped object slip or deformation, it is necessary to be able to determine the state of the object while it is being manipulated by the prosthetic hand. Two of the most important aspects of determining the state of the object are when it is contacted by the prosthesis and when it begins to move within the grasp, indicating object slip.

The prosthesis control unit hosts a RN-42 Bluetooth module (Roving Networks), which allows all signals to be recorded in LabVIEW using serial port communication.

For these tests, contact between the prosthetic hand and the object is characterized as a positive increase in the sensor output. A minimum threshold is set to differentiate between signal noise and object contact; this threshold is chosen as 0.15 N above the resting state of the sensor. The definitions of *contact* and *slip* described in the previous sections are used.

4.5 Results and Discussion

Multiple trials (>4) were run for both objects, each grasping task generated similar results. To concisely summarize, a single result from each object are presented. Fig. 4.11 shows the results from the grasping task with the puck and Fig. 4.12 shows results for the mug.

The top charts in each figure are the normal force signal from the index and middle fingers of the prosthetic hand and the chart directly underneath shows the force derivative of those signals. The corresponding hand adjustment signal as well as the EMG gain reduction are presented below the force and derivative charts. Although the Contact Detection algorithm was not actively running, the gain reduction percent is shown to demonstrate the system's ability to use force values for making EMG gain adjustments.

For the hockey puck grasping task the object is primarily contacted by the index finger. Once contact is made, around 8 s, the finger sensors are activated as indicated

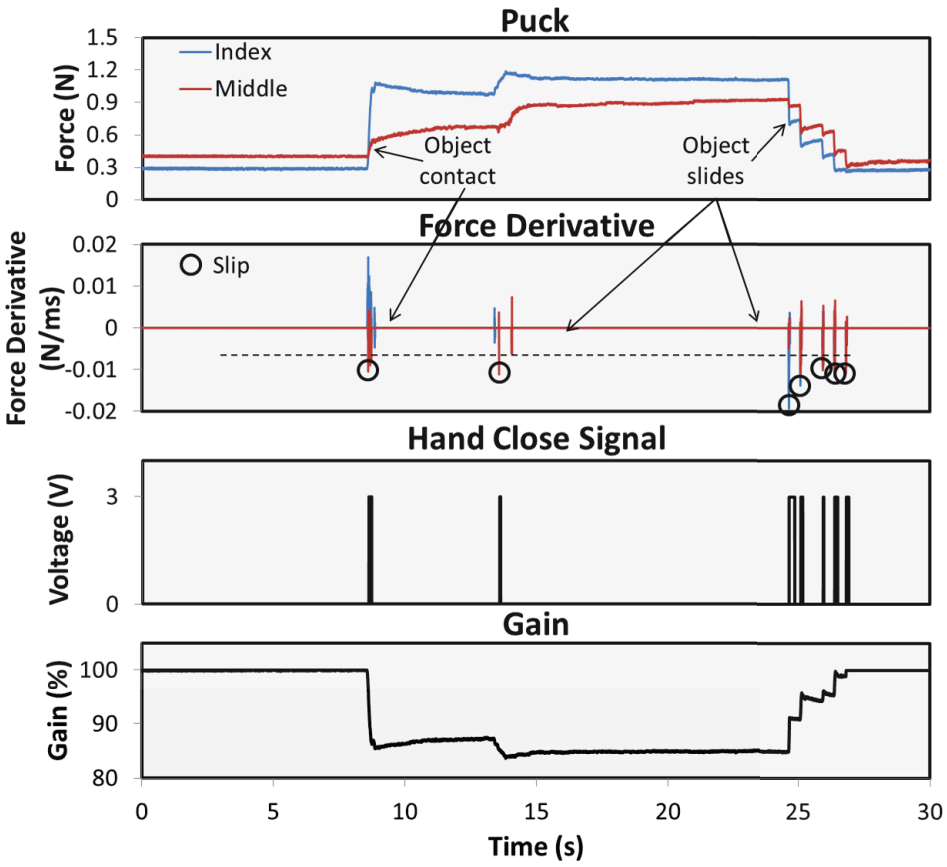

Figure 4.11: Results from the puck grasping task. The top chart shows the applied normal grip force and the one directly below it shows the derivative of that force signal. The corresponding hand adjustments as well as the EMG gain reduction are shown.

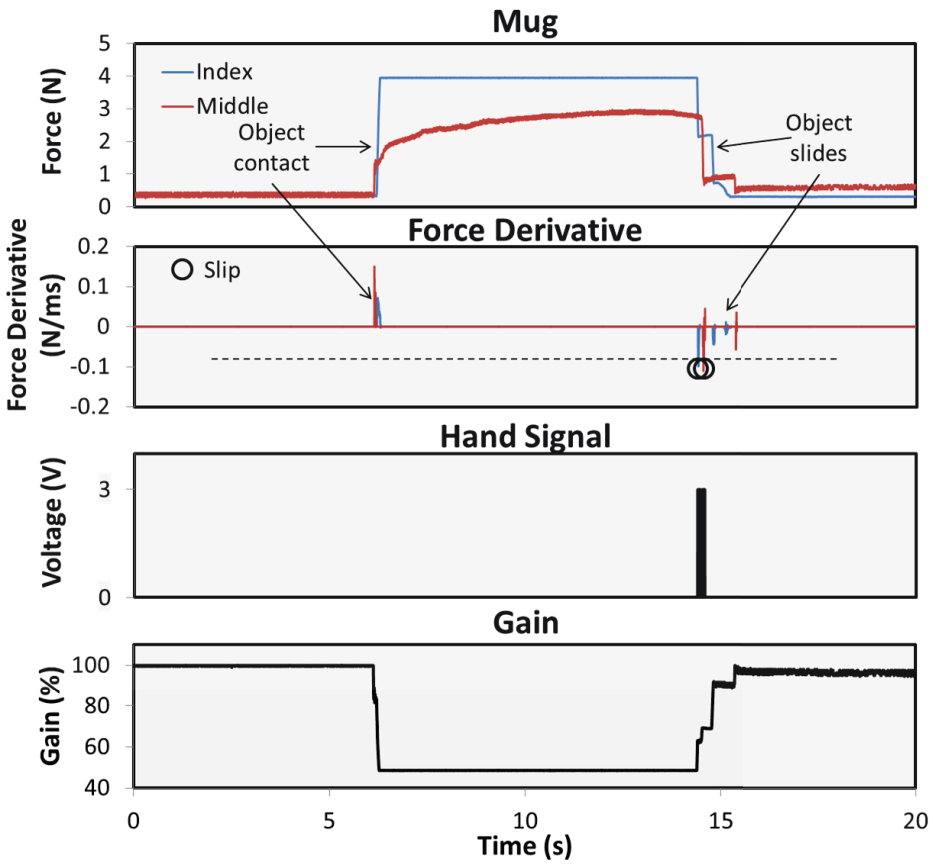

Figure 4.12: Results from the mug grasping task. The top chart shows the applied normal grip force and the one directly below it shows the derivative of that force signal. The corresponding hand adjustments as well as the EMG gain reduction are shown.

by the increase in the force signal. This jump is easily seen with the time derivative of the force signal. It should be noted that the initial force values measured by the sensor, before grasping the object, are nonzero. This is because the sensors are stretched to fit over the phalanges of the prosthetic hand, which causes a reaction force between the phalanx and the sensor. This is reflected by the nonzero force before grasping takes place. This offset is removed before computing any corresponding EMG gain adjustments. By taking the derivative of the force signal, there is no need to zero each sensor because the signals of interest can be isolated as positive or negative spikes. Once contact is made with the object, the finger sensors are activated. A corresponding positive spike is seen, indicating contact between the prosthesis and the object.

The grasped puck shows instability at the 13 s mark as the hand is closed tighter around the object. There is a slight, yet quick, decrease in the force signal, which results in a noticeable negative spike in the force derivative signal. This indicates that the object is slipping across the force sensors. The prosthesis regains a stable grasp on the puck at 14.5 s, which is noticed from the positive spike in the force derivative at the same time. The grasped object is held stationary until 24 s at which time the object begins to slip from the grasp as the hand is slowly opened at a controlled rate.

The onset of object slip is realized with the synchronous decrease in applied grip force on both the index and middle fingers of the prosthetic hand. The step like force signal is characteristic of an object undergoing stick-slip. The abrupt reduction of

the force is translated into negative spikes in the force derivative signal. The object fell completely from the grasp of the hand at 26.5 s.

In a similar fashion, the ceramic mug grasping task shows positive increases in the force derivative signal, indicating object contact. Onset of the mug slipping from the prosthesis grasp is characterized by the negative spikes of the force derivative signal, similar to that seen during the grasping task with the hockey puck. The sturdy nature and geometry of the mug allowed for a higher grasping force from the prosthetic hand; however, instances of slip are characterized as signals below -0.08 N/ms for these tests. This link between grasping tasks is most likely due to the fact that the hockey puck and coffee mug have similar weights. It is interesting to note that the applied grip force for both objects is slightly less for the middle finger than the index finger. This can be attributed to the nature of the prosthetic hand's closing mechanics as well as object shape. The first area of contact with the object made by the prosthesis is with the thumb and index finger. This results in higher grip forces being applied to these particular areas.

This chapter discusses user needs for current upper limb prosthetic devices. Results from a survey of upper limb amputees suggest the need for improving grasping functionality of prosthetic hands. The two control algorithms used in the Reflex system, Contact Detection and Slip Prevention, are presented along with the circuit design that interfaces the textile sensors to the controller. Preliminary results show the system's ability to monitor object contact and slip during grasping with a

prosthesis.

Chapter 5

Experimentation and Results

This chapter describes the experimental methods and the results for the Reflex system. The experimental methods were reviewed and approved by the Johns Hopkins Medicine Institutional Review Boards (IRB) before any testing was performed. The goal of these experiments is to evaluate compliant tactile sensors and the control algorithms described in Section 4.3 as part of a tactile feedback system to enhance upper limb prosthesis control during grasping.

5.1 Experimental Methods

A total of ten able body (*i.e.* no limb loss) participants volunteered for this study. Each participant operated a prosthetic hand with his or her own EMG signals to grab objects. Participants used a bebionic prosthetic hand attached to a brace that was

placed on their arm. Each participant underwent two tasks: A *Compliant Grasping* task in which he or she picks up and moves objects as well as a *Slip Prevention* task, which involves holding an object while weight is added. Every person provided informed consent before, as required by the IRB, before the tasks were performed.

5.1.1 Testing Protocol

For the *Compliant Grasping* test, the participant is required to move a set of items. Each item is grasped, moved approximately 25 cm, and released. The participant is instructed to grab and move each item without breaking it. The items, listed in Table 5.1 and shown in Fig. 5.1, include foam packing peanuts, crackers, hollowed eggs, Styrofoam cups, and unopened soda cans. These items were chosen because they represent a wide range of common objects that an amputee might interact with and also because research using a similar grasping experiment utilized such objects [35]. The force required to break an object (Table 5.1) is determined based on previous publications as well as by breaking the objects while a commercial force sensor measures the applied force [35]. The number of broken items and time to complete each set of movements is recorded during the experimental trials. Each participant moves the objects with his or her able hand, a prosthesis, the prosthesis with sensors attached (but no active feedback to the control unit), and finally the prosthesis with sensors and the *Contact Detection* algorithm running (*i.e.* tactile feedback, see Section 4.3.1).

In the *Slip Prevention* test, the participant closes the prosthesis around a grad-

Table 5.1: Items used in the grasping tasks.

	Mass (g)	**Force to Break (N)**
Foam	0.01	>3
Cracker	3	>5
Egg	5	>25
Cup	3	>10
Can	377	>3,000

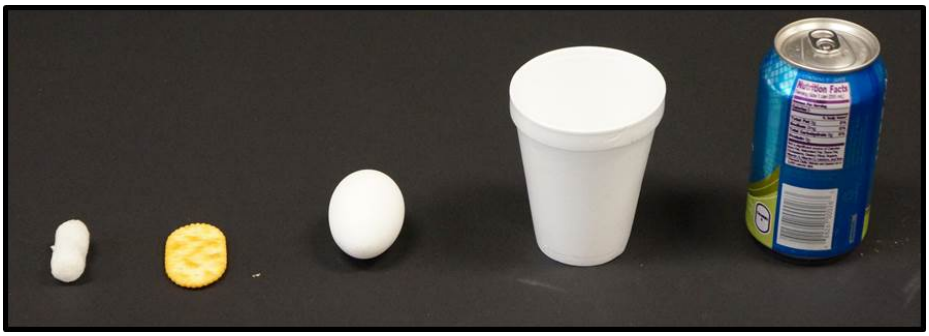

Figure 5.1: Items used for the grasping tasks.

uated cylinder. After a stable grasp, 4 bags of sand are individually added to the cylinder. The first 3 are each 1 N and the final one is 2 N, for a total of 5 N. Another trial involves placing a 12oz (377 N) can of soda into the empty cylinder. Fig. 5.2 shows the method for adding weight, in the form of either sand or a soda can, to the grasped cylinder. The distance the cylinder moves with each weight addition is recorded. If the cylinder falls, it is considered a failed trial. For these experiments, an instance of slip is defined as a change in the grasping force signal of -0.02 N/ms or less.

Each task is performed by the participant's able hand, the prosthesis, the prosthesis with sensors attached but no feedback to the controller, and then finally the prosthesis with sensors that provide tactile feedback to the control unit.

5.1.2 Equipment and Data Acquisition

The Reflex system was embedded within a brace, which was made to allow an able bodied users to move and control a prosthetic hand with their own EMG signals. The brace, Fig. 5.3, is constructed out of thermoplastic and allows the user to place his or her arm within the socket to move a prosthesis. The user has full control over the opening, closing, and movement of the terminal device.

Three textile sensors, each with two sensing elements, were placed on the thumb, index, and middle fingers of the prosthesis. Fig. 5.4 shows the placement of the sensors. The tips and distal regions of these fingers are the primary contact regions

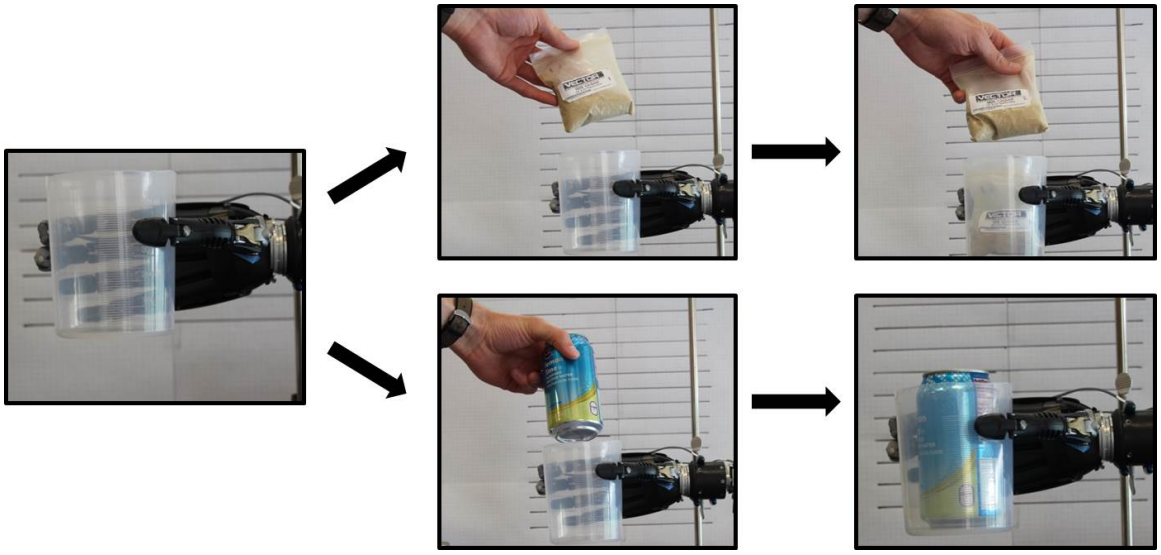

Figure 5.2: Steps for the slip test. Object(s) (sand or soda can) are added to the cylinder. Measurements determine the amount of movement after the addition of weight.

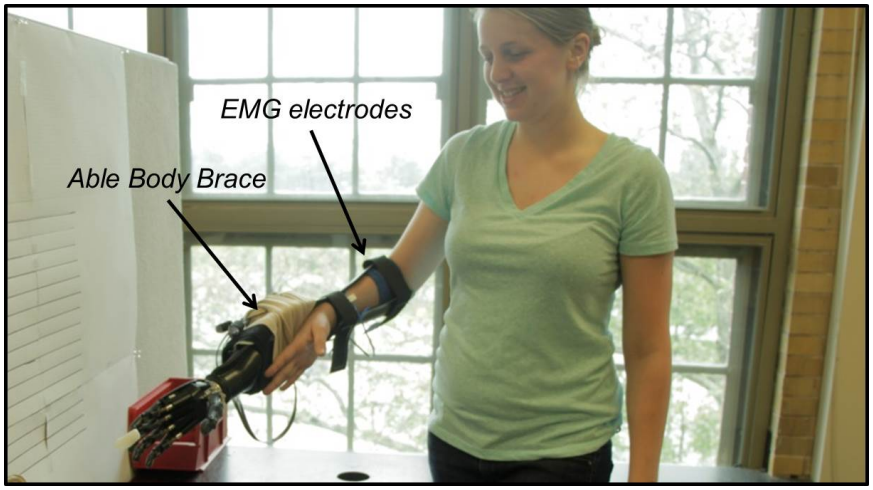

Figure 5.3: Able body brace that allows users to control a prosthesis using natural arm movements and EMG signals.

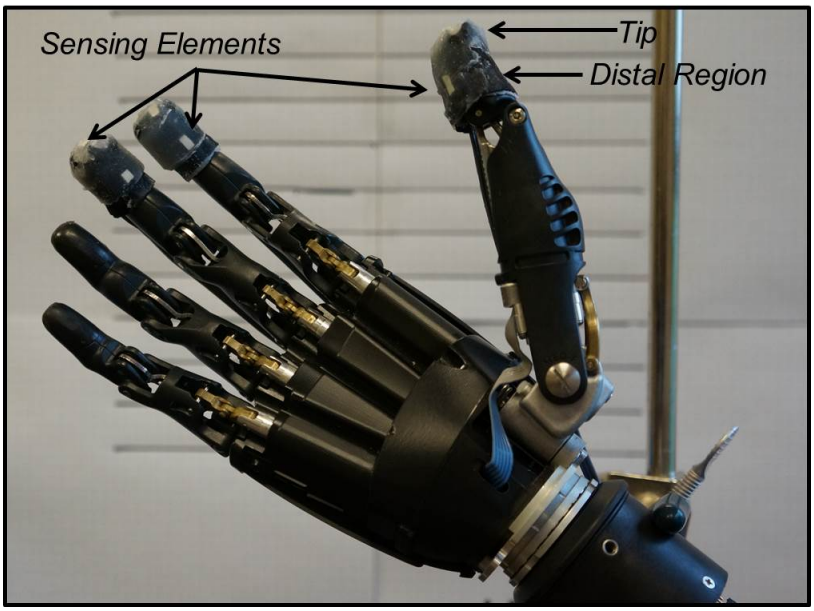

Figure 5.4: Sensor placement on the prosthetic hand.

during grasping, which is where the sensing elements of each cuff are located. This is due to the closing mechanics of the device, as seen in Fig. 5.5. A 3-fingered tripod grip (Fig. 5.5) is used to grasp the objects.

Data were sent wirelessly via Bluetooth communication to a custom signal viewer, which was built using LabVIEW. The signal viewer recorded sensor and EMG data sent from the Reflex control unit. Data were sampled at 260 Hz. Results were saved, plotted and analyzed using MATLAB and Excel. In addition to acquiring signals from the sensors and control unit, every experiment was recorded using a Sony NEX-5R digital camera (16.1 megapixels, 60 fps). Although the video recordings capture the time to complete each task, a stopwatch was also used as a backup. Adobe Premiere Pro was used to analyze the video footage, which included measuring object movement

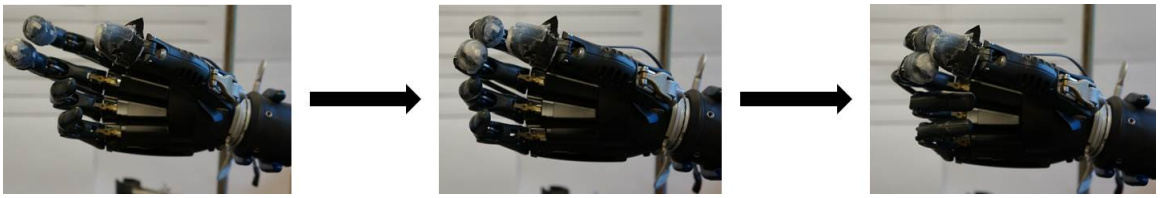

Figure 5.5: Closing mechanics of the bebionic prosthetic hand. The tip and distal region of the thumb, index, and middle fingers are the primary areas of contact during grasping.

during the slip experiments.

5.2 Testing Results

The results are broken up into two subsections: *Compliant Grasping* and *Slip Prevention*. Each subsection provides charts of the force sensor signals during the task as well as the Reflex control unit output. Information regarding the time to complete tasks and the number of failed trials (*i.e* broken items or complete object slip) are presented for the *Compliant Grasping* tests. Results from the *Slip Prevention* tests are presented as failure rates as well as average distance moved by an object that undergoes slip.

5.2.1 Compliant Grasping

As described previously, the *Compliant Grasping* experiments involved moving 5 items without breaking them. Fig. 5.6 shows each item grasped by the prosthesis.

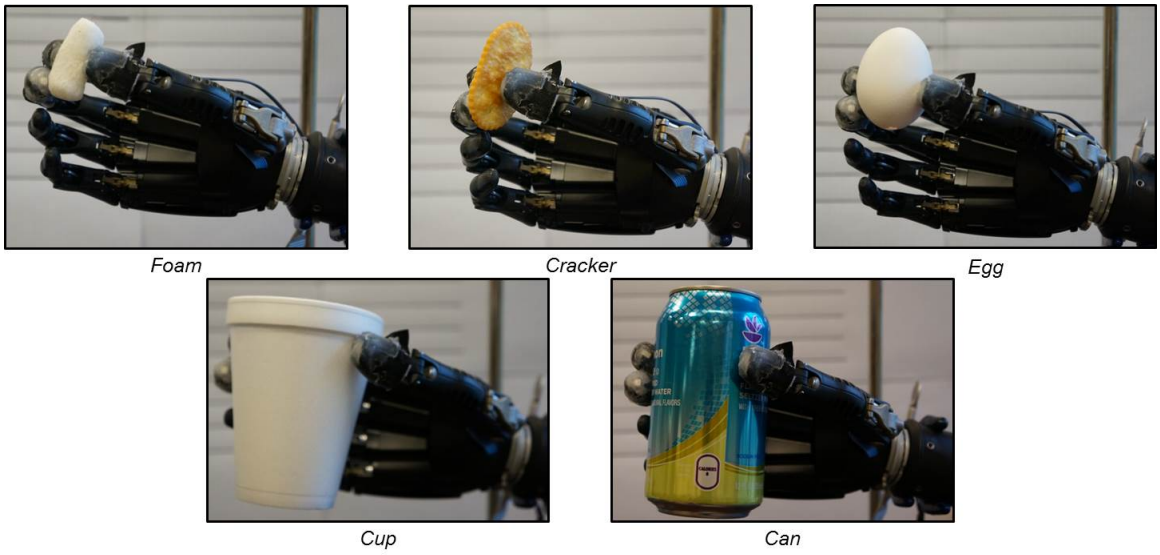

Figure 5.6: Items used for the *Compliant Grasping* experiments. 5 of each item was picked up and moved. The time to complete each task and the number of broken items was recorded.

Figs. 5.7, 5.8, and 5.9 show an average sensor response while grabbing a foam piece, cracker, egg, cup, and can, respectively. The corresponding EMG gain % is shown as well. Although multiple trials were run with each object, results from a single grasp are shown from each object. These results show the sensors' ability to detect small grasping forces, realizing when contact is made with an object.

Although some of the objects are fragile, the Reflex system is able to detect object contact and the force sustained to hold and move an item. From Figs. 5.7, 5.8, and 5.9, it is obvious that even small grasping forces are detected by the system. It is also apparent that the primary areas of contact during grasping are the tip and distal regions of the index finger, the distal region of the middle finger, and the tip of the

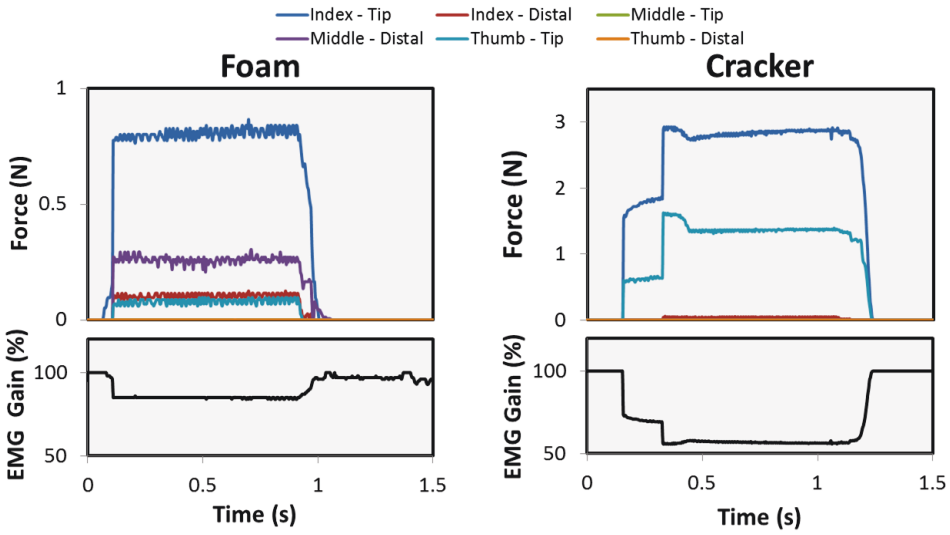

Figure 5.7: Results from a grasping task involving a foam piece (left) and a cracker (right). The corresponding EMG gain %, as output by the Reflex controller, is shown as well.

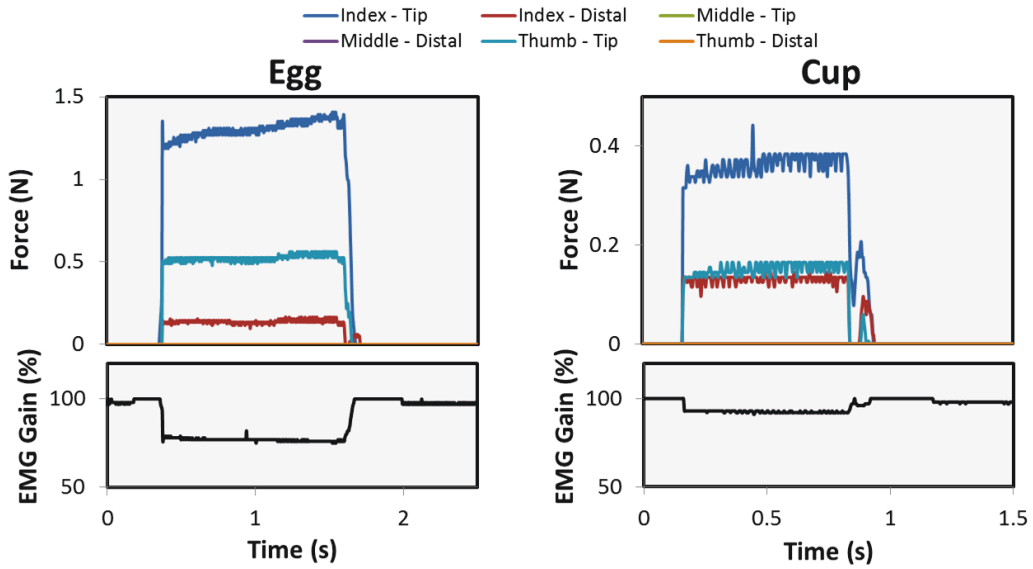

Figure 5.8: Results from a grasping task involving an egg (left) and a cup (right). The corresponding EMG gain %, as output by the Reflex controller, is shown as well.

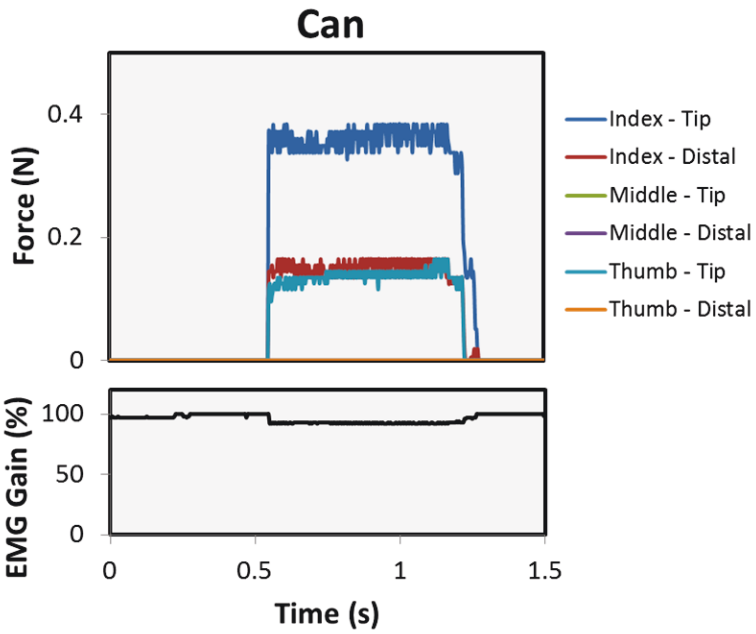

Figure 5.9: Results from a grasping task involving a can. The corresponding EMG gain %, as output by the Reflex controller, is shown as well.

thumb. This is expected due to the closing mechanics of the prosthesis. The bottom portion of these same figures shows the EMG gain % adjustment made by the system control unit during the grasping task.

Table 5.2 shows the percent failure rate for the movement of each item. Failures across all trials are combined and a percentage is presented to show the likelihood of a failed movement task for each item based on the device used (*i.e.* able hand, prosthesis, prosthesis with sensors, or prosthesis with sensors and tactile feedback). It should be noted that a "failure" occurs when an item breaks or, in the case of soda can, falls completely from the grasp of the prosthesis. The results show a decreasing likelihood of objects breaking, with the addition of sensors and the Contact Detection control algorithm. With failure rates of 44% and 32% for the foam and crackers, respectively, with just a prosthesis, a drastic change is seen with the addition of sensors to the device. With sensors attached, users only break 16% of the foam packing peanuts and 10% of the crackers. A similar reduction, although not as large, is seen for the other three grasping tasks (eggs, cups, and cans). When running the Contact Detection algorithm, the chance of breaking foam pieces and crackers is reduced even further. None of the items were broken while using an able hand (as seen in the first column of Table 5.2.

The time it takes to complete each task is normalized using the time required to move items with the participant's able hand. The normalized time index is averaged for each item and the results are presented in Fig. 5.10. There is a decreasing trend

Table 5.2: Percent failure rate of moving items based on device used.

	Able Hand	Prosthesis	Sensors	Contact Detection
Foam	0%	44%	16%	10%
Crackers	0%	32%	10%	8%
Eggs	0%	4%	2%	2%
Cups	0%	2%	0%	0%
Cans	0%	6%	0%	0%

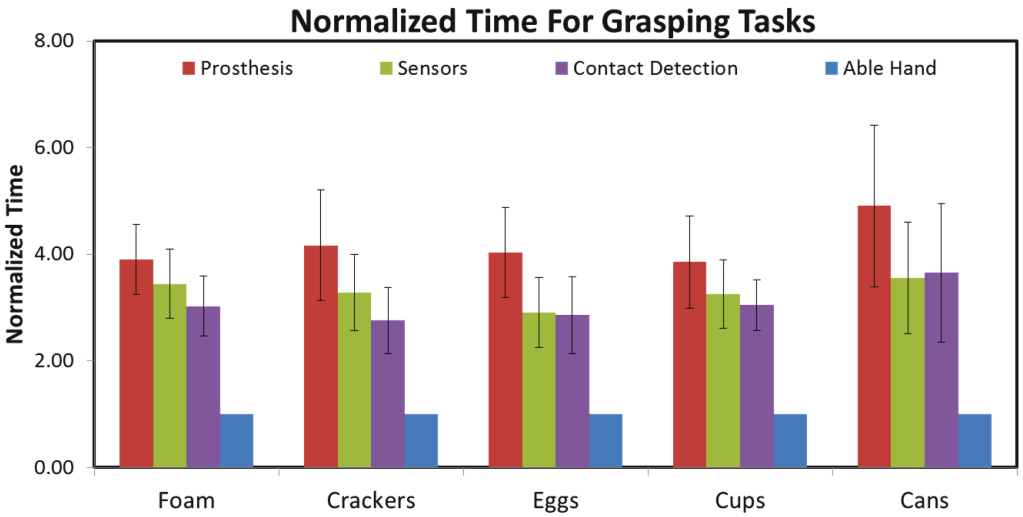

Figure 5.10: Normalized time to complete each movement task. There is a decreasing trend between using a prosthesis and using the prosthesis with sensors attached. The difference between using the sensors and the Contact Detection algorithm is smaller.

in the time it takes to complete the tasks with a prosthesis and a prosthesis with sensors. With the exception of the can moving task, there is a further decrease in average time to complete each task between using a prosthesis with sensors and a prosthesis with Contact Detection. To further clarify, it should be noted that during the grasping tasks with a prosthesis and sensors, there is no direct feedback from the sensors to the system control unit. This is to assess how the compliant nature of the sensors effects the results.

5.2.2 Slip Prevention

The *Slip Prevention* experiments required the study participant to grasp a plastic cylinder. After grasping, weight was added, either in the form of a series of small sand bags or else an unopened can of soda. Fig. 5.11 shows a typical force signal, its derivative, and the corresponding hand close signal sent by the Reflex control unit due to measured instances of slip for these experiments. The primary area of contact while grasping the cylinder is the distal region of the index finger and thumb of the prosthesis. This is because the diameter of the cylinder is approximately 10 cm, causing the hand to contact the object with the distal regions of its phalanges. Table 5.3 shows the percent of failed trails for the slip tests. The likelihood of an object slipping completely from a grasp is higher when participants used just the prosthesis without any sensors. There are very few failed trials once sensors are added to the prosthesis and no failed trials with the implementation of the Slip Prevention control

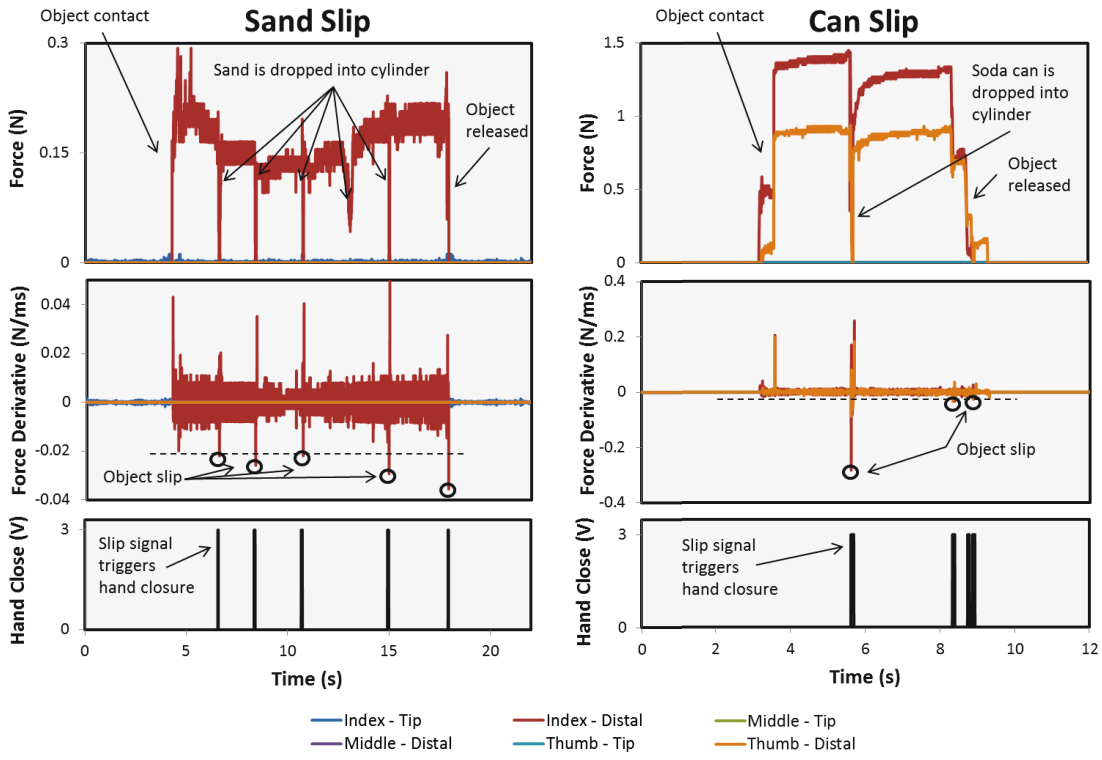

Figure 5.11: Results from the slip grasping tasks. The charts on the left are from a test where bags of sand were added to the grasped object. The charts on the right are from a test where an unopened can of soda was added. The bottom chart on each side shows the hand signal sent from the control unit due to detected instances of object slip. For these two tests, the object did not fall from the grasp of the prosthesis after weight was added.

Table 5.3: Percent of failed trials during the slip tests.

Object Added	Able Hand	Prosthesis	Sensors	Slip Prevention
Sand	0%	9%	3%	0%
Can	0%	38%	3%	0%

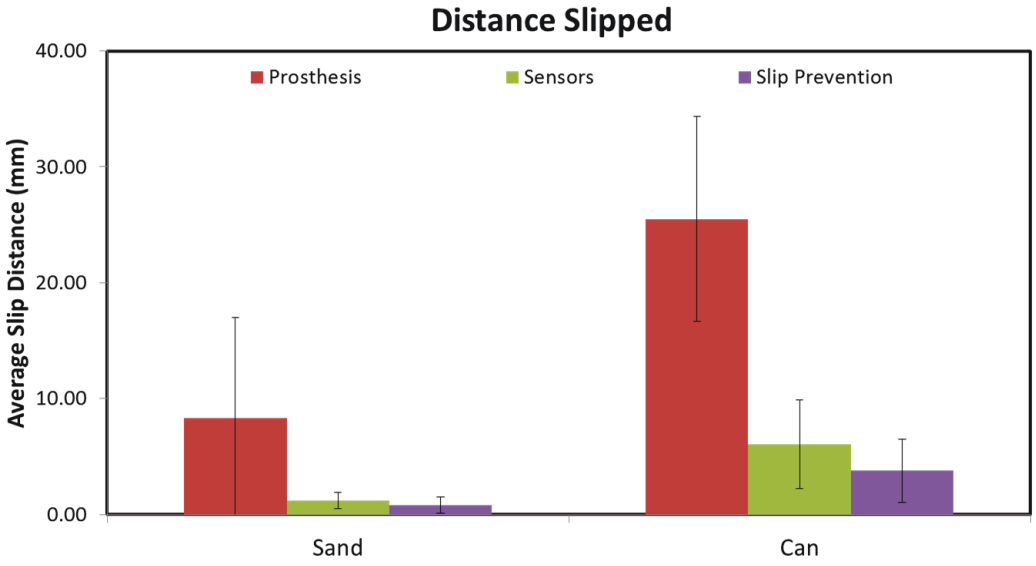

Figure 5.12: Average distance moved by the grasped object after adding weight.

algorithm.

Another useful metric is the distance moved by the object with each addition of weight. Fig. 5.12 shows the average distance the grasped object moved after weight is added. The average distance moved during the slip tests with an able hand are effectively zero and are not reported in Fig. 5.12. Trials where the object completely slipped from the grasp are included in the average distance calculations and are also counted towards the number of failed trials.

5.3 Discussion

The results presented in the previous section are broken up based on the experiment (*Compliant Grasping* and *Slip Prevention*) and discussed in more detail.

5.3.1 Compliant Grasping

Figs. 5.7-5.9 show that the sensor cuffs are capable of detecting forces as small as 0.1 N during grasping and providing tactile feedback for EMG gain adjustments through the Reflex control unit. It should be noted that the operating range of the sensors was quantified as 0.5 N — 20 N (Section 3.3) and there is a reaction force applied to the sensor when it is stretched over the prosthesis phalanx. This reaction force is great enough to to enter the operating range of the sensors, essentially allowing for the reliable detection of small forces (Fig. 5.7). However, the reaction force is removed from the recorded values because each sensor signal is zeroed when the device is powered on. For all items, the sensors measured the applied grasping force during contact. The primary areas of contact for these grasping tasks appears to be the tip and distal region of the index finger, the distal region of the middle finger, and the tip of the thumb. This makes because of the closing mechanics of the prosthesis.

It is clear from Table 5.2 and Fig. 5.10 that the compliant nature of the sensor cuffs offers a significant benefit to decreasing the failure rate of moving items and the time to complete each task. The difference between implementing the Contact Detec-

tion control algorithm is less obvious, although still present. The sensors successfully reduced the rate of breaking objects from 44% with just a prosthesis to 16%. This percentage dropped even more to 10% once the EMG gain adjustment control was implemented. A decrease from 32% to 10% was realized for the task that required participants to move crackers. There is an additional decrease to an 8% failure rate once the Contact Detection control is implemented. This suggests that the most beneficial form of enhancing grasping functionality with a prosthesis is to add compliant tips to the main areas of contact. This is supported further with the results that show a decrease from a failure rate of 4% to 2% for the egg task. In addition, there is a decrease from 2% and 6% for moving the cups and cans, respectively, to 0% for both. There is no difference in failure rate between using compliant sensors and providing tactile feedback to the Reflex controller for the tasks involving eggs, cups, and cans.

Fig. 5.10 shows the average normalized time values to complete each task. Again, it is obvious that the addition of compliant sensors increases grasping ability by reducing the time needed to complete each grasping and movement task. There is also a slight benefit from using the sensor measurements to run the Contact Detection control. The only instance where the average completion time was not further reduced by running the Contact Detection algorithm was during the task involving cans, yet the average normalized time is still less (3.65) than that of just the prosthesis without any compliant sensors or tactile feedback (4.91). The largest difference in time is for the cracker grasping task. The compliant sensor reduce the normalized time from

4.17 to 3.28, but the addition of the Contact Detection algorithm decreases it even further to 2.76. Compared to the task for the cans, which has a reduction from 4.91 to 3.55 with sensors and 3.65 with Contact Detection, there seems to be most benefit for implementing the control algorithm with fragile objects, such as the crackers and foam. These items, although easy to break, have the largest reduction in time to complete once tactile feedback is provided to provide EMG gain adjustments (Fig. 5.7).

An analysis of variance was performed on the average normalized times for each task to evaluate statistical significance of the results. There is no significant statistical difference ($p > 0.05$) between using just compliant sensor fingertips and implementing the Contact Detection control algorithm. There is, however, statistical significance ($p < 0.05$) between using compliant sensors and just a prosthesis for the tasks involving the crackers, eggs, and cans. There is a significant statistical difference between using just a prosthesis for the grasping tasks and using tactile feedback from sensors to implement the Contact Detection algorithm for all trials, except for the task involving the cans. This shows the benefit using tactile feedback with compliant sensor fingertips for grasping tasks with a prosthesis.

5.3.2 Slip Prevention

The results from the slip experiments show the controller's ability to provide closing pulses to the prosthesis, in real-time, to prevent complete object slip. The

derivative of the force signal (Fig. 5.11) enables the Reflex control unit to determine instances of object slip using a threshold of -0.02 N/ms. This method allows the controller to detect slip regardless of the applied grip force, because it is the change in the force signal that indicates object movement. It is apparent in the force signals when weight is added to the cylinder grasped by the user. The added weight causes a sharp decrease in the force signal as the rubber layer of the sensor is stretched, causing a sudden reduction in force. If the change is drastic enough, the control unit detects it and sends a close pulse of approximately 45 ms to the prosthesis. For both the sand and can slip tests presented in Fig. 5.11 the controller sent a hand close signal for every instance of slip detected. This help prevent the object from falling.

When the grasped object slips completely (*i.e.* falls), it is considered a failed trial. The failure rate when using sand to increase weight is 9% for the prosthesis without any sensors or tactile feedback. The addition of sensors decreases this to 3%. Implementation of the Slip Prevention algorithm resulted in a 0% failure rate as well. In a similar fashion, the failure rate when using the unopened can of soda dropped from 38% to 3% when sensors were placed on the prosthesis and then to 0% for the Slip Prevention control (Table 5.3). This suggests that the compliant nature of the sensors is enough to help prevent complete object slip, but the Slip Prevention control algorithm can reduce object slip even more.

The distance moved by the grasped object with the addition of weight (Fig 5.12) provides more insight to the direct benefits of tactile feedback for preventing slip. The

average distance moved when sand was used is 8.3 mm for the prosthesis and only 1.2 mm with sensors attached to the prosthesis. A further decrease in object movement is seen when implementing the Slip Prevention control (0.8 mm). The compliant sensors reduced movement from 25.5 mm with the prosthesis to 6.1 mm when a soda can was used as the weight. The control algorithm had an average movement of 3.8 mm, slightly less than the movement from just sensors without the control. This suggests that the Slip Prevention algorithm is useful in preventing both small and large additions of weight from causing object slip.

An analysis of variance shows that there is statistical significance ($p < 0.05$) between the results from the slip tests with a prosthesis and the prosthesis with attached sensors. There is no significant difference when comparing just the compliant sensors to the Slip Prevention algorithm. This suggests that the largest factor for prevent object slip is through the compliant nature of the interface between the prosthesis with sensors and the grasped object.

The results show that the addition of compliant force sensors offers a clear benefit in grasping delicate objects and also reducing the amount of slip of a grasped object. The addition of tactile feedback from the sensors to the prosthesis control unit offers additional benefit in terms of grasping fragile objects, such as foam packing peanuts and crackers, while also helping further reduce object slip for small weight additions (~ 1 N). However, it appears as if the most beneficial aspect of the Reflex system is the compliant nature of the textile sensors.

Participants of the study were interviewed after the tests and asked to provide any feedback on the system. All of the users agreed that the compliant sensor cuffs provided additional stability while grasping objects and helped reduce the effort required to grasp a fragile object, such as the foam peanuts or crackers. An amputee who witnessed the experiments commented on the need for such compliant fingertips as they greatly enhanced grasping ability. There was also support from amputees regarding the use of a Contact Detection algorithm to reduce EMG signals. Amputees will often use significant effort to grasp fragile objects or else avoid picking them up at all. Every amputee that provided feedback on the Reflex system felt that such an algorithm could be very beneficial in their daily lives.

Chapter 6

Concluding Remarks

This final chapter provides a brief summary of the work presented in this thesis, its findings, and the conclusions made from those findings. As most research projects seem unending, a look at the future directions for this work is included.

6.1 Project Summary

Upper limb amputees lose their ability to use sensory information, particularly tactile perception, for controlling their prosthetic limb. Current prosthetic hands lack any form of tactile feedback as a means to enhance functionality. Despite having technology capable of greatly improving a prosthesis, commercial devices are limited in that they lack a way to use tactile information, such as force and pressure. This work presents a close-loop feedback system, called Reflex, that uses textile-based force

sensors to enhance grasping functionality.

Textile force sensors are designed, fabricated, characterized, and tested as part of the Reflex system for use with upper limb prosthetic devices. In particular, the Reflex system is designed to enhance grasping functionality with a prosthetic hand. The force sensors are made from stretchable fabrics and covered with a 3 mm layer of rubber, to provide compliance to the surface. The sensors are mounted on the thumb, index, and middle fingers of a bebionic prosthetic hand and are used to provide tactile feedback to the control unit of the system. Each sensor has two sensing elements, one on the tip and another on the distal region of the phalanx. An in-depth characterization of the sensors show they offer an operating range of 0.5 — 20 N, which is comparable to commercially available sensors used for prosthetic hand applications.

The sensors were connected using instrumentation amplifiers to increase signal quality. Real-time processing was realized using a custom control unit. The controller was used to take in the analog signals of the sensors in addition to an amputee's EMG signals. The controller is small enough to fit within an amputee's socket. Wireless communication allowed data to be sent to an external PC for recording. The control unit reads in the force values measured by the sensors. Two control algorithms were designed, a *Contact Detection* method, which effectively reduces the user's EMG signal by applying a gain adjustment, and a *Slip Prevention* method, which sends an electrical pulse to close the prosthesis when an instance of slip is detected. Both of these algorithms rely on the tactile feedback provided by the sensors.

Testing showed the benefit of using compliant surfaces for grasping fragile objects as well as for preventing slip after grabbing an object. Experiments were designed to evaluate the tactile feedback system's ability to enhance grasping function with a prosthesis under the control of an actual amputee. Results show that adding compliant sensors to the fingers of a prosthesis greatly reduces the time to grab and move fragile objects. Furthermore, providing tactile feedback to the prosthesis control unit continues to improve the ability to grab and move fragile objects without breaking them.

The Contact Detection algorithm was able to reduce the EMG input signal after detecting contact between the prosthesis and the target object during a grasping task (Figs. 5.7 - 5.9). Results suggest that the compliant nature of the sensors offers the most benefit to grasping, which caused a reduction in the failure rate of the foam from 44% to 16% and from 32% to 10% for the crackers. The addition of tactile feedback to make EMG gain adjustments in real-time is also beneficial, but to a smaller extent, as it further reduced the likelihood of breaking foam pieces to 10% and 8% for the crackers. The sensors also reduced the time required to complete each grasping task, compared to using just a prosthesis (Fig. 5.10). For instance, using sensors reduced the average normalized time to complete the cracker grasping task from 4.17 to 3.28, with an even further reduction to 2.76 while using the Contact Detection control algorithm.

The Slip Prevention algorithm was capable of detecting object slip and providing

an electrical pulse to close the prosthesis in an effort to prevent further slip. To evaluate this control strategy a user grabbed an empty cylinder while weight was added. The sensor cuffs, because of their compliant layer, drastically reduced the likelihood of an object falling from the grasp of a prosthesis with the addition of weight. The initial likelihood for object slip is 9% when sand is added to the grasped object and 38% when a soda can is added. These values drop to 3% for both items when the sensors are used and drop again to 0% with the Slip Prevention control. The use of tactile feedback to actively prevent instances of slip resulted in less movement of the grasped object during the addition of weight. The average distance moved when sand is added dropped from 8.3 mm to 1.2 mm with sensors and to 0.8 mm with Slip Prevention. For the slip tests involving the can, the average movement dropped from 25.5 mm to 6.1 mm with the addition of the sensors and to 3.8 mm with the control algorithm.

Reflex is a closed-loop tactile feedback system that uses force information from compliant sensors that are easily mounted on a prosthetic hand. The system offers two control strategies with the ability to switch between the two based on the environment. On-board processing by the control unit allows real-time hand adjustments based on tactile feedback. This is the first documentation of a system that utilizes tactile feedback from low cost sensors that can be fixed to the phalanges of any upper limb prosthesis while offering multiple control strategies to enhance grasping functionality.

6.2 Future Sensor Design

The sensors used in this work have low material costs, but require careful fabrication steps to ensure functionality. A downside is the time it takes to make each sensor. To move forward, the sensors should be made in a way that reduces failure rate. The current sensors can fall apart over time after taking them on and off the prosthesis. A more stable sensor that fully embeds the sensing element would be necessary for future improvements. One recommendation would be to use SynTouch's most recent sensor, a cheaper version of the BioTac (Section 2.1.2.2), called the NumaTac, which uses an air filled and compliant fingertip pressure sensor [62]. However, using such a sensor would require hardware changes to existing devices to mount the sensors on the fingers. Other possible direction for sensor improvement is to use advanced methods for fabrication, which could improve the quality and durability of the sensors.

6.3 Future Control Strategy

The control algorithms implemented in the Reflex system are basic, yet appear to be functional. Amputees have provided positive feedback regarding the Contact Detection strategy. It seems as if grasping objects is a cognitively expensive task in that amputees have to constantly watch what their prosthesis is interacting with. The benefit of the Contact Detection strategy is that it can help reduce the need for an amputee to watch his or her hand the entire time they are grasping an object. One are

of improvement would be to increase the Contact Detection algorithm's sensitivity, essentially allowing it to make larger reductions of the EMG signal based on smaller contact forces.

The Slip Prevention algorithm could be improved by implementing a proportional scheme that would cause a large amount of slip to trigger a longer closing pulse to the prosthesis. Another addition would be to keep the force values across all active sensors balanced to help eliminate unnecessary torque or an unbalanced grasping force on a grasped object. However, this would require monitoring of static force values, as opposed to changes in the force signal.

6.4 Future Directions

While this work introduces a system that will help enhance the lives of upper limb amputees, there is the added potential to use tactile information to stimulate peripheral nerves in an effort to provide sensations of force, texture, and even proprioception. The notion of providing spike trains directly to a peripheral nerve to elicit these sensations has been proposed and has even sparked a Defense Advanced Research Projects Agency (DARPA) funded project known as HAPTIX [112, 113].

One particular model that could be beneficial for this effort is the basic leaky integrate and fire (LIF) neuron model [114]. In its simplest form, a neuron is modeled

as a leaky integrator of the input $I(t)$.

$$\tau_m \frac{dv}{dt} = -v(t) + RI(t) \tag{6.4.1}$$

where $v(t)$ represents the membrane potential at time t, and τ_m is the membrane time constant. R is the membrane resistance. This is a simple RC circuit where the leakage is due to the resistor and the integration of $I(t)$ is from the capacitor in parallel. When the membrane potential reaches a spiking threshold, v_{th}, it is reset instantaneously to a lower value, v_r. For the case of a constant input ($I(t) = I$), one can assume $v_r = 0$ and Eq. 6.4.1 is then expressed by:

$$v(t) = RI \left[1 - exp(-\frac{t}{\tau_m}) \right] \tag{6.4.2}$$

The asymptotic value of $v(t)$ is simply RI, which if less than v_{th} can't generate a spike. If $RI > v_{th}$ then the model will generate periodic spike firing. Assuming an initial condition of 0 for the membrane potential ($v(0) = v_r = 0$), then the time of the first spike is found to be:

$$t^{(1)} = \tau_m ln \frac{RI}{RI - v_{th}} \tag{6.4.3}$$

which also gives the time between successive spikes. The mean firing rate of the modeled neuron can also be found with:

$$f = \left[\Delta_{abs} + \tau_m ln \frac{RI}{RI - v_{th}} \right]^{-1} \tag{6.4.4}$$

where Δ_{abs} is an absolute refractory period, which is essentially the period following the firing of a nerve fiber when it cannot be stimulated no matter the magnitude of

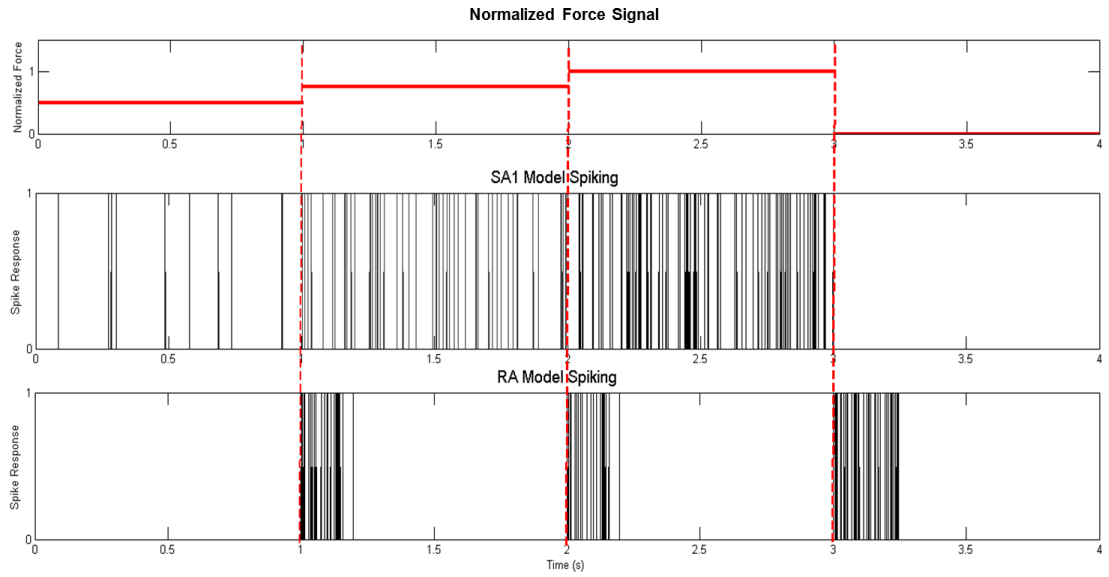

Figure 6.1: Leaky integrate and fire model using a force signal to elicit spiking activity from SA1 and RA mechanoreceptors.

the stimulus. A complete discussion of this model and its extensions can be found in [114].

The point of this model is to provide spiking activity based on an input. One could use force information to elicit spike trains, which could be used for directly stimulating peripheral nerves. This is a method that has been proposed in recent work from theoretical neurobiologists and engineers alike [104]. Fig. 6.1 shows a sample plot of force and the corresponding spike trains that could be generated. There are two types of mechanoreceptors modeled, SA1 (slow adapting) and RA (fast adapting), as described in Section 3.1.2. The top chart of the figure shows force values while the middle and bottom charts show the SA1 and RA modeled response,

respectively.

RA mechanoreceptors respond to rapid changes in a force signal. A neural model can be applied to provide physiological spikes in a peripheral nerve. The frequency of spiking is related to the magnitude of force change. On the other hand, the SA mechanoreceptors respond to steady state pressures, unlike the RA receptors.

While this is just a proof of concept, this type of work could be realized through a tactile feedback system such as the one described in this thesis. The hope is that the work described by this masters' thesis will spark innovation and progress in both our current knowledge and understanding of technology while also improving the lives of upper limb amputees across the globe.

Bibliography

[1] R. Clement, K. Bugler, and C. Oliver, "Bionic prosthetic hands: A review of present technology and future aspirations," *The Surgeon*, vol. 9, no. 6, pp. 336–340, 12 2011. [Online]. Available: http://dx.doi.org/10.1016/j.surge.2011.06.001

[2] "http://www.touchbionics.com/," Touch Bionics.

[3] "http://www.i-biomed.com/," Infinite Biomedical Technologies.

[4] "Developments in dextrous hands for advanced robotic applications," in *Proceedings World Automation Congress, 2004*, vol. 15. Shadow Robot Company, 2004, pp. 123–128.

[5] "http://www.shadowrobot.com/," Shadow Robot Company.

[6] B. Edin, L. Ascari, L. Beccai, S. Roccella, J. Cabibihan, and M. Carrozza, "Bio-inspired sensorization of a biomechatronic robot hand for the grasp-and-

lift task," *Brain Research Bulletin*, vol. 75, no. 6, pp. 785–795, 4 2008. [Online]. Available: http://dx.doi.org/10.1016/j.brainresbull.2008.01.017

[7] J. A. Fishel and G. E. Loeb, "Sensing tactile microvibrations with the biotac comparison with human sensitivity," in *Proceedings 4th IEEE RAS & EMBS International Conference on Biomedical Robotics and Biomechatronics (BioRob)*, 2012, pp. 1122–1127.

[8] *FSR 400 Product Datasheet*, Interlink Electronics. [Online]. Available: http://www.interlinkelectronics.com/

[9] "Flexiforce data sheet," Tekscan. [Online]. Available: http://www.tekscan.com/flexible-force-sensors

[10] H. Forssberg, A. C. Eliasson, H. Kinoshita, R. S. Johansson, and G. Westling, "Development of human precision grip i: Basic coordination of force," *Experimental Brain Research*, vol. 85, no. 2, pp. 451–457, 1991. [Online]. Available: http://dx.doi.org/10.1007/BF00229422

[11] J. Fraden, *Force, Strain, and Tactile Sensors*, 4th ed., ser. Handbook of Modern Sensors: Physics, Designs, and Applications. Springer, 2010, pp. 353–373.

[12] D. P. J. Cotton, P. H. Chappell, A. Cranny, N. M. White, and S. P. Beeby, "A novel thick-film piezoelectric slip sensor for a prosthetic hand," *IEEE Sensors Journal*, vol. 7, no. 5, pp. 752–761, 2007.

BIBLIOGRAPHY

[13] M. Johannes, "Johns hopkins applied physics laboratory - modular prosthetic limb," Applied Physics Lab, 2013. [Online]. Available: http://www.jhuapl.edu/prosthetics/scientists/mpl.asp

[14] T. Someya, "Bionic skin for a cyborg you," 2013. [Online]. Available: http://spectrum.ieee.org/biomedical/bionics/bionic-skin-for-a-cyborg-you

[15] M. Cutkosky, "Biomimetics and dexterous manipulation laboratory." [Online]. Available: http://bdml.stanford.edu/

[16] W. W. Lee, J. J. Cabibihan, and N. V. Thakor, "Biomimetic strategies for tactile sensing," in *IEEE Sensors International Conference*, 2013.

[17] N. I. Glossas and N. A. Aspragathos, "Fuzzy logic grasp control using tactile sensors," *Mechatronics*, vol. 11, no. 7, pp. 899–920, 10 2001.

[18] E. D. Engeberg and S. G. Meek, "Adaptive sliding mode control for prosthetic hands to simultaneously prevent slip and minimize deformation of grasped objects," *IEEE/ASME Transactions on Mechatronics*, vol. 18, no. 1, pp. 376–385, 2013.

[19] "Seer training module," National Cancer Institute. [Online]. Available: http://training.seer.cancer.gov/

[20] E. Kandel, J. Schwartz, T. Jessell, S. Siegelbaum, and A. J. Hudspeth, *Principles of Neural Science, Fifth Edition.* McGraw-Hill Education, 2013.

[21] M. Francomano, D. Accoto, and E. Guglielmelli, "Artificial sense of slip: A review," *IEEE Sensors Journal*, vol. 13, no. 7, pp. 2489–2498, July 2013.

[22] A. Muzumdar, *Powered upper limb prostheses.* Springer, 2004.

[23] H. Sears and J. Shaperman, "Proportional myoelectric hand control: an evaluation," *American Journal of Physical Medicine and Rehabilitation*, vol. 70, pp. 20–28, 1991.

[24] E. D. Engeberg and S. G. Meek, "Adaptive object slip prevention for prosthetic hands through proportional-derivative shear force feedback," in *IEEE/RSJ International Conference on Intelligent Robots and Systems (IROS)*, 2008, pp. 1940–1945.

[25] S. Meek, S. Jacobsen, and P. Goulding, "Extended physiologic tactio: Design and evaluation of a proportional force feedback system," *Journal of Rehabilitation Research Development*, vol. 26, pp. 53–62, 1989.

[26] K. Horch, S. Meek, T. G. Taylor, and D. T. Hutchinson, "Object discrimination with an artificial hand using electrical stimulation of peripheral tactile and proprioceptive pathways with intrafascicular electrodes," *IEEE Transactions on Neural Systems and Rehabilitation Engineering*, vol. 19, no. 5, pp. 483–489, 2011.

[27] I. Birznieks, P. Jenmalm, A. Goodwin, and R. Johansson, "Encoding of direc-

tion of fingertip forces by human tactile afferents," *Journal of Neuroscience*, vol. 21, pp. 8222–8237, 2001.

[28] M. Burstedt, J. Flanagan, and R. Johansson, "Control of grasp stability in humans under different frictional conditions during multidigit manipulation," *Journal of Neuroscience*, vol. 82, pp. 2393–2405, 1999.

[29] E. Biddiss, D. Beaton, and T. Chau, "Consumer design priorities for upper limb prosthetics," *Disability and Rehabilitation: Assistive Technology*, vol. 2, no. 6, pp. 346–357, 2007. [Online]. Available: http://dx.doi.org/10.1080/17483100701714733

[30] P. J. Kyberd, C. Wartenberg, L. Sandsjö, S. Jönsson, D. Gow, J. Frid, C. Almström, and L. Sperling, "Survey of upper-extremity prosthesis users in sweden and the united kingdom," *Journal of Prosthetics and Orthotics*, vol. 19, no. 2, pp. 55–62, 2007. [Online]. Available: http://dx.doi.org/10.1097/JPO.0b013e3180459df6

[31] A. Cranny, D. P. J. Cotton, P. H. Chappell, S. P. Beeby, and N. M. White, "Thick-film force and slip sensors for a prosthetic hand," *Sensors and Actuators A: Physical*, vol. 123 - 124, no. 0, pp. 162–171, 9/23/ 2005. [Online]. Available: http://www.sciencedirect.com/science/article/pii/S0924424705000919

[32] L. Salisbury and A. Colman, "A mechanical hand with automatic proportional control of prehension." pp. 505–511, 1967.

[33] C. Light, P. H. Chappell, B. Hudgins, and K. Engelhart, "Intelligent multifunction myoelectric control of hand prostheses." pp. 139–146, 2002.

[34] G. Loeb and R. Johansson, "Biomimetic tactile sensor," 2010.

[35] B. Matulevich, G. E. Loeb, and J. A. Fishel, "Utility of contact detection reflexes in prosthetic hand control," in *IEEE/RSJ International Conference on Intelligent Robots and Systems (IROS)*, 2013, pp. 4741–4746.

[36] E. Engeberg, M. Frankel, and S. Meek, "Biomimetic grip force compensation based on acceleration of a prosthetic wrist under sliding mode control," in *IEEE International Conference on Robotics and Biomimetics (ROBIO)*, 2009, pp. 210–215.

[37] H. Takeda, N. Tsujiuchi, T. Koizumi, H. Kan, M. Hirano, and Y. Nakamura, "Development of prosthetic arm with pneumatic prosthetic hand and tendon-driven wrist," in *Annual International Conference of the IEEE Engineering in Medicine and Biology Society (EMBC)*, 2009, pp. 5048–5051.

[38] H. Elias, P. Godden, M. Greenhill, and R. Walker, "Humanoid robotic hand actuated by air muscles," U.S. Patent EP1 487 617A1, 2004.

[39] C. Pylatiuk, S. Schulz, and L. Doderlein, "Results of an internet survey of myoelectric prosthetic hand users," *Prosthetics and Orthotics International*, vol. 31, no. 4, pp. 362–370, 2007.

[40] "http://rslsteeper.com/," RSL Steeper.

[41] "http://www.utaharm.com/," Motion Control Inc.

[42] "http://www.ottobockus.com," OttoBock.

[43] "Deka research," DEKA. [Online]. Available: http://www.dekaresearch.com

[44] G. Puchhammer, "The tactile slip sensor: integration of a miniaturized sensory device on an myoelectric hand," *Orthopadie-Technik Quarterly*, vol. 1, pp. 7–12, 2000.

[45] E. Horvath, "Prosthesis drive," U.S. Patent 4 923 477, 1990.

[46] E. D. Engeberg and S. G. Meek, "Backstepping and sliding mode control hybridized for a prosthetic hand," *IEEE Transactions on Neural Systems and Rehabilitation Engineering*, vol. 17, no. 1, pp. 70–79, 2009.

[47] E. D. Engeberg, "A physiological basis for control of a prosthetic hand," *Biomedical Signal Processing and Control*, vol. 8, no. 1, pp. 6–15, 1 2013.

[48] E. D. Engeberg and S. Meek, "Improved grasp force sensitivity for prosthetic hands through force-derivative feedback," *IEEE Transactions on Biomedical Engineering*, vol. 55, no. 2, pp. 817–821, 2008.

[49] R. Andrecioli and E. D. Engeberg, "Grasped object stiffness detection for adaptive pid sliding mode position control of a prosthetic hand," in *4th IEEE RAS &*

EMBS International Conference on Biomedical Robotics and Biomechatronics (BioRob), 2012, pp. 526–531.

[50] ——, "Grasped object stiffness detection for adaptive force control of a prosthetic hand," in *3rd IEEE RAS & EMBS International Conference on Biomedical Robotics and Biomechatronics (BioRob)*, 2010, pp. 197–202.

[51] E. D. Engeberg and S. Meek, "Improved grasp force sensitivity for prosthetic hands through force-derivative feedback," *IEEE Transactions on Biomedical Engineering*, vol. 55, no. 2, pp. 817–821, 2008.

[52] J. R. Flanagan, M. K. O. Burstedt, and R. S. Johansson, "Control of fingertip forces in multidigit manipulation," *Journal of neurophysiology*, vol. 81, no. 4, pp. 1706–1717, April 01 1999.

[53] H. Forssberg, H. Kinoshita, A. C. Eliasson, R. S. Johansson, G. Westling, and A. M. Gordon, "Development of human precision grip," *Experimental Brain Research*, vol. 90, no. 2, pp. 393–398, 1992. [Online]. Available: http://dx.doi.org/10.1007/BF00227253

[54] R. S. Johansson, "Sensory control of dexterous manipulation in humans," in *Hand and Brain: The Neurophysiology and Psychology of Hand Movements*, A. Wing, P. Haggard, and J. Flanagan, Eds. Academic Press, 1996, pp. 381–414.

[55] ——, "Sensory input and control of grip," *Novartis Foundation symposium*, vol. 218, pp. 45–63, 1998.

[56] G. Slota, M. Suh, M. Latash, and V. Zatsiorsky, "Stability control of grasping objects with different locations of center of mass and rotational inertia," *Journal of Motor Behavior*, vol. 44, no. 3, pp. 169–178, 05/01; 2013/02 2012. [Online]. Available: http://dx.doi.org/10.1080/00222895.2012.665101

[57] B. B. Edin, G. Westling, and R. S. Johansson, "Independent control of human finger-tip forces at individual digits during precision lifting." *The Journal of Physiology*, vol. 450, no. 1, pp. 547–564, 05/01 1992. [Online]. Available: http://jp.physoc.org/content/450/1/547.abstract

[58] A. Vallbo and R. Johansson, "Properties of cutaneous mechanoreceptors in the human hand related to touch sensation," *Human Neurobiology*, vol. 3, no. 1, pp. 3–14, 1984.

[59] J. J. Cabibihan, R. Pradipta, and S. S. Ge, "Prosthetic finger phalanges with lifelike skin compliance for low-force social touching interactions," *Journal of Neuroengineering and Rehabilitation*, vol. 8, no. 16, 2011.

[60] N. Wettels, A. R. Parnandi, J.-H. Moon, G. E. Loeb, and G. S. Sukhatme, "Grip control using biomimetic tactile sensing systems," *IEEE/ASME Transactions on Mechatronics*, vol. 14, no. 6, pp. 718–723, 2009.

[61] J. A. Fishel, V. J. Santos, and G. E. Loeb, "A robust micro-vibration sensor for biomimetic fingertips," in *2008 2nd IEEE RAS & EMBS International Conference on Biomedical Robotics and Biomechatronics (BioRob)*, 2008, pp. 659–663.

[62] "http://www.syntouchllc.com," SynTouch.

[63] M. A. Srinivasan, "Surface deflection of primate fingertip under line load," *Journal of Biomechanics*, vol. 22, no. 4, pp. 343–349, 1989.

[64] K. J. Cole and J. H. Abbs, "Grip force adjustments evoked by load force perturbations of a grasped object," *Journal of Neurophysiology*, vol. 60, no. 4, pp. 1513–1522, 1988.

[65] D. Tyler, "Functional neural interface lab," 2013. [Online]. Available: http://bme.case.edu/Tyler/Research

[66] M. R. Tremblay and M. R. Cutkosky, "Estimating friction using incipient slip sensing during a manipulation task," in *IEEE International Conference on Robotics and Automation*, 1993, pp. 429–434 vol.1.

[67] B. L. Gray and R. S. Fearing, "A surface micromachined microtactile sensor array," in *IEEE International Conference on Robotics and Automation*, vol. 1, 1996, pp. 1–6 vol.1.

[68] P. A. Schmidt, E. Maël, and R. P. Wütz, "A sensor for dynamic

tactile information with applications in human-robot interaction and object exploration," *Robotics & Autonomous Systems*, vol. 54, no. 12, p. 1005, 12 2006. [Online]. Available: http://dx.doi.org/10.1016/j.robot.2006.05.013

[69] R. Dahiya and M. Valle, *Tactile Sensing for Robotic Applications*, ser. Sensors, Focus on Tactile Force and Stress Sensors. InTech Education and Publishing, 2008, pp. 289–304.

[70] "www.pressureprofile.com," Pressure Profile Systems, 2013.

[71] Apple. [Online]. Available: http://www.apple.com/

[72] Y. Tenzer, L. P. Jentoft, and D. Howe, "Inexpensive and eaily cusomized tactile array sensors using mems barometer chips," *IEEE Transactions*, 2012.

[73] Y. Tenzer, L. Jentoft, and R. Howe, TakkTile, 2013. [Online]. Available: http://www.takktile.com/

[74] A. Dollar, "Grab lab," 2013. [Online]. Available: http://www.eng.yale.edu/grablab

[75] L. Osborn, R. Kaliki, and N. V. Thakor, "Utilizing tactile feedback for biomimetic grasping control in upper limb prostheses," in *IEEE International Conference on Sensors*, 2013, pp. 1266–1269.

[76] M. Johannes, J. Bigelow, J. Burck, S. Harshbarger, M. Kozlowski, and T. V.

Doren, "An overview of the development process for the modular prosthetic limb," *JHU APL Tech Digest*, vol. 30, no. 3, pp. 207–216, 2011.

[77] Q. Cao, H. Kim, N. Pimparkar, J. P. Kulkarni, C. Wang, M. Shim, K. Roy, M. A. Alam, and J. A. Rogers, "Medium-scale carbon nanotube thin-film integrated circuits on flexible plastic substrates," *Nature*, vol. 454, no. 7203, p. 495, 07/24 2008. [Online]. Available: http://dx.doi.org/10.1038/nature07110

[78] B. Heyneman and M. R. Cutkosky, "Biologically inspired tactile classification of object-hand and object-world interactions," in *IEEE International Conference on Robotics and Biomimetics (ROBIO)*, 2012, pp. 167–173.

[79] "http://www.sinapseinstitute.org/," SINAPSE.

[80] T. Yoshikawa, "Control algorithm for grasping and manipulation by multifingered robot hands using virtual truss model representation of internal force," in *IEEE International Conference on Robotics and Automation (ICRA)*, vol. 1, 2000, pp. 369–376.

[81] T. Yoshikawa, T. Sugie, and M. Tanaka, "Dynamic hybrid position/force control of robot manipulators-controller design and experiment," *IEEE Journal of Robotics and Automation*, vol. 4, no. 6, pp. 699–705, 1988.

[82] N. Hogan, "Stable execution of contact tasks using impedance control," in *IEEE*

International Conference on Robotics and Automation, vol. 4, 1987, pp. 1047–1054.

[83] T. Wimbock, C. Ott, and G. Hirzinger, "Passivity-based object-level impedance control for a multifingered hand," in *IEEE/RSJ International Conference on Intelligent Robots and Systems (IROS)*, 2006, pp. 4621–4627.

[84] S. Ueki, H. Kawasaki, and T. Mouri, "Adaptive coordinated control of multi-fingered hands with sliding contact," in *International Joint Conference SICE-ICASE*, 2006, pp. 5893–5898.

[85] H. Kawasaki, S. Ueki, and S. Ito, "Decentralized adaptive coordinated control of multiple robot arms without using a force sensor," *Automatica*, vol. 42, no. 3, pp. 481–488, 3 2006.

[86] E. A. Al-Gallaf, "Multi-fingered robot hand optimal task force distribution: Neural inverse kinematics approach," *Robotics and Autonomous Systems*, vol. 54, no. 1, pp. 34–51, 1 2006.

[87] J. A. Dominguez-Lopez, R. M. Crowder, R. I. Damper, and C. J. Harris, "Adaptive neurofuzzy control of a robotic gripper with external disturbances," in *IEEE International Conference on Systems, Man and Cybernetics*, vol. 4, 2004, pp. 3193–3198.

[88] Y. Zhao and C.-C. Cheah, "Neural network control of multifingered robot hands

using visual feedback," *IEEE Transactions on Neural Networks*, vol. 20, no. 5, pp. 758–767, 2009.

[89] R. Boughdiri, H. Nasser, H. Bezine, N. K. M'Sirdi, A. M. Alimi, and A. Naamane, "Dynamic modeling and control of a multi-fingered robot hand for grasping task," *Procedia Engineering*, vol. 41, no. 0, pp. 923–931, 2012.

[90] F. Touvet, N. Daoud, J. P. Gazeau, S. Zeghloul, M. A. Maier, and S. Eskiizmirliler, "A biomimetic reach and grasp approach for mechanical hands," *Robotics and Autonomous Systems*, vol. 60, no. 3, pp. 473–486, 3 2012.

[91] N. Daoud, J. P. Gazeau, S. Zeghloul, and M. Arsicault, "A real-time strategy for dexterous manipulation: Fingertips motion planning, force sensing and grasp stability," *Robotics and Autonomous Systems*, vol. 60, no. 3, pp. 377–386, 2012.

[92] D. Goeger, N. Ecker, and H. Woern, "Tactile sensor and algorithm to detect slip in robot grasping processes," in *IEEE International Conference on Robotics and Biomimetics (ROBIO)*, 2009, pp. 1480–1485.

[93] E. Holweg, H. Hoeve, W. Jongkind, L. Marconi, C. Melchiorri, and C. Bonivento, "Slip detection by tactile sensors: algorithms and experimental results," in *IEEE International Conference on Robotics and Automation*, vol. 4, 1996, pp. 3234–3239.

[94] S. Shirafuji and K. Hosoda, "Detection and prevention of slip using sensors with

different properties embedded in elastic artificial skin on the basis of previous experience," in *IEEE International Conference on Robotics and Autonomous Systems*, 6 2011, pp. 459–464.

[95] P. J. Kyberd and P. H. Chappell, "Object-slip detection during manipulation using a derived force vector," *Mechatronics*, vol. 2, no. 1, pp. 1–13, 2 1992.

[96] S. Arimoto, "Intelligent control of multi-fingered hands," *Annual Reviews in Control*, vol. 28, no. 1, pp. 75–85, 2004.

[97] U. Castiello and A. Pierno, "Reaching and grasping," in *Encyclopedia of Neuroscience*, L. R. Squire, Ed. Oxford: Academic Press, 2009, pp. 23 – 28. [Online]. Available: http://dx.doi.org/10.1016/B978-008045046-9.01919-7

[98] U. Castiello, "The neuroscience of grasping," *Nature Reviews Neuroscience*, vol. 6, no. 9, pp. 726–736, Sep 2005.

[99] S. S. Hsiao and M. Gomez-Ramirez, "Neural mechanisms of tactile perception," in *Comprehensive Handbook of Psychology: Volume 3: Behavioral Neuroscience*, 2nd ed., M. Gallagher and R. Nelson, Eds. John Wiley and Sons, Inc, 01/01 2002.

[100] K. O. Johnson and S. S. Hsiao, "Neural mechanisms of tactual form and texture perception," *Annual Review of Neuroscience*, vol. 15, no. 1, pp. 227–250, 1992. [Online]. Available: http://dx.doi.org/10.1146/annurev.ne.15.030192.001303

[101] G. Westling and R. S. Johansson, "Responses in glabrous skin mechanoreceptors during precision grip in humans," *Experimental Brain Research*, vol. 66, no. 1, pp. 128–140, 1987.

[102] R. Johansson and G. Westling, "Roles of glabrous skin receptors and sensorimotor memory in automatic control of precision grip when lifting rougher or more slippery objects," *Experimental Brain Research*, vol. 56, no. 3, pp. 550–564, 1984. [Online]. Available: http://dx.doi.org/10.1007/BF00237997

[103] R. Johansson and J. Flanagan, "Tactile sensory control of object manipulation in humans," in *The Senses: A Comprehensive Reference, Vol 6, Somatosensation*, A. Basbaum, A. Kaneko, G. Shepherd, and G. Westheimer, Eds. San Diego: Academic Press, 2008, pp. 67–86. [Online]. Available: http://dx.doi.org/10.1016/b978-012370880-9.00346-7

[104] S. S. Hsiao, M. Fettiplace, and B. Darbandi, "Sensory feedback for upper limb prostheses," *Progress in Brain Research*, vol. 192, pp. 69–81, 2011.

[105] S. S. Kim, A. Sripati, R. Vogelstein, R. Armiger, A. Russell, and S. Bensmaia, "Conveying tactile feedback in sensorized hand neuroprostheses using a biofidelic model of mechanotransduction," *IEEE Transactions on Biomedical Circuits and Systems*, vol. 3, no. 6, pp. 398–404, Dec 2009.

[106] T. D'Alessio and R. Steindler, "Slip sensors for the control of the grasp in

functional neuromuscular stimulation," *Medical Engineering & Physics*, vol. 17, no. 6, pp. 466–470, 9 1995.

[107] A. Mingrino, A. Bucci, R. Magni, and P. Dario, "Slippage control in hand prostheses by sensing grasping forces and sliding motion," in *IEEE/RSJ/GI International Conference on Intelligent Robots and Systems (IROS)*, vol. 3, 1994, pp. 1803–1809.

[108] R. von Mises, "Mechanik der festen korper im plastisch- deformablen zustand," *Nachrichten von der Gesellschaft der Wissenschaften zu Gottingen, Mathematisch-Physikalische Klasse*, vol. 1, pp. 582–592, 1913. [Online]. Available: http://neo-classical-physics.info/uploads/3/0/6/5/3065888/von_mises_-_plastic_deformation.pdf

[109] R. Budynas, K. Nisbett, and J. E. Shigley, "Failure prevention," in *Shigley's Mechanical Engineering Design*. New York: McGraw-Hill, 2011.

[110] D. Edeer and C. Martin, "Upper limb prostheses - a review of the literature with a focus on myoelectric hands," WorkSafe BC Evidence-Based Practice Group, February 2011.

[111] L. Osborn and R. Kaliki, "Upper limb amputee user needs survey," Infinite Biomedical Technologies, Tech. Rep., 2012.

[112] D. Rager, D. Alvares, I. Birznieks, S. Redmond, J. Morley, N. Lovell, and

R. Vickery, "Generating tactile afferent stimulation patterns for slip and touch feedback in neural prosthetics," in *International Conference of the IEEE Engineering in Medicine and Biology Society (EMBC)*, July 2013, pp. 5922–5925.

[113] "By restoring sense of touch to amputees, haptix seeks to overcome physical and psychological effects of upper limb loss," DARPA, April 2014. [Online]. Available: http://www.darpa.mil/NewsEvents/Releases/2014/04/24.aspx

[114] W. Gerstner and W. Kistler, *Spiking Neuron Models: Single Neurons, Populations, Plasticity*. Cambridge University Press, 2002.

Vita

Luke Osborn was born in Little Rock, AR on October 7, 1989. He received a Bachelor of Science degree in mechanical engineering from the University of Arkansas in the spring of 2012. He enrolled in the biomedical engineering MSE program at Johns Hopkins University in the fall of 2012. He was inducted into the Tau Beta Pi and Pi Tau Sigma honor societies in 2011, was awarded the Mechanical Engineering Department's Senior Scholar Award in 2012, received a National Science Foundation Research Undergraduate Fellowship in 2011, and received two undergraduate research fellowships from 2011—2012. His research focuses on the enhancement of upper limb prosthetic devices, his papers have been accepted at the 2013 IEEE Sensors International Conference as well as the 2014 IEEE International Conference on Biomedical Robotics and Biomechatronics.

Starting at the end of June 2014, Luke will enroll in the PhD program in biomedical engineering at Johns Hopkins University where he will focus on developing tech-

nology for the advanced control of prosthetic limbs through the use of peripheral nerve stimulation based on sensory inputs.